

Identification of the tumour-associated gene *S100A14* and analysis of its regulation

DISSERTATION

zur Erlangung des akademischen Grades

doctor rerum naturalium

(Dr. rer. nat.)

im Fach Biologie

eingereicht an der

Mathematisch-Naturwissenschaftlichen Fakultät I

der Humboldt-Universität zu Berlin

von

Diplom-Biotechnologin Agnieszka Pietas

geb. am 14. April 1975 in Lublin, Polen

Präsident der Humboldt-Universität zu Berlin

Prof. Dr. Jürgen Mlynek

Dekan der Mathematisch-Naturwissenschaftlichen Fakultät I

Prof. Thomas Buckhout, PhD

Gutachter/innen:

1. Prof. Dr. Harald Saumweber
2. PD Dr. Christine Sers
3. Prof. Dr. Iver Petersen

Datum der Promotion: 22.11.2004

Table of Contents

List of Figures.....	IV
List of Tables	VII
List of Abbreviations.....	VIII
Zusammenfassung.....	X
Abstract.....	XII
1 Introduction.....	1
1.1 Multi-Step Progression of Tumours	1
1.2 The S100 Protein Family	3
1.2.1 Genomic Organization and Chromosomal Localization of <i>S100</i> Genes	4
1.2.2 Biological Functions	5
1.2.3 Association with Human Diseases	7
1.3 Aim of This Work	10
2 Materials and Methods	11
2.1 Materials	11
2.1.1 Chemicals	11
2.1.2 Kits	11
2.1.3 Materials.....	12
2.1.4 Enzymes	12
2.1.5 Antibodies	12
2.1.6 Mammalian Cell Lines	13
2.1.7 <i>E. coli</i> Strain	15
2.1.8 RNA Samples from Mammalian Cell Lines	15
2.1.9 Tissue Specimens	16
2.1.10 Plasmids and Expression Constructs	16
2.1.11 Oligonucleotides.....	18

2.2	Methods.....	19
2.2.1	Bacterial Culture.....	19
2.2.2	Culturing of Mammalian Cells	21
2.2.3	Preparation, Enzymatic Manipulation and Analysis of DNA	26
2.2.4	Dual-Luciferase Reporter Assay	33
2.2.5	Preparation and Analysis of RNA.....	34
2.2.6	Analysis of Proteins.....	38
2.2.7	S100A14 Antibody Generation.....	44
2.2.8	Immunofluorescence Analysis.....	45
2.2.9	Immunohistochemistry	46
2.2.10	Tissue Microarrays (TMA) Generation	48
2.2.11	Statistical Analysis.....	48
2.2.12	Bioinformatics.....	48
3	Results.....	50
3.1	Identification of the Human <i>S100A14</i> cDNA	50
3.1.1	Screening of SSH cDNA Libraries.....	50
3.1.2	Sequence Analysis of <i>S100A14</i> cDNA.....	51
3.2	Expression Profile in Tumour Cell Lines, Normal, and Neoplastic Tissues.....	53
3.2.1	<i>S100A14</i> mRNA Level in Tumour Cell Lines.....	53
3.2.2	Expression Profile in Normal Human Tissues	56
3.2.3	<i>S100A14</i> mRNA Level in Tumour Tissues	58
3.2.4	<i>S100A14</i> Protein Expression in Lung Tumours and Association with Clinicopathological Factors.....	60
3.2.5	<i>S100A14</i> Protein Expression in Breast Tumours and Association with Clinicopathological Factors.....	62
3.2.6	<i>S100A14</i> is not Re-Expressed Following Growth of Human Cancer Cell Lines Transplanted into Mice	65
3.3	Subcellular Localization of the <i>S100A14</i> Protein	66
3.4	Genomic Organization and Chromosomal Localization of the <i>S100A14</i> Gene	69

3.5	Identification and Characterization of the Promoter for the <i>S100A14</i> Gene	75
3.6	ERBB Ligands Induce <i>S100A14</i> Expression at the Transcriptional Level in 9442 Cells	79
3.6.1	Effects of Signalling Pathways Inhibition on Activation of <i>S100A14</i> by the EGF	82
3.6.2	EGF-Induced <i>S100A14</i> Gene Expression is Dependent on <i>de novo</i> Protein Synthesis.....	86
3.7	Transcriptional Induction by Protein Kinase C	87
4	Discussion.....	89
4.1	Identification of the <i>S100A14</i> cDNA.....	89
4.2	<i>S100A14</i> is Differentially Expressed in Human Tumours	90
4.3	Identification and Characterization of the Genomic Locus of <i>S100A14</i>	96
4.4	Oncogenic Signalling Pathways Mediate <i>S100A14</i> Transcriptional Induction.....	100
5	References	110
	Danksagung.....	127
	Curriculum Vitae.....	129
	Publications	130
	Eidesstattliche Erklärung	132

List of Figures

Fig. 1	The <i>S100</i> gene cluster on human chromosome 1q21	5
Fig. 2	The scoring system used for immunohistochemical analysis of S100A14.....	47
Fig. 3	Nucleotide and deduced amino acid sequence of the human <i>S100A14</i> gene.....	52
Fig. 4	Alignment of the predicted amino acid sequences of the human S100A14 and the mouse orthologue 1110013O05RIK with the most homologous S100 family members	53
Fig. 5	Expression of the <i>S100A14</i> mRNA in normal human tissues.....	57
Fig. 6	Expression profile of <i>S100A14</i> in human tumours.....	59
Fig. 7	S100A14 protein is overexpressed in primary lung tumour tissue in comparison to normal lung tissue.....	60
Fig. 8	S100A14 localizes to plasma membrane in lung tumour tissue	61
Fig. 9	S100A14 protein is up-regulated in primary breast carcinoma relative to normal breast tissue.....	63
Fig. 10	S100A14 overexpression correlates with ERBB2 overexpression in primary breast tumours.....	63
Fig. 11	S100A14 localizes to plasma membrane in breast cancer tissue	64
Fig. 12	<i>S100A14</i> is not re-expressed in lung cancer cell line xenografts from nude mice	65
Fig. 13	Cellular localization of S100A14-V5 protein in human lung tumour and COS-7 cells	67
Fig. 14	Subcellular localization of the endogenous S100A14 protein in immortalized lung cells, and lung and colon tumour cells	68
Fig. 15	The S100A14 protein is distributed through the cytoplasmic and membranous fractions of 9442 cells	69
Fig. 16	Southern blot analysis of the genomic PAC clones positive for <i>S100A14</i>	71

Fig. 17	Genomic structure of the human <i>S100A14</i>	72
Fig. 18	Southern blot analysis of the <i>S100A14</i> gene in lung cancer cell lines.....	73
Fig. 19	Chromosomal localization of <i>S100A14</i> by FISH.....	73
Fig. 20	<i>S100A14</i> is localized within the <i>S100</i> gene cluster on human chromosome 1q21.....	74
Fig. 21	Transcription activities of <i>S100A14</i> promoter constructs.....	76
Fig. 22	Comparison of nucleotide sequence and potential regulatory elements of the <i>S100A14</i> promoter fragment in mouse and human genomic DNAs.....	78
Fig. 23	Up-regulation of <i>S100A14</i> expression in H322 cells after stimulation with serum.....	79
Fig. 24	Treatment of 9442 and HMEB cells with EGF leads to the induction of <i>S100A14</i>	79
Fig. 25	<i>S100A14</i> is induced by EGF in a time-dependent manner in 9442 cells.....	80
Fig. 26	Induction of <i>S100A14</i> is EGF dose-dependent.....	80
Fig. 27	TGF- α induces <i>S100A14</i> mRNA in 9442 cells.....	81
Fig. 28	Up-regulation of <i>S100A14</i> expression in 9442 cells after stimulation with fresh medium.....	81
Fig. 29	<i>S100A14</i> protein is not induced following treatment with EGF.....	82
Fig. 30	Kinetics of the growth factor-induced response for the ERK1/2, p38, and JNK MAPK pathways and the PI3K cascade.....	83
Fig. 31	The inhibitory efficacy of various pharmacological agents on activation of the ERK1/2, p38, and JNK MAPK pathways and the PI3K cascade.....	84
Fig. 32	ERK1/2 MAPK signalling pathway determines <i>S100A14</i> induction following stimulation with EGF.....	85
Fig. 33	EGF-induced <i>S100A14</i> expression is dependent on <i>de novo</i> protein synthesis.....	86
Fig. 34	PMA exerts stimulation of <i>S100A14</i> via PKC activation.....	88
Fig. 35	Generic <i>S100</i> gene structure.....	97

Fig. 36	Pharmacological modulation of the ERBB-induced signalling pathways	102
Fig. 37	Schematic representation of the signalling pathways leading to <i>S100A14</i> up-regulation in response to EGF and PMA in 9442 cells	107

List of Tables

Table 1	S100 proteins: functions and association with human diseases	7
Table 2	Expression of <i>S100A14</i> mRNA in human cancer cell lines	54
Table 3	Expression of <i>S100A14</i> mRNA in other mammalian cell lines	55
Table 4	Expression of the S100A14 protein in normal human tissues	58
Table 5	Association of S100A14 protein expression in lung tumours with clinicopathological factors	62
Table 6	Association of S100A14 protein expression in breast tumours with clinicopathological factors	65
Table 7	Exon/intron boundaries of the human <i>S100A14</i> gene	72

List of Abbreviations

A	Adenine
aa	Amino acid
ADC	Adenocarcinoma
APS	Ammonium Persulphate
Asp	Asparagine
ATCC	American Type Culture Collection
bp	Base pair
BSA	Bovine Serum Albumine
C	Cytosine
Ca	Carcinoma
cDNA	Complementary DNA
CIAP	Calf Intestinal Alkaline Phosphatase
Da	Dalton
DABCO	1,4-Diazabicyclo (2,2,2)-octane
DAPI	4,6-Diamidino-2-phenylindole hydrochloride
DEPC	Diethylpyrocarbonate
DMEM	Dulbecco Modified Eagle's Medium
DMF	Dimethylformamide
DMSO	Dimethyl Sulfoxide
DNA	Deoxyribonucleic Acid
dNTP	Deoxyribonucleoside Triphosphate
DTT	Dithiothreitol
FCS	Fetal Calf Serum
EB	Elution Buffer
E.coli	Escherichia coli
EDTA	Ethylendiamin-tetra-acetate
EGF	Epidermal Growth Factor
EGFP	Enhanced Green Fluorescent Protein
ER	Oestrogen Receptor
ERBB	Avian erythroblastic leukemia viral oncogene
FITC	Fluorescein Isothiocyanate
G	Guanine
Glu	Glutamine
Gly	Glycine
h	Hour
IPTG	Isopropyl- β -thio- β -D-galactopyranoside
KLH	Keyhole Limpet Hemocyanin
l	Liter
L-15	Leibovitz-15

LB	Luria-Bertani
LAR II	Luciferase Assay Reagent II
LCLC	Large Cell Lung Carcinoma
M	Molar
mM	Milimol
min	Minute
ml	Mililiter
MOPS	3-(N-Morpholino)-propanylsulfon acid
NFκB	Nuclear factor κB
NSCLC	Non-Small Cell Lung Cancer
nt	Nucleotide
OD	Optical Density
ORF	Open Reading Frame
PAGE	Polyacrylamide Gel Electrophoresis
PBS	Phosphate Buffered Saline
PCR	Polymerase Chain Reaction
PKC	Protein Kinase C
PMA	Phorbol 12-myristate 13-acetate
PMSF	Phenyl Methyl-Sulfonyl Fluoride
PR	Progesteron
rpm	Rotations per minute
RPMI	Rosewell Park Memorial Institute
RTK	Receptor tyrosine kinase
SCC	Squamous Cell Carcinoma
SCLC	Small Cell Lung Carcinoma
SDS	Sodium Dodecyl Sulphate
sec	Second
Ser	Serine
SSC	Sodium chloride-Sodium Citrate
T	Thymine
Ta	Annealing Temperature
TBE	Tris-Boric acid-EDTA
TBST	Tris-Buffered Saline Tween-20
TEMED	N,N,N',N'-Tetramethylethylenediamine
TGF-α	Transforming Growth Factor-α
Tm	Melting Temperature
Tris	Tris-(hydroxymethyl)-aminomethan
U	Unit
UTR	Untranslated region
V	Volt
X-gal	5-bromo, 4-chloro-3-indol-β-D-galactopyranoside
μl	Microliter
μM	Micromolar

Zusammenfassung

Durch Analyse der Subtraktion-cDNA Bibliothek einer humanen Lungentumor Zelllinie haben wir ein neues Mitglied der S100 Genfamilie identifiziert und charakterisiert, welches *S100A14* benannt wurde. Die vollständige cDNA hat eine Länge von 1067 bp und kodiert für ein Protein von 104 Aminosäuren, welches die S100-spezifische Kalzium-bindende Domäne enthält und die größte Homologie zu S100A13 zeigt. Das Gen wird in normalen humanen Epithelien ubiquitär exprimiert, zeigt jedoch Expressionsverluste in vielen Tumorzelllinien aus unterschiedlichem Gewebe. Im Gegensatz zu Tumorzelllinien ist *S100A14* auf mRNA- und Proteinebene in vielen humanen Primärtumoren stärker exprimiert, unter anderem in Lungen- und Brustkarzinomen. Das Protein ist vorzugsweise in der Region der Plasmamembran und im Zytoplasma lokalisiert.

Das Gen liegt auf Chromosom 1 im Bereich der Bande 1q21, einer Region mit hoher chromosomaler Instabilität in Malignomen, in der sich auch mindestens 16 weitere *S100* Gene befinden. Es ist aus vier Exons und drei Introns aufgebaut und erstreckt sich über 2165 bp genomischer DNA.

In der 5' Region proximal der transkriptionellen Initiationsstelle des *S100A14* Gens wurde mit Hilfe von Deletionsmutationen eine minimale Promoteregion identifiziert, die vermutlich zur basalen Promoteraktivität beiträgt.

Um den Mechanismus der erhöhten *S100A14* Expression in Lungen- und Brustkarzinomen zu verstehen, haben wir die Effekte des EGF (epidermal growth factor) und des TGF- α (transforming growth factor- α) untersucht. Beide Faktoren sind Liganden des ERBB Rezeptors und induzieren in der immortalisierten bronchialen Epithelzelllinie *S100A14* Expression. Unter Verwendung spezifischer Inhibitoren konnte gezeigt werden, dass für die EGF-vermittelte transkriptionelle Induktion der ERK1/2 Signalweg (extracellular signal-regulated kinase) verantwortlich ist und eine *de novo* Proteinsynthese erfordert. Diese Ergebnisse unterstützend konnte immunhistologisch eine signifikante Korrelation zwischen der Überexpression von ERBB2 und *S100A14* in primären Brustkarzinomen nachgewiesen werden.

Phorbolester-12-Myristat-13-Acetat (PMA) verstärkte gleichfalls die *S100A14* mRNA Expression in 9442 Zellen, was eine Regulation durch die Protein Kinase C (PKC) vermuten lässt. Die PMA-induzierte Expression von *S100A14* wird ebenso wie die TGF- α /EGF-Induktion durch die Aktivierung des ERK1/2 Signalweges vermittelt.

In Anbetracht der großen Bedeutung der ERK1/2 und PKC Signalwege in der Tumorentstehung und Tumorprogression ist zu vermuten, dass *S100A14* über die aberrante Regulation dieser Signalwege an die maligne Transformation gekoppelt ist.

Schlagwörter: S100A14, S100, EGF, TGF- α , PKC, PMA, ERK1/2

Abstract

By analysing a human lung tumour cell line subtraction cDNA library, we have identified and characterized a novel member of the human *S100* gene family that we designated *S100A14*. The full-length cDNA is 1067 bp and encodes a putative protein of 104 amino acids. The predicted protein contains the S100-specific EF-hand calcium-binding domain and shares the highest sequence homology to *S100A13*. The gene is ubiquitously expressed in normal human tissues of epithelial origin, with the highest expression in colon. *S100A14* transcript was found to be down-regulated in many immortalized and tumour cell lines from diverse tissues. In contrast to the tumour cell lines, *S100A14* shows up-regulation at the mRNA and protein level in many human primary tumours, including lung and breast carcinomas. *S100A14* protein localizes predominately to the plasma membrane and the cytoplasm.

We localized the *S100A14* gene to a region of chromosomal instability on human chromosome 1q21, where at least 16 other *S100* genes are clustered. We subsequently resolved the gene structure of *S100A14* in human by demonstrating its organization of four exons and three introns spanning a total of 2165 bp of genomic sequence. By analysing the proximal 5' upstream region of the *S100A14* transcription initiation site, we identified the minimal promoter region which possibly contributes to the basal activity of the promoter fragment.

To elucidate mechanisms whereby *S100A14* expression is enhanced in lung and breast tumours, we studied the effects of epidermal growth factor (EGF) and transforming growth factor- α (TGF- α) on its expression. Both are ligands of ERBB receptor and induced *S100A14* expression in the immortalized bronchial epithelial cells. By use of specific inhibitors, we found that EGF-mediated transcriptional induction of *S100A14* involves extracellular signal-regulated kinase (ERK1/2) signalling and requires *de novo* protein synthesis. In support of these findings, we demonstrated by immunohistochemistry a significant correlation between ERBB2 and *S100A14* protein overexpression in primary breast carcinomas.

Our studies showed that the phorbol ester 12-myristate 13-acetate (PMA) increases *S100A14* mRNA expression in immortalized bronchial epithelial cells

suggesting regulation by protein kinase C (PKC). Similar to TGF- α /EGF induction, the PMA-induced *S100A14* expression was also mediated by activation of the ERK1/2 signalling cascade.

Considering the importance of the ERK1/2 and PKC signalling pathways in tumour development and progression we suggest that it is the aberrant regulation of these signalling cascades that couples *S100A14* to malignant transformation.

Keywords: S100A14, S100, EGF, TGF- α , PKC, PMA, ERK1/2

1 Introduction

1.1 Multi-Step Progression of Tumours

Several lines of evidence indicate that tumorigenesis in humans is a multi-step process, formally analogous to Darwinian evolution, in which a succession of genetic and epigenetic changes, each conferring a different type of growth advantage, leads to the progressive conversion of normal cells into cancer cells (Nowell, 1976). The accumulation of genetic changes liberates neoplastic cells from the homeostatic mechanisms that govern normal cell proliferation. Observations of human cancers and animal models implicate a limited number of molecular pathways, the disruption of which contributes to most cancers. In humans, at least four to six distinct somatic mutations are required to reach this state (Renan, 1993; Kinzler et al., 1996).

Several properties are shared by most of human tumours: self-sufficiency in growth signals, insensitivity to growth-inhibitory signals, evasion of programmed cell death (apoptosis), limitless replicative potential, sustained angiogenesis, and tissue invasion and metastasis (Hanahan and Weinberg, 2000). Each of these novel capabilities acquired during tumour development represents the successful breaking of an anti-cancer defense mechanism applied by cells and tissues.

Molecular studies have identified three groups of genes, which are frequently deregulated in cancer:

1. proto-oncogenes, which are activated by mutations and become oncogenes. Their acquired oncogenic functions lead to uncontrolled cellular growth and proliferation.
2. tumour-suppressor genes, which normally negatively regulate cell growth and proliferation preventing the development of tumour. Loss or mutational inactivation of these genes leads to the deregulation of cell cycle progression as well as other intracellular processes resulting in cancer progression.
3. genes responsible for maintaining the genomic integrity and genes encoding the DNA-repair system. Loss of function of these genes results in a genetic instability that is characteristic of tumour cells.

Development of gene-expression profiling as well as advances in tumour diagnosis revealed, however, a striking conceptual inconsistency in the prevailing multi-step model of tumour progression (Bernards and Weinberg, 2002). Gene-expression pattern of metastatic tumour cells is often strikingly similar to that of the cells confined to the primary tumour mass from which they were derived. Equally relevant are other studies in which the gene-expression profiles of the dominant populations of breast-cancer cells within a primary tumour mass have been used to predict, with 90% accuracy, whether the tumour will remain localized or whether the patient will experience metastases and disease relapse.

Based on these findings, it is suggested that a subset of the mutant alleles acquired by incipient tumour cells early in tumorigenesis confer not only the selected replicative advantage, but also, later in tumorigenesis, the tendency to metastasize. This tendency will become manifest only much later in tumour progression, in the context of yet other mutations that have struck the genomes of descendant cells.

This reasoning has important implications. First, genes and genetic changes specifically and exclusively involved in orchestrating the process of metastasis do not exist. Instead, it is the particular combination of genes that enables cells to create primary tumour mass that also empowers them to become metastatic. Second, because important components of the genotype of metastasis are already implanted in cells relatively early in tumorigenesis, even relatively small primary tumour cell populations may already have the ability to dispatch metastatic cells to distant sites in the body.

Moreover, several independent lines of evidence seem to support the idea that tumorigenesis is governed not only by the tumour cells *per se*, but also by the microenvironment (Chang and Werb, 2001). For example, tumour-associated fibroblasts can direct tumour progression (Olumi et al., 1999), and endothelial cells foster tumour angiogenesis (Carmeliet and Jain, 2000). Inflammatory cells might also promote tumour development, as shown by studies on skin tumorigenesis in K14-HPV16 transgenic mice that lack mast cells or metalloproteinase-9 (Coussens et al., 1999; Coussens et al., 2000).

1.2 The S100 Protein Family

Calcium (Ca^{2+}) functions as a universal second messenger that plays a regulatory role in a great variety of cellular processes such as memory and transmission of nerve impulses, muscle contraction, secretion, cell motility and volume regulation, cell growth and differentiation, gene expression, cross-talk between different enzyme systems, apoptosis, and necrosis (Berridge et al., 2000). The Ca^{2+} signalling networks are composed of many molecular components including the large family of Ca^{2+} -binding proteins characterized by the EF-hand structural motif (Kawasaki et al., 1998). Certain members, notably calbindin D28k and parvalbumin, serve as cytosolic Ca^{2+} buffers, whereas others, such as calmodulin, troponin C, and the S100 proteins, are Ca^{2+} -dependent regulatory proteins.

S100 proteins represent the largest subgroup within the EF-hand protein family. They have received increasing attention in recent years due to their association with various human pathologies including cancer, neurodegenerative disorders, inflammation, and cardiomyopathy (Heizmann et al., 2002). Moreover, they have been of value in the diagnosis of these diseases. Twenty-two members have been identified so far. Unlike the ubiquitous calmodulin, most of them show cell- and tissue-specific expression.

S100 proteins are small (10 to 12 kDa) acidic proteins that form homo- and heterodimers. They are characterized by a pair of helix-loop-helix (the EF-hand) motifs connected by a central hinge region. The two EF-hand structural motifs display different affinities for calcium. The C-terminal EF-hand contains the canonical Ca^{2+} -binding loop consisting of 12 amino acids. The N-terminal EF-hand consists of 14 amino acids and is specific for S100 proteins. Upon Ca^{2+} binding S100 proteins undergo a conformational change required for target recognition and binding. Generally, the dimeric S100 proteins bind four Ca^{2+} per dimer. Besides Ca^{2+} , a number of S100 proteins bind Zn^{2+} with a wide range of affinities. For S100B, S100A5, and S100A13 Cu^{2+} binding was reported (Nishikawa et al., 1997; Schäfer et al., 2000; Mandinova et al., 2003).

Another distinguishing feature of S100 proteins is that individual members are localized within specific cellular compartments from which some of them relocate upon Ca^{2+} or Zn^{2+} activation (Davey et al., 2001). A signalling event is thus transduced in a temporal and spatial manner by specific targeting for each S100

protein. Furthermore, some S100 proteins are secreted from cells acting in a cytokine-like manner. The individual members are believed to utilize distinct pathways (ER-Golgi route, tubulin- or actin-dependent) for their translocation/secretion into the extracellular space (Hsieh et al., 2002). S100B and S100A12 specifically bind to the surface receptor RAGE (receptor for advanced glycation endproduct) – a multiligand member of the immunoglobulin superfamily (Schmidt et al., 2000). The extracellular levels of S100B thereby play a crucial role in that nanomolar concentrations of S100B have trophic effects on cells whereas pathological levels (as found in Alzheimer's patients) induce apoptosis (Huttunen et al., 2000).

Characteristic of the S100 protein family is that most *S100* genes form a cluster on human chromosome 1q21, a region frequently involved in chromosomal rearrangements and deletions in human cancers (Schäfer et al., 1995; Weterman et al., 1996; Gendler et al., 1990).

S100 proteins were recently found to be reliable diagnostic markers for hypoxic brain damage and for monitoring the outcome after cardiac arrest (S100B; Böttiger et al., 2001), acute myocardial infarction (S100A1; Kiewitz et al., 2000), amyotrophic lateral sclerosis (S100A6; Hoyaux et al., 2000), for the classification of astrocytomas and glioblastomas (Camby et al., 2000; Camby et al., 1999), melanoma metastasis formation (S100B; Krähn et al., 2001), as prognostic indicators for gastric cancer (S100A4; Yonemura et al., 2000), laryngeal (S100A2; Lauriola et al., 2000) and esophageal squamous cell carcinomas (S100A4; Ninomiya et al., 2001), and for breast cancer (Platt-Higgins et al., 2001).

1.2.1 Genomic Organization and Chromosomal Localization of *S100* Genes

The structural organization of *S100* genes is highly conserved both within an organism and in different species (Heizmann et al., 2002). A typical *S100* gene consists of three exons whereby the first exon carries exclusively 5' untranslated sequences. The second exon contains the ATG translation start codon and codes for the N-terminal EF-hand, and the third exon encodes the carboxy-terminal canonical EF-hand. Presently, 16 *S100* genes are found in a tight gene cluster on human chromosome 1q21 within a genomic region of 260 kb (Fig. 1).

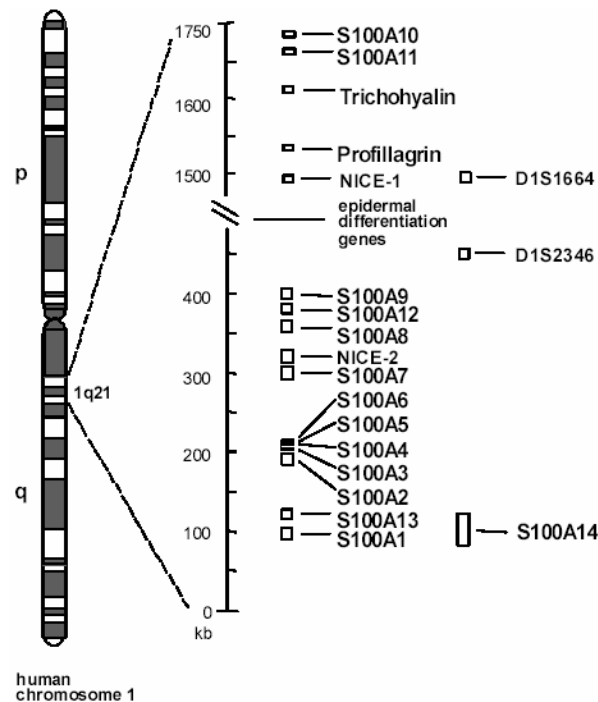


Fig. 1 The *S100* gene cluster on human chromosome 1q21. Genes located in the cluster region are indicated as well as two commonly used genomic markers (D1S1664 and D1S2346). p and q indicate the short and the long arm of the chromosome, respectively.

Four additional *S100* genes are found on other human chromosomes: Xp22 (calbindin-D9K), 21q22 (*S100B*), 4p16 (*S100P*) and 5 (*S100Z*). Within the gene cluster, epidermal differentiation genes as well as a gene of unknown function called *NICE2* interrupt the *S100* genes. Furthermore, there are three proteins encoded in 1q21 that carry in the N-terminus an S100-like domain, namely trichohyalin, profilaggrin, and C1 or f10. The small distances between the genes on the chromosome and the phylogenetic tree indicate that *S100* genes most likely originate from late gene duplication events. It is interesting that the clustered organization of the human genes seems to be evolutionarily conserved, at least in the mouse. In other species, *S100* genes are less well characterized.

1.2.2 Biological Functions

S100 proteins generally are involved in a large number of cellular activities such as signal transduction, cell differentiation, regulation of cell motility, transcription and cell cycle progression. Such activities can be expected since S100 proteins are thought to modulate the activity of target proteins in a Ca^{2+} - (and possibly also in a Zn^{2+} - and Cu^{2+} -) dependent manner, thereby transferring the signal from the

second messenger. Therefore, understanding the biological function of S100 proteins will crucially depend on the identification of their target proteins. During the last decade, a large number of such possible interactions have been described involving enzymes, cytoskeletal elements as well as transcription factors.

Apart from these intracellular functions, some S100 proteins like S100A8/S100A9, S100B, S100A4 and probably others can be secreted from cells, as noted above, and exhibit cytokine-like extracellular functions. These include chemotactic activities related to inflammation (S100A8/A9 and A12), neurotrophic activities (S100B), and angiogenic effects (S100A4 and S100A13). In all cases, the mechanisms of secretion as well as the nature of high affinity surface receptors remain largely unknown. One candidate receptor to mediate at least some of the described extracellular functions is the RAGE, which is activated upon binding of S100A12, S100A13, S100P, and S100B (Hofmann et al., 1999; Huttunen et al., 2000; Arumugam et al., 2004; Hsieh et al., 2004). It is currently not known whether RAGE is a universal S100 receptor.

Generation of animal models has been initiated to study the physiological significance of S100 proteins. Ectopic overexpression in the mouse has been described for *S100B* and *S100A4*. In the case of *S100B*, enhanced expression in the brain led to hyperactivity associated with an impairment of hippocampal function (Gerlai and Roder, 1995). In contrast to this mild phenotype, expression of *S100A4* in oncogene-bearing transgenic mice can induce metastasis of mammary tumours, suggesting that *S100A4* plays an important role in the acquisition of the metastatic phenotype (Ambartsumian et al., 1996; Davies et al., 1996).

Inactivation through homologous recombination in mouse embryonic stem cells has been demonstrated for *S100B*, *S100A8*, and *S100A1*. While inactivation of *S100B* has no obvious consequences for life (Xiong et al., 2000), *S100A8* null mice die via early resorption of the mouse embryo (Passey et al., 1999), a result that suggests a role for this protein in prevention of maternal rejection of the implanting embryo. *S100A1* null mice have significantly reduced responses to acute and chronic hemodynamic stress that are associated with reduced cardiac calcium sensitivity (Du et al., 2002).

Since S100 proteins can form homo- and heterodimers and usually more than one S100 protein is expressed in a given cell type, functional redundancy or

compensatory mechanisms might explain the lack of phenotype observed in some animal models.

1.2.3 Association with Human Diseases

Several S100 proteins are closely associated with human diseases (Table 1).

Table 1 S100 proteins: functions and association with human diseases

Protein	Postulated functions	Disease association
S100A1	Regulation of cell motility, muscle contraction, phosphorylation, Ca^{2+} -release channel, transcription	Cardiomyopathies
S100A2	Tumour suppression, nuclear functions, chemotaxis	Cancer, tumour suppression
S100A3	Hair shaft formation, tumour suppression, secretion, and extracellular functions	Hair damage, cancer
S100A4	Regulation of cell motility, secretion and extracellular functions, angiogenesis	Cancer (metastasis)
S100A5	Ca^{2+} , Zn^{2+} , and Cu^{2+} -binding protein in the CNS and other tissues; unknown function	Not known
S100A6	Regulation of insulin release, prolactin secretion, Ca^{2+} homeostasis, tumour progression	Amyotrophical lateral sclerosis
S100A7	S100A7-fatty acid binding protein complex regulates differentiation of keratinocytes	Psoriasis, cancer
S100A8/ S100A9	Chemotactic activities, adhesion of neutrophils, myeloid cell differentiation, apoptosis, fatty acid metabolism	Inflammation, wound healing, cystic fibrosis
S100A10	Inhibition of phospholipase A2, neurotransmitter release, in connection with annexin II regulates membrane traffic, ion currents	Inflammation
S100A11	Organization of early endosomes, inhibition of annexin I function, regulation of phosphorylation, physiological role in keratinocyte cornified envelope	Skin diseases, ocular melanoma
S100A12	Host-parasite interaction, differentiation of squamous epithelial cells and extracellular functions	Mooren's ulcer (autoimmune disease), inflammation
S100A13	Regulation of FGF-1 and synaptotagmin-1 stress-induced release; involved in the formation of Cu^{2+} -dependent IL-1 α :S100A13 heterotetramer that facilitates the export of both proteins	Angiogenesis, vascular response to injury
S100A15	unknown	Psoriasis
S100A16	unknown	Malignant transformation
S100B	Cell motility, proliferation, inhibition of microtubule assembly, transcription, regulation of nuclear kinase, extracellular functions, e.g. neurite extension	Alzheimer's disease, Down syndrome, melanoma, amyotrophic lateral sclerosis, epilepsy
S100P	Function in the placenta	Malignant transformation
S100Z	Function in spleen and leukocytes	Aberrant in some tumours
Calbindin D9K	Ca^{2+} buffer and Ca^{2+} transport	Vitamin D deficiency, abnormal mineralization

A few S100 proteins have been proposed to play important roles in tumour progression and suppression and are recognized as potential tumour markers.

The association of S100 proteins with cancer development originates in the finding that the evolutionary conserved gene cluster on human chromosome 1q21 is implicated in gene rearrangements during tumour development. As discussed below, up-regulation in tumours has been reported for *S100A1*, *S100A4*, *S100A6*, *S100A7*, *S100A8*, *S100A9*, *S100A10*, *S100A16*, *S100B*, and *S100P*, whereas *S100A2* and *S100A11* have been postulated to be tumour suppressor genes.

S100A1 and *S100B* are overexpressed in human cancers and have been suggested to play a role in the hyperactivation of Ndr kinase in melanomas (Millward et al., 1998). Inhibition of p53 activity by *S100B* could be one mechanism, whereby overexpressed *S100B* is involved in neoplastic transformation. Blood levels of *S100B* are used to monitor malignant melanomas (Krähn et al., 2001).

S100A4 has been implicated in invasion and metastasis. The prognostic significance of its selective expression in various cancers has been exploited. In gastric cancer the opposite expression of *S100A4* in relation to a tumour suppressor E-cadherin was found to be a powerful aid in histological typing and in evaluating the metastatic potential/prognosis of patients with this type of cancer (Yonemura et al., 2000). It was also demonstrated that extracellular *S100A4* could act as an angiogenic factor and might induce tumour progression via an extracellular route stimulating angiogenesis (Kriaievska et al., 2002).

S100A5 has been postulated to be a marker of recurrence in WHO grade I meningiomas (Hancq et al., 2004).

S100A6 has been found overexpressed in human pancreatic adenocarcinomas (Logsdon et al., 2003) as well as in intrahepatic tumours, where it was activated by TNF- α and NF κ B (Joo et al., 2003).

S100A7 (psoriasin) expression has been associated with psoriasiform hyperplasia, tumour progression in breast cancer and a worse prognosis in estrogen receptor-negative invasive ductal breast carcinomas (Emberley et al., 2003) as well as with gastric tumours (El-Rifai et al., 2002). In addition, *S100A7* is a potential tumour marker for non-invasive follow-up of patients with urinary bladder squamous cell carcinoma (Ostergaard et al., 1999).

The two calgranulins – *S100A8* and *S100A9* – are differentially expressed at sites of acute and chronic inflammation. Recent reports, however, indicate that

they are also overexpressed during skin carcinogenesis (Gebhardt et al., 2002), in poorly differentiated lung adenocarcinomas (Arai et al., 2001), gastric tumours (El-Rifai et al., 2002), and at the invasive margin of colorectal carcinomas (Stulik et al., 1999).

S100P expression has been noted in various cancer cell lines. It is associated with cellular immortalization in breast cancer cell lines (Guerreiro et al., 2000). In colon cancer cell lines, its expression is elevated in doxorubicin-resistant cells (Bertram et al., 1998). S100P is expressed in prostate cancer, where its expression is androgen-sensitive (Averboukh et al., 1996) and in pancreatic adenocarcinoma, where its expression has been localized to the neoplastic epithelium of pancreas (Logsdon et al., 2003). Furthermore, it was found that S100P expression correlates with decreased survival in patients with lung cancer (Beer et al., 2002).

S100A10 is an annexin 2 protein ligand and a key plasminogen receptor of the extracellular cell surface that is overexpressed in esophageal squamous cell carcinomas (Zhi et al., 2003), renal cell carcinomas (Teratani et al., 2002), and gastric tumours (Rifai et al., 2002). It was shown that S100A10 stimulates the conversion of plasminogen to plasmin on the tumour cell surface thereby contributing to the increased invasiveness of tumour cells (Zhang et al., 2004).

The recently identified *S100A16* is up-regulated at the transcriptional level in tumours of the bladder, lung, thyroid gland, pancreas, and ovary (Marenholz and Heizmann, 2004).

By contrast, S100A2 is markedly down-regulated in breast tumour biopsies and can be re-expressed in mammary carcinoma cells by 5-azadeoxycytidine treatment (Wicki et al., 1997). A prognostic significance of S100A2 in laryngeal squamous-cell carcinoma has also been found allowing discrimination of high and low risk patients in the lymph-node negative subgroup to provide better therapy (Lauriola et al., 2000). Using DNA array technology, *S100A2* was identified as differentially expressed in normal versus tumorigenic human bronchial epithelial cells (Feng et al., 2001).

A role for S100A11 as a tumour suppressor protein was postulated. This was based on its down-regulation in immortalized versus normal cells (Sakaguchi et

al., 2000) and the observation that microinjection of an anti-S100A11 antibody into normal confluent quiescent cells induced DNA synthesis (Sakaguchi et al., 2003).

1.3 Aim of This Work

The primary aim of the study was to identify novel tumour-associated genes with potential application in the detection or treatment of cancer. The starting point was a collection of partial cDNA clones of yet unknown genes from a suppression subtractive hybridization (SSH) cDNA library preferentially representing genes that were down-regulated in the small cell lung carcinoma cell line as compared to normal human bronchial epithelial cells.

An unknown human transcript was selected for further characterization in view of its differential expression in tumour cell lines and in primary tumours, as well as its homology to a protein family known to be associated with tumorigenesis.

I aimed to elucidate the rationale for the differential expression of the gene in tumours as well as to evaluate its potential clinical relevance. A further intention was to shed light on the mechanism of regulation of the gene in order to determine its association with malignant transformation.

2 Materials and Methods

2.1 Materials

2.1.1 Chemicals

All chemicals used in this work were purchased from Roche Diagnostics GmbH, Mannheim, Germany; Calbiochem, CA, USA; Sigma-Aldrich Chemie GmbH, Munich, Germany; Sigma, MS, USA; Biozym Diagnostik GmbH, Oldendorf, Germany; Merck, Darmstadt, Germany; Serva Electrophoresis GmbH, Heidelberg, Germany; R&D Systems Inc., MN, USA.

Milli-Q 18.2 MΩ · cm water was used in all procedures if required.

2.1.2 Kits

5'-RACE Kit	BD Biosciences, CA, USA
BEGM Bullet Kit	Clonetics, San Diego, CA, USA
ChemMate Detection Kit	DAKO, Glostrup, Denmark
Developer RP X-OMAT EX	Eastman Kodak Company, NY, USA
Dual-Luciferase Reporter Assay System	Promega, WI, USA
ECL Western Blotting Detection Kit	Amersham Pharmacia Biotech, Freiburg, Germany
Endofree Plasmid Maxiprep Kit	Qiagen GmbH, Hilden, Germany
ExpressHyb solution	BD Biosciences, CA, USA
FastTrack 2.0 Kit for Isolation of mRNA	Invitrogen, CA, USA
Fixer RP X-OMAT LO	Eastman Kodak Company, NY, USA
Megaprime DNA Labelling System	Amersham Pharmacia Biotech, Buckinghamshire, UK
Opti-MEM I Reduced Serum Medium	Invitrogen, CA, USA
Plasmid Mini and Maxi Kit	Qiagen GmbH, Hilden, Germany
Protease Inhibitors Cocktail	Roche Diagnostics GmbH, Mannheim, Germany
QIAquick PCR Purification Kit	Qiagen GmbH, Hilden, Germany
QIAquick Nucleotide Removal Kit	Qiagen GmbH, Hilden, Germany
Qiaquick Gel Extraction Kit	Qiagen GmbH, Hilden, Germany
Rapid Ligation Kit	Roche Diagnostics GmbH, Mannheim, Germany
SequaGel XR	National Diagnostics, GE, USA
Thermoscript RT-PCR System	Invitrogen, CA, USA
Thermo-Sequenase Fluorescent-Labeling Cycle-Sequencing Kit	Amersham Pharmacia Biotech, Buckinghamshire, UK
TRIzol	Invitrogen, CA, USA

2.1.3 Materials

Hybond-N membrane	Amersham Pharmacia Biotech, Buckinghamshire, UK
Hybond-N+ membrane	Amersham Pharmacia Biotech, Buckinghamshire, UK
Hybond-P PVDF membrane	Amersham Pharmacia Biotech, Buckinghamshire, UK
Kodak X-ray Film	NEN Life Science Products, MA, USA
Hybond Hyperfilm	Amersham Pharmacia Biotech, Buckinghamshire, UK
Human Multiple Tissue Northern (MTN) Blot	BD Biosciences, CA, USA
Cancer Profiling Array	BD Biosciences, CA, USA
Metaphases of normal human lymphocytes	Vysis, IL, USA

2.1.4 Enzymes

Ampli Taq DNA Polymerase	Perkin Elmer, MA, USA
Calf Intestinal Alkaline Phosphatase (CIAP)	Promega, Mannheim, Germany
Restriction Endonucleases: <i>Bam</i> HI, <i>Xba</i> I, <i>Kpn</i> I, <i>Sac</i> I, <i>Pst</i> I, <i>Xho</i> I, <i>Sal</i> I, <i>Not</i> I, <i>Eco</i> RI	Promega, Mannheim, Germany

2.1.5 Antibodies

Anti- β -actin	Sigma-Aldrich, Inc., MS, USA
Anti-AKT	Cell Signalling Technology, Inc., MA, USA
Anti-ER	Novocastra, Newcastle, UK
Anti-ERBB2	DAKO, Glostrup, Denmark
Anti-c-JUN	Cell Signalling Technology, Inc., MA, USA
Anti-Ki-67	Dianova, Hamburg, Germany
Anti-p38	Cell Signalling Technology, Inc., MA, USA
Anti-Phospho-AKT (Ser473)	Cell Signalling Technology, Inc., MA, USA
Anti-Phospho-HSP27 (Ser82)	Cell Signalling Technology, Inc., MA, USA
Anti-Phospho-c-JUN (Ser63)	Cell Signalling Technology, Inc., MA, USA
Anti-Phospho-p38 (Thr180/Tyr182)	Cell Signalling Technology, Inc., MA, USA
Anti-Phospho-p44/42 MAPK (Thr202/Tyr204)	Cell Signalling Technology, Inc., MA, USA
Anti-Phospho-SAPK/JNK (Thr183/Tyr185)	Cell Signalling Technology, Inc., MA, USA
Anti-PR	DAKO, Glostrup, Denmark
Anti-S100A14 affinity-purified	A. Pietas, Charité, Berlin, Germany
Anti-SAPK/JNK	Cell Signalling Technology, Inc., MA, USA
Anti-pan-Ras	BD Biosciences, CA, USA
Anti- α -tubulin	Monosan, Sanbio b.v., Netherlands
Anti-V5	Invitrogen, CA, USA

FITC(DTAF)-Conjugated Goat Anti-Mouse IgG (H + L)	Jackson ImmunoResearch Laboratories, Baltimore, MD, USA
FITC(DTAF)-Conjugated Goat Anti-Rabbit IgG (H + L)	Jackson ImmunoResearch Laboratories, Baltimore, MD, USA
Horseradish Peroxidase-Conjugated Rabbit Anti-Mouse	DAKO, Glostrup, Denmark
Horseradish Peroxidase-Conjugated Goat Anti-Rabbit	Amersham Pharmacia Biotech, Buckinghamshire, UK

2.1.6 Mammalian Cell Lines

HBE	Normal human bronchial epithelial cells; Clonetics, San Diego, CA, USA
SAE	Normal human small-airway epithelial cells; Clonetics, San Diego, CA, USA
H378	SCLC; ATCC, Rockville, MD, USA
H82	SCLC; ATCC, Rockville, MD, USA
COLO 677	SCLC; German Collection of Microorganisms and Cell Cultures, Braunschweig, Germany
H446	SCLC; ATCC, Rockville, MD, USA
CPC-N	SCLC; German Collection of Microorganisms and Cell Cultures, Braunschweig, Germany
DMS-79	SCLC; ATCC, Rockville, MD, USA
H209	SCLC; ATCC, Rockville, MD, USA
DMS-114	SCLC; ATCC, Rockville, MD, USA
H187	SCLC; ATCC, Rockville, MD, USA
N417	SCLC; ATCC, Rockville, MD, USA
H526	SCLC metastatic; ATCC, Rockville, MD, USA
COLO 668	Brain metastasis of SCLC; German Collection of Microorganisms and Cell Cultures, Braunschweig, Germany
SHP77	Large cell variant of SCLC; ATCC, Rockville, MD; German Collection of Microorganisms and Cell Cultures, Braunschweig, Germany
COLO 699	ADC; German Collection of Microorganisms and Cell Cultures, Braunschweig, Germany
DV-90	ADC; German Collection of Microorganisms and Cell Cultures, Braunschweig, Germany
H322	ADC; ATCC, Rockville, MD, USA
D51	ADC; I. Petersen, Charité, Berlin, Germany
D54	ADC; I. Petersen, Charité, Berlin, Germany
D117	ADC; I. Petersen, Charité, Berlin, Germany
H125	ADC; ATCC, Rockville, MD, USA
H23	ADC; ATCC, Rockville, MD, USA
A549	ADC; German Collection of Microorganisms and Cell Cultures, Braunschweig, Germany
H2228	ADC; ATCC, Rockville, MD, USA
H2030	ADC; ATCC, Rockville, MD, USA

H157	SCC; ATCC, Rockville, MD, USA
H2170	SCC; ATCC, Rockville, MD, USA
H226	SCC mesothelioma; ATCC, Rockville, MD, USA
A427	Lung Ca; German Collection of Microorganisms and Cell Cultures, Braunschweig, Germany
BEN	Lung Ca, lymph node metastasis; German Collection of Microorganisms and Cell Cultures, Braunschweig, Germany
D97	LCLC; I. Petersen, Charité, Berlin, Germany
HBE4-E6/E7	HBE immortalized with E6 and E7 genes of HPV-16; ATCC, Rockville, MD, USA
9442 (BET-1A)	HBE immortalized with SV40 early region; ATCC, Rockville, MD, USA
BEAS-2B	HBE immortalized with SV40 early region; ATCC, Rockville, MD, USA
YP44	HBE immortalized with SV40 early region; kindly provided by Dr. Cheng, Cancer Institute, Beijing, China
HMEC	Normal human mammary epithelial cells; Clonetics, San Diego, CA, USA
HMEB	HMEC immortalized with telomerase and SV40 early region; kindly provided by Dr. B. Weinberg, Whitehead Institute for Biomedical Research, Massachusetts Institute of Technology, USA
MCF-10A	Spontaneously immortalized mammary epithelial cells; kindly provided by Dr. A. Gontarewicz, Charité, Berlin, Germany
MCF-7	Breast Ca; kindly provided by Dr. A. Gontarewicz, Charité, Berlin, Germany
SK-BR-3	Breast Ca; kindly provided by Dr. A. Gontarewicz, Charité, Berlin, Germany
MDA-MD-231	Breast Ca; kindly provided by Dr. A. Gontarewicz, Charité, Berlin, Germany
HT-29	Colon Ca; kindly provided by Dr. K. Jürchott, Charité, Berlin, Germany
SW-480	Colon Ca; kindly provided by Dr. K. Jürchott, Charité, Berlin, Germany
HCT-116	Colon Ca; kindly provided by Dr. K. Jürchott, Charité, Berlin, Germany
CaCo-2	Colon Ca; kindly provided by Dr. K. Kölbl, Charité, Berlin, Germany
WiDr	Colon Ca; kindly provided by Dr. K. Kölbl, Charité, Berlin, Germany
Lovo	Colon Ca; kindly provided by Dr. A. Siegert, Charité, Berlin, Germany
CX-2	Colon Ca; kindly provided by Dr. A. Siegert, Charité, Berlin, Germany
HRT-18	Colon Ca; kindly provided by Dr. A. Siegert, Charité, Berlin, Germany
HEP-2	Head and neck Ca; kindly provided by J. Möller, Charité, Berlin, Germany
D36-1/95	Head and neck Ca; I. Petersen, Charité, Berlin, Germany
D36-2/95	Head and neck Ca; I. Petersen, Charité, Berlin, Germany
D6/95	Head and neck Ca; I. Petersen, Charité, Berlin, Germany
D3/02	Head and neck Ca; I. Petersen, Charité, Berlin, Germany
D40/97	Head and neck Ca; I. Petersen, Charité, Berlin, Germany
IMR-90	Fetal lung fibroblasts; kindly provided by Dr. A. Gontarewicz, Charité, Berlin, Germany
HAKAT	Immortalized keratinocytes; kindly provided by Dr. N. Fusenig, DKFZ, Heidelberg, Germany
HEK 293	Human embryonic kidney epithelial cells; kindly provided by Dr. A. Gontarewicz, Charité, Berlin, Germany

COS-7	African green monkey kidney fibroblasts; kindly provided by Dr. I. Nazarenko, Charité, Berlin, Germany
RAW 264.7	Mouse macrophagoid immortalized cells; ATCC, Rockville, MD, USA
L-cells	Mouse fibroblasts; ATCC, Rockville, MD, USA
L-Wnt 3 cells	Mouse fibroblasts transfected with Wnt-3A; ATCC, Rockville, MD, USA
C57MG	Mouse mammary epithelial cells, kindly provided by Dr. R. Nusse, Stanford University School of Medicine, USA

2.1.7 *E. coli* Strain

One Shot TOP10F'	F' <i>{lacI^qTn 10(Tet^R)}</i> <i>mcrAD(mrr-hsdRMS-mcrBC)</i> Φ80/ <i>lacZΔM15 deoR recA1 endA1</i>	Invitrogen, CA, USA
------------------	--	---------------------

2.1.8 RNA Samples from Mammalian Cell Lines

H596	Lung Ca; Cancer Profiling Array, BD Biosciences, CA, USA
DU 145	Prostate Ca; kindly provided by Dr. A. Gontarewicz, Charité, Berlin, Germany
PC-3	Prostate Ca; kindly provided by Dr. A. Gontarewicz, Charité, Berlin, Germany
Kato III	Metastasis of gastric Ca; kindly provided by Dr. A. Gontarewicz, Charité, Berlin, Germany
EJ	Bladder Ca; kindly provided by Dr. A. Gontarewicz, Charité, Berlin, Germany
HeLa	Cervical Ca; kindly provided by Dr. A. Gontarewicz, Charité, Berlin, Germany
Daudi	Burkitt's lymphoma; Cancer Profiling Array, BD Biosciences, CA, USA
K562	Chronic myelogenous leukemia; Cancer Profiling Array, BD Biosciences, CA, USA
HL-60	Promyelocytic leukemia; Cancer Profiling Array, BD Biosciences, CA, USA
MOLT-4	Lymphoblastic leukemia; Cancer Profiling Array, BD Biosciences, CA, USA
Raji	Burkitt's lymphoma; Cancer Profiling Array, BD Biosciences, CA, USA
G361	Melanoma; Cancer Profiling Array, BD Biosciences, CA, USA
SKOV-3	Ovarian Ca; kindly provided by Dr. A. Gontarewicz, Charité, Berlin, Germany
OVCAR-3	Ovarian Ca; kindly provided by Dr. A. Gontarewicz, Charité, Berlin, Germany
HT 1080	Fibrosarcoma; kindly provided by Dr. A. Gontarewicz, Charité, Berlin, Germany
ROSE 199	Rat ovarian surface epithelial cells; kindly provided by Dr. A. Gontarewicz, Charité, Berlin, Germany
ROSE A2/1	Rat ovarian surface epithelial cells transfected with <i>KRas</i> ; kindly provided by Dr. A. Gontarewicz, Charité, Berlin, Germany
ROSE A2/5	Rat ovarian surface epithelial cells transfected with <i>KRas</i> ; kindly provided by Dr. A. Gontarewicz, Charité, Berlin, Germany
208F	Immortalized rat fibroblasts; kindly provided by Dr. A. Gontarewicz, Charité, Berlin, Germany
FE-8	<i>HRAS</i> -transformed derivative of 208F; kindly provided by Dr. A. Gontarewicz, Charité, Berlin, Germany
IR-4	208F cells transfected with IPTG-inducible <i>Ras</i> ; kindly provided by Dr. A. Gontarewicz, Charité, Berlin, Germany

2.1.9 Tissue Specimens

Tumour specimens used in this study include xenografts of the following lung cancer cell lines transplanted subcutaneously into immunodeficient mice: CPC-N, H526, H446, H82, H209, N417 (SCLC); Colo 668 (brain metastasis of SCLC); D54 (adenocarcinoma), and D97 (LCLC). They were obtained from experiments conducted by Prof. Dr. I. Petersen on tumorigenicity of various human cultured lung cancer cell lines in nude mice (unpublished results). These specimens were shock frozen in liquid nitrogen and stored at -80°C until RNA extraction.

Normal human colon tissue and tumour tissue specimens used in the immunohistochemical analysis were obtained from surgical resections at the Department of Surgery of the Charité Hospital at the Humboldt University Berlin. Operation specimens were transferred to the Institute of Pathology within 1 hour after surgical removal. Generally, no adjuvant radiotherapy or chemotherapy was applied before surgery. These specimens were shock frozen in liquid nitrogen and stored at -80°C until RNA extraction.

2.1.10 Plasmids and Expression Constructs

S100A14-V5	The expression construct was generated by PCR-amplification of the ORF of the S100A14 cDNA using H1043for-tr and H1043rev-tr primers. The amplified fragment of 316-bp was ligated into the <i>Bam</i> HI and <i>Xba</i> I sites of the pcDNA3.1/V5 vector.
pcDNA3.1/V5	Invitrogen, CA, USA
D1-4 human <i>S100A14</i> genomic construct	The human <i>S100A14</i> genomic construct was generated by cloning of the 3173-bp positive fragment (hybridizing with S100A14 coding region, intron 2, and 3 in Southern blot analysis) produced by <i>Bam</i> HI digestion of the PAC clone D11609 into pBluescript II KS(+) phagemid vector.
pBluescript II KS(+) phagemid vector	Stratagene, La Jolla, Canada
H1043	The DKFZp404H1043 clone containing the human full-length S100A14 cloned in pSPORT1 vector, was provided by RZPD, Heidelberg, Germany.
H1043(-)0.5/10	The human full-length <i>S100A14</i> expression construct was generated by subcloning from the H1043 clone by restriction digestion with <i>Not</i> I and <i>Xba</i> I.
pGL3-Basic	The firefly luciferase reporter vector lacking eukaryotic promoter and enhancer elements upstream of the firefly luciferase gene.

pRL-TK	The <i>Renilla</i> luciferase reporter vector containing the herpes simplex virus thymidine kinase promoter region upstream of <i>Renilla</i> luciferase gene.
p500-luc	The p500-luc luciferase reporter vector was generated by restriction digestion with <i>KpnI</i> (multiple cloning site) and <i>SacI</i> (endogenous restriction site; position 496 bp in D1-4) of the <i>S100A14</i> genomic construct D1-4. The fragment of 495-bp was ligated into the compatible restriction sites of the pGL3-Basic firefly luciferase reporter vector.
p300-luc	The p300-luc luciferase reporter vector was generated by restriction digestion with <i>PstI</i> (endogenous restriction site; position 192 bp in D1-4) of the p500-luc fragment. The resulting <i>PstI</i> - <i>SacI</i> (-313 bp to -12 bp) restriction fragment was amplified by PCR using the oligonucleotides Prom2b-for and Prom2b-rev. The amplified fragment of 300-bp was ligated into <i>KpnI</i> and <i>SacI</i> sites of the pGL3-Basic firefly luciferase reporter vector.
p250-luc	The p250-luc luciferase reporter vector was generated by restriction digestion with <i>PstI</i> (endogenous restriction site; position 192 bp in D1-4) of the p500-luc fragment. The resulting <i>PstI</i> (the multiple cloning site)- <i>PstI</i> (-573 bp to -313 bp) restriction fragment was amplified by PCR using the oligonucleotides Prom1b-for and Prom1b-rev. The amplified fragment of 192-bp was ligated into <i>KpnI</i> and <i>SacI</i> sites of the pGL3-Basic firefly luciferase reporter vector.
p2A-luc	The p2A-luc deletion construct was created by PCR-amplification of the fragment (-313 bp to -269 bp) of the p300-luc, using prom2A-for and prom2A-rev primers. The amplified fragment of 51-bp was ligated into the <i>KpnI</i> and <i>SacI</i> sites of the pGL3-Basic firefly luciferase reporter vector.
p2B-luc	The p2B-luc deletion construct was created by PCR-amplification of the fragment (-313 bp to -206 bp) of the p300-luc, using prom2A-for and prom2B-rev primers. The amplified fragment of 107-bp was ligated into the <i>KpnI</i> and <i>SacI</i> sites of the pGL3-Basic firefly luciferase reporter vector.
p2C-luc	The p2C-luc deletion construct was created by PCR-amplification of the fragment of the p300-luc (-208 bp to -12 bp) using prom2C-for and prom2C-rev primers. The amplified fragment of 196-bp was ligated into the <i>KpnI</i> and <i>SacI</i> sites of the pGL3-Basic firefly luciferase reporter vector.
EGFP (enhanced green fluorescent protein)	BD Biosciences, San Diego, TX, USA
p65/Flag	The p65 expression vector containing p65 full-length cDNA fused with Flag epitope, was a generous gift from Dr. C. Scheidereit, MDC, Berlin, Germany.
pcDNA3/Flag	The empty vector pcDNA3/Flag was a generous gift from Dr. C. Scheidereit (MDC, Berlin, Germany).
pCR2.1 TA Cloning Vector	Invitrogen, Groningen, Netherlands
m-S100A14	The IMAGp998M1311375Q3 clone containing the mouse full-length S100A14 cDNA cloned in pCMV-SPORT6 phagemid vector, was provided by RZPD (Berlin, Germany).

2.1.11 Oligonucleotides

IRD-labelled oligonucleotides were purchased from MWG-Biotech, Ebersberg, Germany. Non-labelled oligonucleotides were purchased from BioTeZ GmbH, Berlin-Buch, Germany.

Oligonucl.	Labelling	Sequence
Prom1b-for		5'– TTA GGG GTA CCC CCC AGG CAG GCT TGA GTG – 3'
Prom1b-rev		5'– TTA TAT CGA GCT CGT GCA GGG CAG GGA AGG – 3'
Prom2b-for		5'– TAG GGG TAC CCC TGC AGT TCG CCA GGG C – 3'
Prom2b-rev		5'– GCG ACC ACG AGC TCA GCT CTT ATA CCT G – 3'
18S-for		5'– GGG GAG GTA GTG ACG AA – 3'
18S-rev		5'– ACA AAG GGC AGG GAC TT – 3'
Prom2A-for		5'– TTA GGG GTA CCC CTG CAG TTC GCC AGG GCC – 3'
Prom2A-rev		5'– TTA TAT CGA GCT CGA CTT CGA GAC CTC ATG GG – 3'
Prom2B-rev		5'– TTA TAT CGA GCT CGG ATC AGC ATG CAG AGT CAC – 3'
Prom2C-for		5'– TTA GGG GTA CCC CTG CTG ATC GGA GGC CAG – 3'
Prom2C-rev		5'– TTA TAT CGA GCT CGA GCT CTT ATA CCT GGG GG – 3'
GAPDH-for		5'– GAA CGG GAA GCT TGT CAT CA – 3'
GAPDH-rev		5'– GTA GCC AAA TTC GTT GTC ATA C – 3'
mA14-for		5'– ATG GGA CAG TGT CGG TCA – 3'
mA14-rev		5'– TCA GCT CCG AGT AAC AGG – 3'
pGL3basic-f	IRD800	5'– CTA GCA AAA TAG GCT GTC CC – 3'
pGL3basic-r	IRD800	5'– CTT TAT GTT TTT GGC GTC TTC CA – 3'
exon1 for		5'– CTC AGC GGC TGC CAA CAG – 3'
exon2 for		5'– CAG TGT CGG TCA GCC AAC – 3'
exon3 for		5'– GAA CTT TCA CCA GTA CTC CG – 3'
D1-4prom-for		5'– CAT GAG GTC TCG AAG TCC – 3'
D1-4prom-rev		5'– CAG CTC ACC TGA GCT CAG – 3'
H1043for-2		5'– TCA TGC CGA GCA ACT GTG G – 3'
H1043rev-2		5'– GCC TCT CCA GCT TCA CAC T – 3'
H1043for-3		5'– GCT GCC AAC AGA TCA TGA – 3'
H1043rev-3		5'– TTG GCT GAC CGA CAC TGT – 3'
H1043 f		5'– CAA CAG AAC TCT CAC CAA AG – 3'
H1043 r		5'– TCC AGA GGG AGT TCT CAG T – 3'
H1043 i1 for		5'– GGC TGC CAA GTA AGG AAA C – 3'
H1043 i1 rev		5'– TCA TGA TCT GCT TAG AGG AG – 3'
H1043 i2 for		5'– AAC GCA GAG GTG GGC TCA T – 3'
H1043 i2 rev		5'– CTG AGC ATC CTG AGG GCA G – 3'
H1043 i3 for		5'– TCT CAT GCC GGT ATG GAC – 3'
H1043 i3 rev		5'– CCA CAG TTG CTC TGA GGG – 3'

H1043for-tr		5'– CGG GAT CCC GCA CCA TGG GAC AGT GTC GG – 3'
H1043rev-tr		5'– GCT CTA GAG CGT GCC CCC GGA CAG GCC T – 3'
GPS1		5'– AGG CCT CTC CAG CTT CAC ACT CTT G – 3'
NGPS1		5'– CAA CAG AAC TCT CAC CAA AG – 3'
NGPS2		5'– GCC TCT CCA GCT TCA CAC T – 3'
D1-4 T7-1	IRD800	5'– AGG CTG CTG CAA TAG CAG – 3'
D1-4 T7-2	IRD800	5'– TCT AAG CAG ATC ATG AGC – 3'
D1-4 T7-3	IRD800	5'– CAT CTC ATG CCG GTA TGG – 3'
H1043 M13	IRD800	5'– TGA GGT CAG ATC TCA GAA C – 3'
H1043 T7	IRD800	5'– CCT ACT TAT AAA CTC CCT A – 3'
pcDNA3.1R	IRD800	5'– CCT CGA CTG TGC CTT CTA – 3'
pcDNA3.1R-2	IRD800	5'– TAG AAG GCA CAG TCG AGG – 3'
M13	IRD800	5'– GTA AAA CGA CGG CCA G – 3'
M13R	IRD800	5'– CAG GAA ACA GCT ATG AC – 3'
T7	IRD800	5'– TAA TAC GAC TCA CTA TAG GG – 3'

2.2 Methods

2.2.1 Bacterial Culture

2.2.1.1 Routine Culturing and Storage Conditions

E.coli cultures were routinely grown at 37°C on Luria Bertani (LB) agar or in the LB broth, containing Ampicillin (50 µg/ml) or Kanamycin (25 µg/ml).

For long-term storage, a fresh overnight culture was prepared as follows: bacteria were streaked onto an agar plate containing the selective antibiotic, and incubated at 37°C overnight. Individual bacterial colonies were picked into Greiner tubes (Greiner Bio-One, Germany) containing 3 ml LB broth, and incubated for 14-16 hours at 37°C with shaking at 160 rpm. Then 800 µl of 2 x bacteria storage medium and 800 µl of bacterial culture were added into the storage tube. The vials were immediately transferred to -70°C and stored until use. To recover a bacteria culture, a small amount of the frozen stock was inoculated into 3 ml LB broth, containing the appropriate antibiotic, and incubated overnight at 37°C with shaking at 160 rpm.

2 x Bacteria storage medium

8.25 g $K_2HPO_4 \cdot 3H_2O$

1.80 g KH_2PO_4

0.45 g Na-citrate $\cdot 2H_2O$

0.09 g $MgSO_4 \cdot 7H_2O$

5.90 g $(NH_4)_2SO_4$

35.75 ml 87% Glycerol

sterile H_2O was added to a final volume of 500 ml and the medium was filter-sterilised under sterile conditions.

1 x LB broth

1% Bacto tryptone

0.5 % Bacto yeast extract

1% NaCl

1 x LB agar

LB broth with 1.5% Bacto agar

To prepare agar plates, the LB agar was cooled to $\sim 50^\circ C$, appropriate antibiotics were added and 15 ml of LB agar per 100-mm plate were poured. For β -galactosidase assay, LB agar plates were prepared with 80 $\mu g/ml$ X-gal (5-bromo-4-chloro-3-indol- β -D-galactopyraniside) and 20 mM IPTG (isopropyl- β -thio- β -D-galactopyraniside). IPTG was prepared in sterile water, and X-gal in dimethylformamide (DMF).

2.2.1.2 Transformation

Chemically competent TOP10F' *E.coli* were thawed on ice and mixed gently. The cells were transformed with an aliquot of 2 μl of the ligation reaction and incubated for 30 min on ice. Next, the cells were incubated for 30 sec in the $42^\circ C$ water bath and placed on ice. 250 μl of pre-warmed SOC medium (Invitrogen) were added, the vials were placed horizontally and shaken at 220 rpm and $37^\circ C$ for 1 hour in a rotary shaker incubator. Finally, 50 and 200 μl of each transformed culture were spread on separate LB agar plates containing 50 $\mu g/ml$ ampicillin and incubated overnight at $37^\circ C$.

Individual transformants were selected for plasmid miniprep DNA isolation by Plasmid Mini Kit and analysed by restriction endonuclease digestion and sequencing. The plates were sealed with parafilm and stored at 4°C for up to four weeks.

2.2.2 Culturing of Mammalian Cells

2.2.2.1 Routine Culturing

Mammalian cell lines were maintained at 37°C and 95% humidity in the presence of 5% CO₂. Cells were typically grown in T-75 flasks and 100-mm dishes (BD Biosciences).

The cell lines used in this study were cultivated in the following media:

Cell line	Medium
HBE	BEGM
SAE	SAGM
HBE-E6/E7	BEGM
9442 (BET-1A)	BEGM
BEAS-2B	BEGM
YP44	BEGM
H378	RPMI + 10% FCS
H82	RPMI + 10% FCS
COLO 677	RPMI + 10% FCS
H446	RPMI + 10% FCS
CPC-N	McCoys + 10% FCS
DMS-79	RPMI + 10% FCS
H209	RPMI + 10% FCS
DMS-114	Waymouth's + 10% FCS
H187	RPMI + 10% FCS
N417	RPMI + 10% FCS
H526	RPMI + 10% FCS
COLO 668	RPMI + 10% FCS
SHP77	RPMI + 10% FCS
COLO 699	RPMI + 10% FCS
DV-90	RPMI + 10% FCS
H322	RPMI + 10% FCS
D51	Leibovitz 15 medium (L-15) + 10% FCS + 1% glutamine
D54	L-15 + 10% FCS + 1% glutamine
D117	L-15 + 10% FCS + 1% glutamine
H125	RPMI + 10% FCS

H23	RPMI + 10% FCS
A549	F12/Ham + 10% FCS
H2228	RPMI + 10% FCS
H2030	RPMI + 10% FCS
H157	RPMI + 10% FCS
H2170	RPMI + 10% FCS
H226	RPMI + 10% FCS
A427	RPMI + 10% FCS
BEN	Dulbecco modified Eagle's medium (DMEM) + 10% FCS + 2 mM glutamine + 4.5 g/l glucose
D97	L-15 + 10% FCS + 1% glutamine
HMEC	MEBM
HMEB	MEBM + G418 (0.4 mg/ml) + hygromycin (0.1 mg/ml) + puromycin (1 ng/ml)
MCF 10A	DMEM:F12 HAM + 5% horse serum + 10 µg/ml insulin + 5 µg/ml hydrocortisone + 20 ng/ml EGF + 100 ng/ml cholera toxin
MCF-7	DMEM + 10% FCS + 2 mM glutamine
SK-BR 3	DMEM + 10% FCS + 2 mM glutamine
MDA MD 231	DMEM + 10% FCS + 2 mM glutamine
HT-29	L-15 + 10% FCS + 1% glutamine
SW-480	L-15 + 10% FCS + 1% glutamine
HCT-116	L-15 + 10% FCS + 1% glutamine
CaCo-2	RPMI + 10% FCS
WiDr	RPMI + 10% FCS
Lovo	DMEM + 10% FCS + 2 mM glutamine + 4.5 g/l glucose
CX-2	RPMI + 10% FCS
HRT-18	RPMI + 10% FCS
HEP-2	RPMI + 10% FCS
D36-1/95	L-15 + 10% FCS + 1% glutamine
D36-2/95	L-15 + 10% FCS + 1% glutamine
D6/95	L-15 + 10% FCS + 1% glutamine
D3/02	L-15 + 10% FCS + 1% glutamine
D40/97	L-15 + 10% FCS + 1% glutamine
IMR-90	DMEM + 20% FCS + 2 mM glutamine
HAKAT	DMEM + 10% FCS + 2 mM glutamine
HEK 293	DMEM + 10% FCS + 2 mM glutamine + 4.5 g/l glucose
COS-7	DMEM + 10% FCS + 2 mM glutamine
RAW 264.7	DMEM + 10% FCS + 2 mM glutamine + 4.5 g/l glucose
L-cells	DMEM + 10% FCS + 2 mM glutamine + 4.5 g/l glucose
L-Wnt 3 cells	DMEM + 10% FCS + 2 mM glutamine + 4.5 g/l glucose + G418 (400 µg/ml)
C57MG	DMEM + 10% FCS + 2 mM glutamine + 4.5 g/l glucose + 10 µg/ml insulin

For sub-culturing of the cells, the medium was removed, and the cells were rinsed once with 1 x PBS buffer. Then, the buffer was removed and 2 ml of trypsin-EDTA solution was added per 75-cm² culture flask. The cells were incubated for a few minutes at 37°C until they detached. Then, 8 ml of a fresh culture medium was added, aspirated, and dispensed into new culture flasks. Fresh medium was added every 2 to 3 days.

Trypsin-EDTA 10 x stock solution (Biochrom AG) contained 0.5% Trypsin and 0.2% EDTA. For use in cell culture, the solution was diluted 1:10 with PBS, filter-sterilized, and frozen at -20°C in 80 ml aliquots. Before use, an aliquot was thawed in a water bath at 37°C and used as described above.

10 x PBS

2 g/l KCl

2 g/l KH₂PO₄

21.6 g/l Na₂HPO₄*7 H₂O

pH was adjusted to 7.4

2.2.2.2 Freezing and Thawing Procedure

Following trypsinization, the cells were transferred into a 15 ml Falcon tube and centrifuged at 1 000 x g for 5 min at room temperature. The cell pellet was resuspended in 1 ml of storage medium, transferred into a cryo-tube and placed in a cryo-container with isopropanol. The cells were kept at -70°C for 24 hours to allow them to freeze slowly. After this time, they were stored in liquid nitrogen. Storage medium consisted of the respective cell culture medium supplemented with 5% DMSO.

Thawing of cells was performed quickly in a 37°C water bath for ~2 min. Then, the cells were transferred immediately into a culture flask containing pre-warmed culture medium. The next day, the medium was replaced with the fresh one to remove traces of DMSO.

2.2.2.3 Cell Treatments

For the treatment with EGF, TGF- α , and TNF- α , 9442 (BET-1A) cells were grown to ~70% confluence in regular medium (BEBM) supplemented with growth factors (BEGM) for 3 days. After this time, subconfluent cultures were treated with

50 ng/ml of human recombinant EGF, 20 ng/ml of human recombinant TGF- α , and 25 ng/ml of human recombinant TNF- α without medium change, cultured for the indicated times, and harvested. The growth and treatment of cells as well as the RNA and protein extraction were performed at least 3 independent times.

For the stimulation with medium, BEBM medium was supplemented with a double set of growth factors (BEGM; we refer to this as “stimulation medium”). After 3 days of incubation in regular culture medium, the medium was replaced with the “stimulation medium” and cells were cultured for the indicated times and harvested.

To determine the kinetics of MAPK pathways stimulation, 9442 cells were grown in regular medium for 3 days and then stimulated for various periods of time (5, 15, 30, 60, 90, 120 min) with “stimulation medium”.

In order to determine the effective drug concentration, 9442 cells were grown in regular medium for 3 days and then preincubated for 1 hour with 10 μ M AG1478, 20 μ M U0126, 40 μ M SB203580, 40 μ M SP600125, 40 μ M LY294002, respectively, without medium change. Next, the cells were stimulated with “stimulation medium” for the optimal time course determined from the stimulation kinetics studies. The drug concentrations were chosen based on maximal suppressive efficacy and minimal cell toxicity. Stock solutions of 15.8 mM AG1478, 10 mM U0126, 25 mM SB203580, and 22.7 mM SP600125 were prepared in DMSO, and 50 mM LY294002 in 100% ethanol. As a control, cells were treated with the vehicle, DMSO or ethanol, respectively.

For inhibition studies, 9442 cells were incubated for 12 hours (RNA analysis) and 24 hours (protein analysis) with EGF or TGF- α without medium change, in the presence or absence of the inhibitors, which were added 1 hour prior to treatment with the growth factors.

To inhibit protein synthesis, cells were pretreated for 1 hour with cycloheximide (2-10 μ g/ml) before adding EGF. Stock solution of 100 mg/ml cycloheximide was prepared in DMSO.

Protein kinase C (PKC) was induced by treatment with phorbol 12-myristate 13-acetate (PMA; 10 nM and 100 nM) for the indicated times. Inhibition of PKC was carried out by preincubating cells for 1 hour with a broad PKC inhibitor bisindolylmaleimide I (5 μ M) before stimulation with PMA or EGF. Stock solutions

of 2 mg/ml PMA and 3 mM bisindolylmaleimide I were prepared in 100% ethanol and DMSO, respectively. Control plates were treated with the vehicle.

For the treatment with thapsigargin, cells were preincubated with the stimulation buffer containing 1 mM CaCl_2 for 10 min (Davey et al., 2001). Then, 0.5 μM thapsigargin was added and the cells were incubated for 15 and 30 min at 37°C, fixed and immunostained for the endogenous S100A14 protein. Stock solution of 1.5 mM thapsigargin was prepared in DMSO. Control incubations were performed with DMSO as the vehicle. For Zn^{2+} treatment, cells were incubated with 40 μM of ZnCl_2 for 15 and 30 min at 37°C.

Stimulation buffer

140 mM NaCl

5 mM KCl

1 mM MgCl_2

10 mM Glucose

10 mM HEPES

1 mM CaCl_2

H_2O was added and the solution was filter-sterilised.

Lung tumour cell lines (H525, COLO 668, COLO 667, H157, SHP-77, D117, H23, N417) were treated with 20 μM 5-aza-2'-deoxycytidine for 5 days and processed for RNA. Stock solution of 10 mM 5-aza-2'-deoxycytidine was prepared in 1 x PBS, pH 6.0.

Stimulation of HEK 293 and Lovo cells with EGF and $\text{TNF-}\alpha$ was performed 24 hours after the transfection with p2C promoter construct, following 24 hours incubation in serum-containing, or serum-free medium. Cells were incubated for 6, 12, and 24 hours in the presence or absence of EGF and $\text{TNF-}\alpha$ and harvested after indicated times.

2.2.2.4 Transfection of Mammalian Cells

Cationic lipid-mediated transfection was employed as a method of introducing DNA into cells.

A total of 6×10^4 cells/well of the H157, A549, and COS-7 cells were seeded in 6-well plates a day before transfection. The cells were transfected with 0.8 μg

(H157), 1.9 µg (COS-7), and 3.8 µg (A549) of *S100A14-V5* construct using 5.2 µl of Lipofectin reagent (Invitrogen, MD, USA), 6 µl, and 12 µl of LipofectAMINE reagent (Invitrogen, MD, USA), respectively. Transfection was performed according to the following protocol: for each transfection, DNA and Lipofectin/LipofectAMINE were diluted into separate aliquots (200 µl) of Opti-MEM I Reduced Serum Medium (Invitrogen). Diluted Lipofectin Reagent was allowed to stand at room temperature for 30 min. The two solutions were then combined, mixed gently and incubated at room temperature for 15 min (Lipofectin) or 45 min (LipofectAMINE) for lipid-DNA complexes formation. The cells were washed once with Opti-MEM, then 800 µl of Opti-MEM was added per well and the cells were overlaid with lipid-DNA complexes. Cells were then incubated for 5 hours at 37°C in a CO₂ incubator. After this time, DNA-lipid containing medium was replaced with growth medium. Cells were assayed for gene expression 48 hours after transfection.

To control the transfection efficiency, cells were transfected with an EGFP plasmid (enhanced green fluorescent protein) and viewed 48 hours after transfection using inverted microscope equipped with UV-lamp. The number of green fluorescent cells was visually estimated. Mock-transfected cells were used as negative controls.

2.2.3 Preparation, Enzymatic Manipulation and Analysis of DNA

2.2.3.1 Mini-Preparation of Plasmid DNA

Mini-preparation of plasmid DNA was performed with Qiagen Plasmid Miniprep Kit according to the manufacturer's recommendations. For isolation of ~15 µg of plasmid DNA, 3 ml overnight culture of *E.coli* in LB medium was prepared. DNA was eluted in 15 µl of the elution buffer (EB; 10 mM Tris-HCl, pH 8.5) and stored at -20°C.

2.2.3.2 Large-Scale Preparation of Plasmid DNA

For large-scale plasmid isolation, the Qiagen Plasmid Maxiprep Kit was used. Plasmid DNA preparations for transfection experiments were performed with Qiagen Endofree Plasmid Maxiprep Kit. Plasmid DNA was isolated according to

the supplier's manual. A 150 ml (Qiagen Plasmid Maxiprep Kit) or 100 ml (Qiagen Endofree Plasmid Maxiprep Kit) *E.coli* overnight culture was prepared for each experiment. The pellet was resuspended in a volume of EB buffer that the final concentration of DNA was ~1.0-1.5 µg/µl.

2.2.3.3 *Measurement of DNA Concentration*

Concentration of DNA was measured using a GeneQuant II RNA/DNA spectrophotometer (Pharmacia Biotech). Typical OD 260/280 ratios were ~1.7-1.8.

2.2.3.4 *Digestion of DNA with Restriction Endonucleases*

Digestion of DNA with restriction endonucleases was performed according to the recommendations of the manufacturer. For the digestion of 1-2 µg of DNA, 10 U of enzyme were added with an appropriate buffer in a final volume of 20 µl. Reactions were incubated for 14-16 hours.

For cloning experiments, the digested DNA was subsequently separated in agarose gel, excised from the gel, and purified with QIAquick Gel Extraction Kit. Alternatively, QIAquick PCR Purification Kit was used to purify PCR-amplified fragments with incorporated restriction sites. An additional purification step for DNA was included for cloning experiments. The DNA was precipitated with 0.5 volumes of 4 M NaAc, pH 5.2 and 2.5 volumes of cold 100% ethanol, and incubated for 1 hour at -20°C. For PCR-amplified and subsequently digested DNA fragments, Pellet Paint Co-Precipitant (Novagen) was included in the precipitation reaction. Then, the solution was centrifuged at 14 000 x g and 4°C for 30 min, the pellet was washed with 1 ml 70% ethanol, and centrifuged a second time at 14 000 x g and 4°C for 5 min. Finally, the pellet was shortly air-dried and resuspended in 10 µl of EB buffer.

2.2.3.5 *Vector Dephosphorylation*

To exclude self-ligation of the vector DNA, the protruding 5'-end of the vector was dephosphorylated with calf intestinal alkaline phosphatase (CIAP). The reaction was performed according to the recommendations of the supplier. One unit of CIAP was diluted for immediate use in 1 x CIAP Reaction Buffer and incubated with the vector DNA at 37°C for 30 minutes. After that time, another aliquot of

diluted CIAP was added and the incubation was continued at 37°C for additional 30 minutes. The reaction was stopped by incubation at 75°C for 15 minutes. The dephosphorylated DNA was then purified by QIAquick PCR Purification Kit followed by DNA precipitation.

2.2.3.6 DNA Ligation

Ligation of DNA fragments into plasmid vectors was performed with Rapid DNA Ligation Kit. Experiments were performed according to the protocol of the supplier. A maximum of 200 ng of total DNA (vector + insert) at the molar ratios of vector DNA to insert DNA 1:2 and 1:5 were used. The reactions were incubated for 5 min at room temperature and then placed on ice. To determine the efficiency of ligation, 5 µl of the reaction mix were run on an agarose gel and visualised with ethidium bromide.

2.2.3.7 Polymerase Chain Reaction (PCR)

Amplification of DNA was performed according to the following protocol:

Template DNA	25.0 ng – 0.5 µg
10 x PCR buffer (including 15 mM MgCl ₂)	2.50 µl
dNTP mix (each 10 nM)	1.00 µl
5'- and 3'- oligonucleotide primers	1.00 µl (each)
Ampli Taq DNA polymerase (1U)	0.25 µl
H ₂ O filled up to	25.0 µl

For amplification of DNA fragments from PAC genomic clone, 5% DMSO was added to the reaction.

Typical cycling profiles were programmed in Primus 96 Plus Thermal Cycler (MWG-Biotech) as follows:

Denaturation of double-stranded DNA	95°C	30 sec	30 cycles
Annealing of oligonucleotides to the template DNA	T _a	30 sec	
Elongation	72°C	30/60 sec	
Extension	72°C	5 min	
Chilling	4°C	up to 1 h	

Annealing temperatures were calculated using the formula: $T_a = T_m - 2^{\circ}\text{C}$, where T_m is the melting temperature of the primers used for amplification. T_m of each oligonucleotide primer was calculated as follows: $T_m = 4 \times (G + C) + 2 \times (A + T)$, where G – guanine, C – cytosine, T – thymine, A – adenine.

2.2.3.8 Purification of PCR-Amplified Fragments of DNA

Purification of PCR-amplified DNA fragments was performed with QIAquick PCR Purification Kit according to the supplier's protocol. Purified PCR fragments were controlled by agarose gel electrophoresis.

2.2.3.9 Sequencing

Sequencing analysis was performed on a LI-COR automated DNA sequencer (MWG-Biotech) using fluorescent primers labelled with the tricarbo-cyanine dye IRD800 at their 5'-end.

Gel components were pre-mixed the following way:

- 30 ml Sequagel XR (Biozym)
- 7.5 ml Sequagel-buffer (Biozym)
- 150 μl 10% Ammonium persulfate (APS)
- 15 μl TEMED

and polymerised for 1 hour.

Cycle sequencing reactions were done using the Thermo-Sequenase Fluorescent-Labeling Cycle-Sequencing Kit according to a protocol of the supplier. The reactions were pre-mixed the following way:

- 4 μl H_2O
- 4 μl plasmid DNA (100-300 ng/ μl)
- 4 μl IRD800-labelled primer (2 pmol/ μl)

to a total reaction volume of 12 μl .

The pre-mix was distributed in four tubes, 3 μl in each, and 1.3 μl of Thermo-Sequenase DNA Polymerase and Termination Mix A/C/G/T was added to each tube.

The following parameters were used for a cycle-sequencing:

30 sec	95°C	30 cycles
15 sec	Ta	
1 min	70°C	

Each reaction was stopped with 4 µl of a Stop/Loading Buffer. Samples were then analysed by electrophoresis or stored at -20°C.

The reaction tubes were heated for 5 min at 70°C to denature the samples. Then 1.3 µl/well was loaded onto sequencing gel, and run overnight. Data were analysed using a LI-COR user program.

2.2.3.10 *Electrophoretic Separation of DNA*

Gel electrophoretic separation of DNA was performed in 1 to 2% agarose gels run at 30 to 80V with 0.5 x TBE as a running buffer. Samples were diluted in 6 x Loading Dye (Promega) and loaded on gels containing 0.1 µg/ml ethidium bromide for visualisation.

10 x TBE

108 g Tris-base

55 g Boric acid

40 ml 0.5 M EDTA, pH 8.0

adjusted with H₂O to 1 l

2.2.3.11 *Elution of DNA Fragments from a Gel*

For elution of DNA fragments from agarose gels, the QIAquick Gel Extraction Kit was used. DNA fragments were excised from the gel on UV light and handled as recommended by the manufacturer. DNA was eluted in 30 µl of EB buffer, purified, and concentrated by ethanol precipitation.

2.2.3.12 *Southern Blot Analysis*

For Southern blot analysis, DNA samples were loaded onto a 1% agarose gel and run at 50V for 4 hours or overnight. Following electrophoresis, the gel was processed for blotting by depurination, denaturation, and neutralization. The gel was rinsed in H₂O between each step.

For depurination, the gel was placed in 0.25 M HCl and agitated gently for 15 min. Then, the gel was submerged in denaturation buffer (0.5 M NaOH/1.5 M NaCl) and incubated for 45 min with gentle agitation. To neutralize the gel, it has been submerged in neutralization buffer (0.5 M Tris-HCl/1.5 M NaCl) and incubated for 30 min with gentle agitation. Then, the neutralization solution was replaced with the fresh one and incubated for further 30 min.

The DNA was transferred from the gel onto the Hybond-N+ membrane by vacuum transfer using the Vacuum blotter (Model 785, BIO-RAD) for 90 min. 10 x SSC was used as a transfer buffer. The membrane was pre-wetted with H₂O and then submerged for 5 min in transfer buffer. Following the transfer, the membrane was rinsed for 5 min in 2 x SSC, air-dried, and cross-linked by UV exposure at 120 000 microjoules/cm². The membrane was wrapped in plastic foil and stored at 4°C until use.

DNA probes were labelled with [α -³²P] dCTP by random oligonucleotide priming using Megaprime DNA Labeling System, according to the manufacturer's recommendations. Typically, 25 ng of labelled probe was used for each hybridization. Unincorporated nucleotides were removed using QIAquick Nucleotide Removal Kit, according to the protocol of the supplier. Subsequently, the radioactively labelled probe was denatured at 98°C for 5 min and quickly placed on ice.

Prehybridization and hybridization were carried out in glass tubes in a commercial hybridization oven. The membrane was placed RNA-side-up in a hybridization tube, ~5 ml of pre-warmed ExpressHyb solution were added and it was prehybridized with rotation at 60°C for 30 min. Following prehybridization, the denatured probe was added into the hybridization solution and the incubation was continued at 60°C overnight.

The next day, the blot was rinsed quickly in 2 x SSPE/0.1% SDS wash solution. Then, the washing solution was replaced with the fresh one and incubated with rotation for 1 hour at room temperature. After that time, the solution was replaced with 0.1 x SSPE/0.1% SDS wash solution and incubated with rotation for 1 hour at 60°C. After the final wash, the membrane was immediately covered with plastic wrap and mounted. Autoradiography was

performed by exposition to Kodak X-ray film at -70°C in a cassette with two intensifying screens.

For re-probing the membrane, the probe was stripped from the membrane by incubation with shaking for 10 min in 0.5% SDS solution pre-warmed to 80-100°C. The membrane was then covered with plastic wrap and stored at 4°C until use.

20 x SSC

3 M NaCl

0.3 M Natrium citrate

20 x SSPE

3.6 M NaCl

0.2 M Natrium phosphate

0.02 M EDTA, pH 8.0

pH was adjusted to 7.7, H₂O was added to a final volume of 1 liter and the solution was autoclaved.

2.2.3.13 Cancer Profiling Array Analysis

Cancer Profiling Array (BD Biosciences) consists of SMART-amplified cDNA from 241 tumour and corresponding normal tissues from individual patients, along with eight negative and positive controls (yeast total RNA; yeast tRNA; *E.coli* DNA; human Cot-1 DNA; poly(A); ubiquitin cDNA; human genomic DNA). Samples on the array are normalized to four different housekeeping genes: ubiquitin, 23-kDa highly basic protein, β -actin, and glutamase dehydrogenase. The array also includes the following human cancer cell lines: HeLa; Burkitt's lymphoma, Daudi; chronic myelogenous leukemia K562; promyelocytic leukemia HL-60; melanoma G361; lung carcinoma A549; lymphoblastic leukemia MOLT-4; colorectal adenocarcinoma SW480, and Burkitt's lymphoma, Raji.

The 369-bp PCR fragment of the human S100A14 cDNA, corresponding to the complete protein coding region, was used as a hybridization probe. The probe was prepared using H1043f and H1043r primers.

Hybridization was performed according to the manufacturer's recommendations and as described above for Southern blot, except for the following modifications: the array membrane was prehybridized in 15 ml of prewarmed

ExpressHyb solution with 1.5 mg yeast tRNA at 65°C for 2 hours. The radioactively labelled cDNA probe was mixed with 100 µg of yeast tRNA, denatured at 98°C for 10 min, and hybridized to the array at 65°C overnight. Following exposure to a phosphor screen for 14 hours and 7 hours, the array was scanned with the GS-250 Molecular Imager (BIO-RAD, Munich, Germany) at a 800-µm resolution. The results were quantified using the Molecular Analyst Software Version 1.4 by applying a grid to the image to measure the intensity of the hybridization signal of every spot. After background subtraction, the image was normalized using all spots on the membrane as reference points. The threshold values for up- and down-regulation were chosen based on careful inspection of tumour/normal intensity ratios for all the spots on the membrane (intensity ratio >2 for up-regulation and <0.5 for down-regulation).

2.2.3.14 Fluorescence in situ Hybridization (FISH) Analysis

The FISH analysis was performed by Ms. N. Deutschmann (Institute of Pathology, Berlin, Germany) as described by Lichter and Ried (Godsen, 1994). The DNA from the genomic PAC clones I22230, A12752, and D11609 was purified with Qiagen Maxi Kit and labelled by nick-translation with biotin-16-dUTP (Roche). Next, hybridization on metaphases of normal lymphocytes was performed. Images were captured with a cooled charge-coupled device camera (Photometrics, Tucson, Arizona) and processed using a custom made program (Karyomed, KaryoMedics, Germany).

2.2.3.15 5' Rapid Amplification of cDNA Ends (5' RACE)

The 5'-end of the *S100A14* cDNA was determined with 5' RACE Kit according to the supplier's manual, using poly(A) RNA from normal colon tissue. The gene-specific primers for 5' RACE included GPS1, NGPS1, and NGPS2. The PCR products were cloned into the pCR2.1 TA Cloning Vector and 24 clones were sequenced.

2.2.4 Dual-Luciferase Reporter Assay

Human embryonic epithelial kidney cells HEK 293 were plated in 6-well plates at 1.5×10^5 cells/well a day before transfection. The cells were transfected for

6 hours using a transfection mixture consisting of 200 μ l of Opti-MEM, 4 μ l of LipofectAMINE, 1 μ g of Firefly luciferase reporter constructs driven by the *S100A14* promoter fragments, and 0.1 μ g of pRL-TK *Renilla* luciferase reporter vector as an internal control for transfection efficiency.

For co-transfection experiments, cells were transfected with a total of 1 μ g DNA, consisting of a mixture of 0.5 μ g of the p2C-luc plasmid and 0.5 μ g of the expression vector encoding wild type p65. Where necessary, “empty” vector for p65 (pcDNA3Flag) or pGL3-Basic vector were included to maintain constant amounts of DNA.

The assays for firefly and *Renilla* luciferase activity were performed using the Dual-Luciferase Reporter Assay Kit (Promega), as recommended by the manufacturer. Forty-eight hours after transfection, the cells were washed once with 1 x PBS and cell lysates were prepared by passive lysis in 250 μ l of freshly prepared 1 x passive lysis buffer (Promega). Firefly and *Renilla* luciferase activities were assayed in 20 μ l of cell lysate pre-dispensed into 5-ml Sarstedt tubes, followed by sequential autoinjection of 25 μ l LAR II and Stop&Glo reagents using the Lumat LB9507 luminometer fitted with automatic injection system (Berthold Technologies, Germany). The luminometer was programmed to perform a 2-second per measurement delay, followed by a 10-second measurement period for each reporter assay.

Luciferase read-out was obtained from triplicate transfections and averaged. Firefly luciferase activity was normalized to the *Renilla* luciferase activity, and the results were expressed as relative luciferase activity.

2.2.5 Preparation and Analysis of RNA

2.2.5.1 RNA Preparation

Total RNA from cultured cells was isolated using TRIzol (Invitrogen). Cells growing on 100-mm dishes were washed once with pre-cooled 1 x PBS and lysed by adding 2 ml of TRIzol reagent and passing the cell lysate several times through a pipette. Then the lysed cells were scraped off with a sterile cell scraper (Sarstedt) and transferred to 11-ml Sarstedt tubes. The samples were then extracted with 0.4 ml of chloroform (0.2 ml chloroform per 1 ml of TRIzol reagent) by inversion

mixing. Phase separation was achieved by placing the samples at room temperature for 5 min, and centrifuging at 9 000 x g and 4°C for 20 min. The aqueous layer was mixed with 1 ml of isopropanol (0.5 ml isopropanol per 1 ml of TRIzol reagent) to precipitate the RNA. Samples were incubated at room temperature for 10 min, then centrifuged at 10 000 x g and 4°C for 10 min. The RNA pellet was washed with 2 ml of 80% ethanol (1 ml ethanol per 1 ml of TRIzol reagent), and centrifuged at 7 500 x g and 4°C for 5 min. The pellet was air-dried, resuspended in DEPC-treated water, and the RNA was quantified using a GeneQuant II RNA/DNA spectrophotometer (Pharmacia Biotech). The concentration of RNA was adjusted to ~1.0-1.5 µg/µl. Typical OD 260/280 ratios were ~1.4-1.5. To assess the integrity of the RNA preparations, a test formaldehyde-agarose gel electrophoresis was performed.

Tissue samples were homogenized in 4 ml of TRIzol reagent using a power homogenizer (MICRA). The homogenized samples were incubated at room temperature for 5 min and followed the standard RNA extraction procedure as outlined above.

Poly(A) RNA was isolated using FastTrack 2.0 Kit (Invitrogen) according to the recommendations of the manufacturer.

DEPC-treated H₂O

1 l H₂O

1 ml Diethylpyrocarbonate (DEPC)

The solution was stirred on a magnetic stirrer overnight in a fume hood and autoclaved the next day.

2.2.5.2 Electrophoretic Separation of RNA

A 10-µg aliquot of total RNA was size-fractionated on 1% denaturing agarose gel in the presence of 2.2 M formaldehyde.

To denature the RNA sample, a denaturation reaction was set up:

RNA	10.0 µg
10 x MOPS	1.0 µl
Formaldehyde	3.5 µl
Formamide	10.0 µl
10 x Gel-loading buffer	2.0 µl

The RNA solution was incubated for 10 min at 55°C and then quickly chilled on ice. After loading, the gel was run in 1 x MOPS electrophoresis buffer at 50V for ~5 hours, visualised and photographed on a UV transilluminator.

Denaturing agarose gel

1 g Agarose

72.2 ml of DEPC-treated H₂O

agarose was dissolved by boiling in a microwave oven and cooled to ~50°C. In a chemical fume hood, 10 ml of 10 x MOPS electrophoresis buffer and 17.8 ml of formaldehyde were added and the gel was casted.

10 x MOPS

0.2 M MOPS

50 mM Sodium acetate

10 mM EDTA, pH 8.0

pH was adjusted to 7.0 with NaOH

10 x Gel-loading buffer

500 µl Formamide

2 µl EDTA, pH 8.0

5 µl Ethidium bromide

0.1% w/v Bromophenol blue

2.2.5.3 Northern Blot Analysis

Electrophoretically separated RNA was transferred from gel onto Hybond-N membrane by upward capillary transfer. Prior to the transfer, the gel was rinsed with H₂O. The membrane was prepared for the transfer by immersing in 10 x SSC for 5 min and the gel was placed on a solid support in an inverted position. Then, the membrane was placed on the top of the gel, followed by 6 pieces of Whatman 3MM papers and a stack of paper towels. A glass plate was put on it and weighted down with a 500-g weight. The transfer occurred overnight in 20 x SSC buffer. The next day, the membrane was immersed for 5 min in 2 x SSC, air-dried, and cross-linked by UV irradiation. If not used immediately, the membrane was stored at 4°C.

The radioactive labelling of the probe, hybridization, washing of the blots, and stripping of radiolabelled probes were carried out as described for Southern blot analysis (Section 2.2.3.12). Following modifications to the protocol were introduced for Northern blot analysis: the hybridization temperature was 64°C and the membrane washing times were 40 min. All the washing steps were performed with solutions prepared with DEPC-treated H₂O. As a hybridization probe, the PCR fragment of the human *S100A14* cDNA corresponding to the complete protein coding region was used. To confirm equal RNA loading and transfer, the 180-bp fragment of the mouse 18S cDNA that cross-hybridizes with human 18S RNA was used.

Typically, the blots were exposed to a phosphor screen for different time periods and scanned with the GS-250 Molecular Imager (BIO-RAD, Munich, Germany) at a 200-µm resolution. The results were quantified using the Molecular Analyst Software Version 1.4. Alternatively, if autoradiography was performed, the autoradiographs were scanned to quantify the intensity of the radiographic bands using a scanning laser BIO-RAD Laboratories Imaging Densitometer Model GS-670 and densitometry was performed.

2.2.5.4 Reverse Transcriptase-PCR (RT-PCR) Analysis

For the detection and expression analysis of the *S100A14* mRNA, the THERMOSCRIPT RT-PCR System (Invitrogen) was applied. First, cDNA synthesis was performed using 3 µg of total RNA primed with gene-specific primer H1043-rev and control gene primer GAPDH-rev. The RNA was reverse-transcribed at 55°C for 1 hour according to the manufacturer's recommendations. The reaction was terminated by heating at 85°C for 5 min. In the second step, PCR amplification was carried out using 2 µl of the cDNA synthesis reaction and primed with gene specific primers designed from open reading frame: ex1-for or ex3-for, and H1043-rev. A control PCR reaction for GAPDH was performed in parallel using the primer pair: GAPDH-for and GAPDH-rev. Amplification resulted in DNA fragments of 249-bp (ex1-for and H1043-rev), 425-bp (ex1-for and H1043-rev), and 800-bp (GAPDH-for and GAPDH-rev). PCR products were analysed on a 1.2% agarose gel and viewed on UV light.

2.2.6 Analysis of Proteins

2.2.6.1 Protein Isolation from Mammalian Cells

For protein isolation, cells were washed twice with cold 1 x PBS and lysed with denaturing hypotonic lysis buffer on ice. The lysed cells were scraped off the plates, transferred into 1.5-ml Eppendorf tubes, and incubated with shaking for 10 min at 95°C. Then, the protein samples were aliquoted and stored at -20°C.

Denaturing hypotonic lysis buffer

1% SDS

10 mM Tris-HCl, pH 7.5

2 mM EDTA, pH 8.0

2.2.6.2 Subcellular Fractionation

Cells were washed twice with cold 1 x PBS and lysed in hypotonic lysis buffer (1.2 ml per 100-mm plate) for 10 min. The cell lysate was homogenized in a pre-cooled Dounce homogenizer by repeated strokes and centrifuged for 10 min at 2 700 x g to pellet the nuclei using a Sorvall SA-600 rotor. The nuclear pellet was resuspended in a volume of 50 µl of 2 x SDS sample buffer.

The postnuclear supernatant was transferred into Beckman tubes (13 x 15 mm) and centrifuged for 30 min at 60 000 x g and 4°C to pellet the membranes using a Beckman TLN 100.3 rotor. The crude membranes were resuspended in a volume of 100 µl of 2 x SDS sample buffer.

The postmembrane supernatant was further fractionated by methanol/chloroform precipitation to recover cytoplasmic proteins. Four ml methanol were added to the postmembrane supernatant, then 1 ml chloroform was added and mixed, then 3 ml of H₂O were added and mixed. The solution was centrifuged at 15 000 x g for 15 min at 4°C. The upper phase was discarded, and 6 ml methanol were added, mixed and centrifuged again at 15 000 x g for 15 min at 4°C. The pellet was dried and resuspended in 100 µl of 2 x SDS sample buffer.

Following dissolving of the pellets in 2 x SDS sample buffer, samples were incubated with shaking for 10 min at 95°C, centrifuged for 5 min at 14 000 x g, and stored at -20°C until use.

The resulting fractions were tested for their enrichment in soluble, membrane, and nuclear fractions by Western blotting with anti- α -tubulin, anti-pan RAS, and anti-phospho-c-JUN antibodies, respectively.

Hypotonic lysis buffer

10 mM Tris-HCl, pH 8.0

0.1 mM DTT

1 mM PMSF

1 tab/10 ml protease inhibitor Complete tabs (Roche)

2 x SDS sample buffer

120 mM Tris-HCl, pH 6.8

200 mM DTT

4% w/v SDS

10% w/v Glycerol

0.002% w/v Bromophenol blue

2.2.6.3 Determination of Protein Concentration

Protein content was determined by colorimetric amido-black method as described by Schaffner and Weissmann (1973).

A standard curve for bovine serum albumine (BSA) was created by preparing 0.5, 0.75, 1, 2, 4, 8, and 10- μ g duplicate dilutions of 200 mg/ml stock solution of BSA.

Then, 1 μ l of protein standards (applied in duplicates) and 1 μ l of protein sample were applied to the nitrocellulose membrane (Schleicher & Schüll). The membrane was placed in 0.1% amido-black for 1 min and then washed extensively with shaking using freshly prepared destaining solution. The destaining solution was replaced several times till the membrane was completely destained. The protein spots were cut out, put into Eppendorf tubes, and 800 μ l of elution solution were added. The tubes were placed in an Eppendorf shaker and shaken for 30 min.

Absorbance of standards and protein samples was measured at 630 nm in disposable 1.5 ml semi-micro cuvettes (Brand) using Biochrom 4060 software in UV-Visible Spectrophotometer (Pharmacia LKB). Protein concentration was

determined by plotting absorbance of the protein samples against the standard curve using Microsoft Excel program.

Destaining solution

90 ml Methanol

2 ml Acetic acid

8 ml H₂O

Elution solution

50 ml Ethanol

10 µl 0.5 M EDTA, pH 8.0

0.5 ml 5 M NaOH

49.5 ml H₂O

2.2.6.4 One-Dimensional SDS Gel Electrophoresis (PAGE)

Protein samples were separated by polyacrylamide gel electrophoresis (PAGE) using the standard Laemmli method.

Protein samples were mixed with 1 volume of 2 x SDS sample buffer and denatured for 5 min at 95°C. Equal amounts of proteins were loaded onto 12% gel and run ~4 hours at 65V in 1 x running buffer using Mini-PROTEAN 3 Cell electrophoresis tank (BIO-RAD). Protein separation was controlled by running a Prestained Broad Range Protein Marker (BIO-RAD).

Separating gel: 10 ml of 12% gel

3.35 ml H₂O

2.5 ml 1.5 M Tris-HCl, pH 8.8

4.0 ml 30% Acrylamide/Bisacrylamide

100 µl 10% SDS

50 µl APS

10 µl TEMED

Stacking gel: 5 ml of 4% gel

3.05 ml H₂O

1.25 ml 0.5 M Tris-HCl, pH 6.8

0.66 ml 30% Acrylamide/Bisacrylamide

50 µl 10% SDS

50 µl APS

10 µl TEMED

5 x running buffer

15.1 g/l Tris-base

72.0 g/l Glycine

5.0 g/l SDS

An alternative protocol was used for S100A14 gel electrophoresis. Protein samples were mixed with 1 volume of 2 x tricine sample buffer and denatured for 5 min at 95°C. Equal amounts of proteins were loaded onto 15% Tris-tricine gel and run in 1 x cathode (upper tank) and 1 x anode (lower tank) electrophoresis buffer for ~1 hour at 35V and ~5 hour at 50V.

2 x Tricine sample buffer

2.0 ml 0.5 M Tris-HCl, pH 6.8

2.4 ml Glycerol

4.2 ml 20% SDS

0.31 g DTT

0.02% w/v Coomassie blue

adjusted with H₂O to 10 ml

Separating gel: 10 ml of a 15% gel

1.66 ml H₂O

3.32 ml 3 M Tris-HCl, pH 8.45

1.06 ml Glycerol

3.75 ml 40% Acrylamide/Bisacrylamide

150 µl 20% SDS

50 µl APS

10 µl TEMED

Stacking gel: 5 ml of 4% gel

2.71 ml H₂O

1.66 ml 3 M Tris-HCl, pH 8.45

0.5 ml 40% Acrylamide/Bisacrylamide

75 µl 20% SDS

50 µl APS

10 µl TEMED

Cathode electrophoresis buffer

12.11 g/l Tris-base

17.92 g/l Tricine

1 g/l SDS

stored at 4°C

Anode electrophoresis buffer

24.22 g Tris-base

diluted to 1 l with H₂O, adjusted to pH 8.9, and stored at 4°C

2.2.6.5 Western Blot Analysis

Following electrophoresis, the stacking gel was discarded, and the separating gel was submerged in transfer buffer for 20 min. During that time, PVDF membrane (Amersham) was activated in methanol for 11 sec, washed in H₂O for 5 min, and equilibrated in transfer buffer for 10 min. On a semidry transfer unit (PeqLab Biotechnology GmbH) 6 sheets of Whatman paper pre-wetted in transfer buffer, the PVDV membrane, the gel, and 6 sheets of pre-wetted Whatman paper were assembled. The protein transfer proceeded for 45 min at 200 mA.

Transfer efficiency was controlled by Coomassie blue staining of the gel for 30 min, followed by destaining and visualisation. After the transfer, the membrane was washed briefly in TBST buffer and blocked for 1 hour in 10 ml of blocking buffer at room temperature with shaking on a rotor platform. After the blocking procedure, the membrane was washed 3 x 5 min in 20 ml TBST, and incubated overnight with the primary antibody in 5% BSA solution (5% BSA in TBST) at 4°C. The next day, the membrane was washed 3 x 10 min in 20 ml TBST, and incubated with the corresponding secondary antibody for 1 hour. The membrane was washed again 3 x 10 min in TBST, and the immunocomplexes were detected with an Enhanced Chemiluminescence Kit (ECL, Amersham), as recommended by the supplier.

For S100A14 detection, the membranes were incubated with the primary antibody for 2 hours in blocking buffer at room temperature.

For re-probing, the membranes were incubated in stripping buffer for 30 min at 70°C and washed 3 x 10 min in TBST. The membranes were subsequently blocked in blocking buffer and immunoblotted with a primary antibody as outlined above.

Primary antibodies, corresponding secondary antibodies, and their dilutions

Primary antibody	Dilution	Secondary antibody	Dilution
Anti- β -actin	1:10 000	Peroxidase-conjugated rabbit anti-mouse	1:5000
Anti-AKT	1:1000	Peroxidase-conjugated goat anti-rabbit	1:5000
Anti-c-JUN	1:1000	Peroxidase-conjugated goat anti-rabbit	1:5000
Anti-p38	1:1000	Peroxidase-conjugated goat anti-rabbit	1:5000
Anti-Phospho-AKT (Ser473)	1:1000	Peroxidase-conjugated goat anti-rabbit	1:5000
Anti-Phospho-HSP27 (Ser82)	1:1000	Peroxidase-conjugated goat anti-rabbit	1:5000
Anti-Phospho-c-JUN (Ser63)	1:1000	Peroxidase-conjugated goat anti-rabbit	1:5000
Anti-Phospho-p38 (Thr180/Tyr182)	1:1000	Peroxidase-conjugated goat anti-rabbit	1:5000
Anti-Phospho-p44/42 MAPK (Thr202/Tyr204)	1:1000	Peroxidase-conjugated goat anti-rabbit	1:5000
Anti-Phospho-SAPK/JNK (Thr183/Tyr185)	1:1000	Peroxidase-conjugated goat anti-rabbit	1:5000
Anti-S100A14 affinity-purified	1:2700	Peroxidase-conjugated goat anti-rabbit	1:5000
Anti-SAPK/JNK	1:1000	Peroxidase-conjugated goat anti-rabbit	1:5000
Anti-pan-RAS	1:800	Peroxidase-conjugated rabbit anti-mouse	1:5000
Anti- α -tubulin	1:5000	Peroxidase-conjugated rabbit anti-mouse	1:5000
Anti-V5	1:5000	Peroxidase-conjugated rabbit anti-mouse	1:5000

Transfer buffer

5.81 g Tris-base

2.93 g Glycine

1.875 ml 20% SDS

200 ml Methanol

H₂O was added to 1 l

TBST

10 ml 1 M Tris-base, pH 8.0

30 ml 5 M NaCl

500 µl Tween-20

H₂O was added to 1 l

Coomassie blue staining solution

50% v/v Methanol

0.05% v/v Coomassie blue R-250

10% v/v Acetic acid

40% H₂O

Coomassie blue destaining solution

5% v/v Methanol

7% v/v Acetic acid

88% H₂O

Blocking buffer

5% Non-fat dry milk (Difco, Becton Dickinson, MD, USA) in TBST

Stripping buffer

25 ml Tris-HCl, pH 6.7

20 ml 20% SDS

1.4 ml 14.3 M β-Mercaptoethanol

H₂O was added to 200 ml

2.2.7 S100A14 Antibody Generation

The anti-S100A14 polyclonal antibody was raised by immunizing two rabbits with the NH₂ – CEAAKSVKLERPVRGH – COOH peptide located in the C-terminus of S100A14 protein (Eurogentec, Belgium). Animals were immunized four times at 2-weeks intervals by subcutaneous injection of 50-100 µg of peptide in an

emulsion with KLH. The titer of the antiserum was determined by ELISA using 100 ng of the antigen peptide. A dilution of maximally 1:1000 (antiserum SA1349) is possible for the detection of 4 µg of the antigen peptide. The antibody was affinity-purified with the antigen peptide using standard methods (Eurogentec, Belgium).

Potential cross-reactivity of the antibody with other S100 family members was examined by Western blot using recombinant S100 proteins: S100A1, S100A2, S100A3, S100A4, S100A5, S100A6, S100A8, S100A9, S100A12, S100A13, S100B, and a protein extract from HBE cells as a positive control. The recombinant proteins were kindly provided by Prof. Dr. C. Heizmann (University of Zürich, Switzerland) and Dr. C. Kerkhoff (University of Münster, Germany). No cross-reactivity with any S100 protein tested was detected confirming that the C-terminal peptide used for rabbit immunisation is indeed S100A14-specific (data not shown).

2.2.8 Immunofluorescence Analysis

For immunofluorescence analysis, cells were seeded and grown on 18 x 18 mm glass cover slips. After fixation with freshly prepared 3% paraformaldehyd in 1 x PBS for 15 min at room temperature, cells were permeabilized with 0.2% Triton X-100 for 2 min, washed 3 x 5 min with 1 x PBS and incubated for 1 hour in blocking buffer (10% FCS in 1 x PBS).

The S100A14 affinity-purified antibody was diluted 1:2000, and anti-V5 antibody 1:200 in blocking buffer. Cover slips were incubated with the primary antibodies for 2 hours at room temperature, then washed 3 x 5 min in PBS, and incubated with the secondary antibodies for 1 hour. Fluorescein isothiocyanate (FITC)-conjugated goat anti-mouse IgG (H + L) antibody at 1:200 and FITC-conjugated goat anti-rabbit antibody at 1:200 were used. Nuclei were stained with 4,6-diamidino-2-phenylindole (DAPI) (Sigma, Steinheim, Germany) for 5 min. Cover slips were then washed with PBS, air-dried, and mounted on glass slides with DABCO anti-fade reagent (Merck, Darmstadt, Germany). They were examined using Leica confocal laser-scanning microscope (Jena, Germany).

2.2.9 Immunohistochemistry

Immunohistochemical staining of tissue sections was performed by Ms. B. Thews, Ms. K. Witkowski, and Ms. K. Petri at the Immunohistochemistry Laboratory of the Institute of Pathology, Charité in Berlin.

Paraffin-embedded archive material was retrieved from the files of the Institute of Pathology of the Charité University Hospital. One- μ m sections were cut from the blocks, mounted on superfrost slides (Menzel-Gläser, Germany) or ChemMate Capillary Cap Microscope slides (DAKO), dewaxed with xylene and gradually hydrated. Antigen retrieval was performed by pressure cooking in 0.01 M citrate buffer for 5 min. The primary antibody was incubated at room temperature for 30 min. The biotinylated secondary antibody reagent of the ChemMate Detection Kit (DAKO, Denmark), that reacts equally well with rabbit and mouse immunoglobulins, was applied as recommended by the supplier. Detection took place by indirect streptavidin-biotin method with alkaline phosphatase as the reporting enzyme according to the manufacturer's instructions. Chromogen-Red (ChemMate Detection Kit) served as chromogen, afterwards the slides were briefly counterstained with haematoxylin and aquaeously mounted.

Primary antibodies, corresponding secondary antibodies, and their dilutions

Primary antibody	Dilution	Secondary antibody
Anti-S100A14	1:1000	ChemMate biotinylated goat anti-rabbit
Anti-ERBB2	1:1000	ChemMate biotinylated goat anti-rabbit
Anti-Ki-67	1:1000	ChemMate biotinylated goat anti-mouse
Anti-ER	1:100	ChemMate biotinylated goat anti-mouse
Anti-PR	1:500	ChemMate biotinylated goat anti-mouse

Specificity of the S100A14 antibody was verified by incubating tissue sections with pre-immune serum, demonstrating completely negative staining.

Immunostained slides were analysed under a Zeiss Axioskop light microscope and scored after the entire slide had been evaluated. The immunohistochemical evaluation was performed by Prof. Dr. I. Petersen.

In order to analyse the expression level of S100A14, we introduced a semiquantitative scoring system consisting of four different staining patterns to

distinguish between positive and negative staining. The highest positive score has been assigned to score 3, where the entire tissue shows strong positive staining. Moderately positive staining represents score 2. Score 1 was assigned to borderline positive staining of the protein and score 0 represents the complete negative staining (Fig. 2).

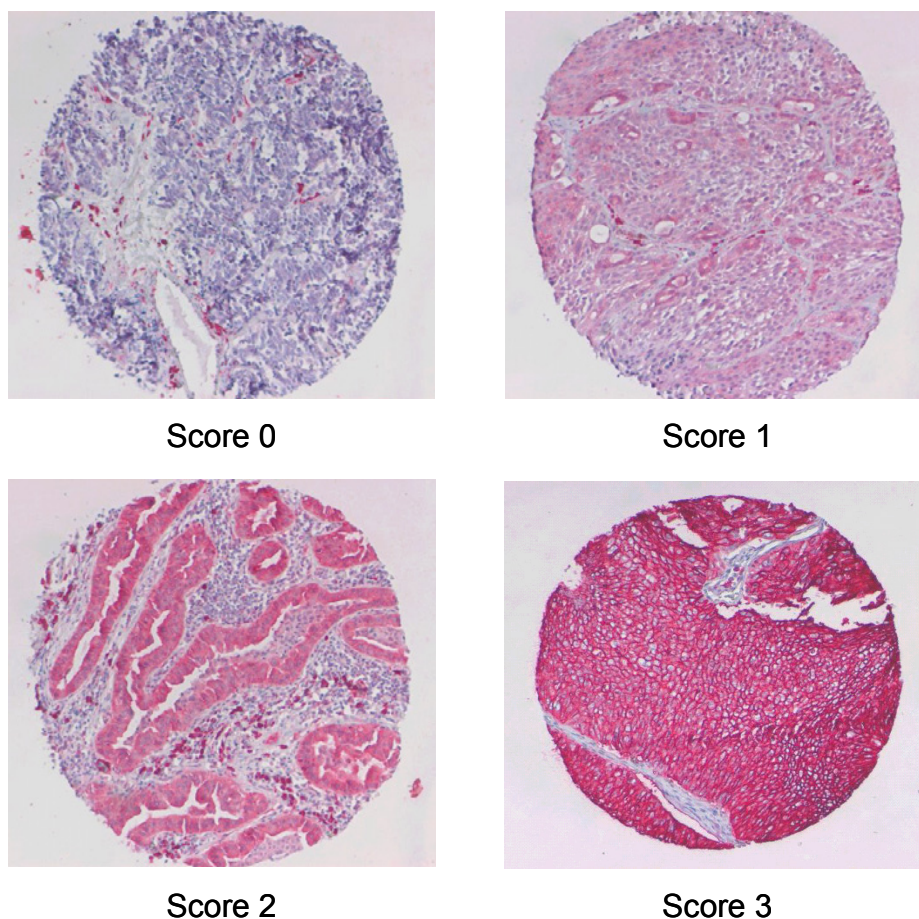


Fig. 2 The scoring system used for immunohistochemical analysis of S100A14. Examples shown are lung tumour tissue spots stained with anti-S100A14 antibody. The four different scores used are indicated.

ERBB2 immunostaining was evaluated using the method employed by the HercepTest (DAKO) according to the degree and the proportion of plasma membrane staining. ERBB2 expression was negative for a score of 0 to 1+. A score of 0 was defined as no staining or plasma membrane staining in less than 10% of tumour cells. A score of 1+ comprised faint or partly stained plasma membrane in more than 10% of tumour tissue. Tumours with scores of 2 or greater were considered to be positive for ERBB2 overexpression. A score of 2+ was defined as weak to moderate complete plasma membrane staining in more

than 10% of tumour cells. A score of 3+ was interpreted as strong, complete plasma membrane staining in more than 10% of tumour cells.

2.2.10 Tissue Microarrays (TMA) Generation

Tissue microarrays containing normal human tissues, as well as breast and lung tumours were generated by Dr. Y. Yongwei and Ms. N. Deutschmann. The normal human tissue array consisted of 29 tissue samples, the lung tumour array consisted of 150 tissue samples, and the breast tumour array was composed of 146 tissue samples. All the tissue samples were derived from randomly selected patients who underwent surgical resections performed at the Department of Surgery, University Hospital Charité between 2000 and 2002.

Suitable areas for tissue retrieval were marked on standard haematoxylin-eosin (HE) sections. Then, tissue cylinders with a diameter of 1.0 or 0.6 mm were punched out of the paraffin block and transferred into a recipient array block using a manual tissue arrayer purchased from Beecher Instruments (Woodland, USA). The tissue array was cut in 1- μ m sections without any sectioning aid like adhesive tapes or additionally coated slides.

Limitations of the tumour material and slide damages were the main reasons for the missing specimens on the tissue microarray slides. Tissue spots with heterogeneous expression patterns for S100A14 were subsequently examined by whole tissue section immunohistostaining.

2.2.11 Statistical Analysis

The Fisher's exact test for categorical variables was used to compare immunohistochemical results for S100A14 with other immunohistochemical markers and clinicopathologic characteristics. All analysis were two-tailed, and the criterion of significance was set at $p < 0.05$. The statistical analysis was undertaken using the SPSS statistical package (Version 11.5).

2.2.12 Bioinformatics

Blast analysis was performed to search for homologies at the nucleotide level and for pairwise sequence alignments (National Center for Biotechnology Information, <http://www.ncbi.nlm.nih.gov/BLAST>). Recognition sites for restriction enzymes

were identified with the Webcutter program at the Web address <http://www.firstmarket.com/cutter/cut2.html>. *S100A14* promoter region was analysed by TRANSFAC 4.0 (<http://www.transfac.gbf.de/TRANSFAC>), using the MatInspector V2.2 program. Parameters for MatInspector were set for 1.0 core similarity (a 4-nt highly conserved sequence) and 0.85 matrix similarity, employing the vertebrates matrix group. ClustalW 1.8 program was used for multiple alignments of DNA sequences (<http://www.ebi.ac.uk>).

The ExPASy nucleotide translation tool (Swiss Institute of Bioinformatics, <http://www.expasy.ch/tools/dna.html>) was applied to translate cDNA in all six possible open reading frames. Sequence homologies at the amino acid level were determined with the EMBnet-CH Blast program and potential posttranslational modification sites with the PROSITE program (all the programs are available at the ExPASy Molecular Biology Server). Hydrophobicity analysis based on the method of Kyte and Doolittle was performed using the program ProtScale at the ExPASy Molecular Biology Server. Protein secondary structure was predicted with the PSIPred V2.0 (University College London, UK <http://bioinf.cs.ucl.ac.uk/psipred>).

3 Results

3.1 Identification of the Human *S100A14* cDNA

3.1.1 Screening of SSH cDNA Libraries

To identify new potential cancer diagnostic or therapeutic targets, suppression subtractive hybridization (SSH) transcript profiling was performed between normal human cultured bronchial epithelial cells (HBE) and the metastatic small cell lung carcinoma cell line H526 (Difilippantonio et al., 2003).

The quality of the SSH library was confirmed by Northern blot analysis, indicating that 69% (236/342) of the clones were differentially expressed in the tumour cell line. In an initial evaluation we used a limited panel of cell lines including HBE cells, as well as lung tumour cell lines 2170, H526, and D51, representing the three major subtypes (squamous cell carcinoma, adenocarcinoma, and small cell lung carcinoma). Thirty-one cDNAs scored as differentially expressed in at least two of the tumour cell lines were analysed more extensively on an extended panel of cell lines including small airway epithelial cells (SAE), four immortalized HBE cells, and 32 lung cancer cell lines. The DNA sequences of isolated cDNA fragments were then determined and compared with those deposited in the GenBank database.

Based on our interest in further examining those transcripts with no homology to any known gene, 6 partial cDNAs representing transcripts that were abundantly expressed in normal lung epithelial cells but were absent or under-represented in the majority of lung tumour cell lines were selected for further analysis. These cDNA fragments were sent to the German Resource Center of the Human Genome Project (RZPD, Heidelberg, Germany) for screening of human cDNA libraries enriched in full-length cDNAs. Three of those cDNA fragments represented the same unknown gene. Screening of the human lung, trachea, and primary keratinocyte cDNA libraries yielded 13 positive clones out of which 9 were confirmed positive by Southern blot analysis. Out of 5 clones containing the longest inserts determined by *NotI/SalI*-restriction digest, clones DKFZp404H1043, DKFZp404B1018, and DKFZp719J2437 were identified as candidate full-length cDNA clones. Clone DKFZp404H1043 (designated H1043) with cDNA insert of

1057 bp was chosen for further characterization. The insert size was in accordance with the transcript size estimated by Northern blot analysis.

On the nucleotide level no homology to any known gene was found. Analysis of the predicted protein sequence revealed an S100-specific EF-hand Ca^{2+} -binding domain as well as a high homology to the S100A13 calcium-binding protein. Therefore, we designated the transcript *S100A14* and submitted it to the NCBI GenBank database under Accession No NM_020672 (LocusID LOC57402).

To verify the full-length cDNA sequence of *S100A14* we performed 5' RACE on human colon cDNAs since this organ showed the most abundant expression of the transcript in our Northern blot analysis. It provided additional 5' UTR sequence, not present in the H1043 clone. The predominant cDNA product was 1067 bp in length.

3.1.2 Sequence Analysis of *S100A14* cDNA

The cDNA was predicted to contain an open reading frame (ORF) of 104 amino acids (nt 109-423), a 5' untranslated region (UTR) of 108 bp, and a 3' UTR of 644 bp. The putative ATG initiation codon was embedded in a strong Kozak consensus sequence (CACCATGG) (Kozak, 1996) and was preceded by an in-frame stop codon. A polyadenylation signal (nt 1028-1033) and a poly(A)-tail beginning after nucleotide 1053 oriented the fragment and provided further evidence for the predicted ORF. The nucleotide sequence and the predicted open reading frame of *S100A14* are shown in Fig. 3.

Computer-assisted analysis of the deduced amino acid sequence revealed an S100-specific EF-hand Ca^{2+} -binding domain at the N-terminus (aa 33-45) consisting of 13 amino acids. The second putative canonical EF-hand motif has been deduced from the secondary structure and hydrophobicity analysis of the protein. It contained only 2 out of 6 conserved residues (Asp76 and Glu80) and might start at Gly72 ending at Ser83. In addition, the protein was predicted to contain a N-glycosylation site (aa 75-78), a protein kinase C phosphorylation site (aa 94-96), 5 casein kinase II phosphorylation sites (aa 16-19, 42-45, 73-76, 77-80, 83-86), and a N-myristoylation site (aa 2-7).

The calculated molecular weight of *S100A14* is 11 662 Da and the isoelectric point is 4.99. Protein secondary structure analysis indicated two helix-loop-helix

structural motifs characteristic of calcium-binding sites. There was an extended hydrophilic loop at the extreme N-terminus in contrast to other S100 family members.

	CTCCTGTCTTGTCTCAGCGGCTGCCAACAGATCATGAGCCATCAGCTC	48
	CTCTGGGGCCAGCTATAGGACAACAGAACTCTCACCAAAGGACCAGACACAGTGAGCACC	108
	<u>ATGGGACAGTGT</u> CGGT <u>CAGCCAACGCAGAGGATGCTCAGGAATTCAGTGATGTGGAGAGG</u>	168
1	M G Q C R S A N A E D A Q E F S D V E R	
	GCCATTGAGACCCCTCATCAAGAACTTTCACCAGTACTCCGTGGAGGGTGGGAAGGAGACG	228
21	A I E T L I K N F H Q Y S V E G G K E T	
	CTGACCCCTTCTGAGCTACGGGACCTGGTCACCCAGCAGCTGCCCCATCTCATGCCGAGC	288
41	L T P S E L R D L V T Q Q L P H L M P S	
	AACTGTGGCCTGGAAGAGAAAATTGCCAACCTGGGCAGCTGCAATGACTCTAAACTGGAG	348
61	N C G L E E K I A N L G S C N D S K L E	
	TTCAGGAGTTTCTGGGAGCTGATTGGAGAAGCGGCCAAGAGTGTGAAGCTGGAGAGGCCT	408
81	F R S F W E L I G E A A K S V K L E R P	
	GTCCGGGGGCACTGAGAACTCCCTCTGGAATTCTTGGGGGGTGTGGGGAGAGACTGTGG	468
101	V R G H *	
	GCCTGGAGATAAACTTGTCTCCTCTACCACCACCCTGTACCCTAGCCTGCACCTGTCTCT	528
	CATCTCTGCAAAGTTCAGCTTCCTTCCCCAGGTCTCTGTGCACTCTGTCTTGGATGCTCT	588
	GGGGAGCTCATGGGTGGAGGAGTCTCCACCAGAGGGAGGCTCAGGGGACTGGTTGGGCCA	648
	GGGATGAATATTTGAGGGATAAAAATTGTGTAAGAGCCAAAGAATTGGTAGTAGGGGGAG	708
	AACAGAGAGGAGCTGGGCTATGGGAAATGATTTGAATAATGGAGCTGGGAATATGGCTGG	768
	ATATCTGGTACTAAAAAAGGGTCTTTAAGAACCTACTTCCTAATCTCTTCCCCAATCCAA	828
	ACCATAGCTGTCTGTCCAGTGCTCTCTTCCTGCCTCCAGCTCTGCCCCAGGCTCCTCCTA	888
	GACTCTGTCCCTGGGCTAGGGCAGGGGAGGAGGGAGAGCAGGGTTGGGGGAGAGGCTGAG	948
	GAGAGTGTGACATGTGGGGAGAGGACCAGCTGGGTGCTTGGGCATTGACAGAATGATGGT	1008
	TGTTTTGTATCATTTGATTA <u>ATA</u> AAAAAAAAAATGAAAAAAGTGAAAAAAAAAAAAAAAAA	1067

Fig. 3 Nucleotide and deduced amino acid sequence of the human S100A14 gene. The predicted start codon and polyadenylation signal are underlined. An asterisk indicates the putative stop codon. Numbers to the left correspond to the single-letter amino acid sequence. Numbers to the right correspond to the nucleotide sequence.

The deduced protein of S100A14 shares 68% similarity and 38% identity to S100A13 (Accession No Q99584) being the closest human match. Significant similarity was also found with S100A4 (62% similarity; 30% identity), S100A2 (60% similarity; 30% identity), S100A10 (58% similarity; 31% identity), and S100A9 (55% similarity; 34% identity), as illustrated in Fig. 4. Furthermore, in the

SwissProt database we identified an apparent mouse orthologue, 1110013O05RIK protein (Accession No Q9D2Q8), showing 97% similarity (93% identity) using the human *S100A14* amino acid sequence as a query. A comparison between the *S100A14* cDNA and RIKEN 1110013O05 (1110013O05Rik) cDNA (GenBank Accession No NM_025393) revealed 87% identity.

S100A14	MGQCRSANAEDAQEFSDVERAIETLIKNFHOYS-VEGGKETLTPSELRLDVTQQLPHLMP	59
RIK	MGQCRSANAEDAQEFSDVERAIETLIKNFHKYS-VAGKKETLTPAELRLDVTQQLPHLMP	59
S100A13	-----MAAEPLTELEESIETVVVTFFTFARQEGRKDSLVSNEFKELVTQQLPHLLK	51
S100A4	-----MACPLEKALDVMVSTFHKYSGKEGDKFKLNKSELKELLITRELPSFLG	47
S100A2	-----MCSLEQALAVLVVTFHKYSCQEGDKFKLSKGEMKELLHKELPSFVG	47
S100A10	-----PSOMEHAMETMMFTFHKFAGDKG--Y-LTKEDLRVLMKEFFPGFLE	43
S100A9	-----MTCKMSQLERNIETIINTFHOYSVKLGHPDTLNQGEFFKELVRKDLQNFILK	50
S100A14	----SNCGLEEKIANLGSCNDSKLEFRSFWELIGEAAKSVKLER--PVRGH-----	104
RIK	----SNCGLEEKIANLGNCSNDSKLEFGSFWELIGEAAKSVKMER--PVTRS-----	104
S100A13	----DVGSLDEKMKSLDVNDSSELKFNEYWRILIGELAKEIRKKKDLKIRKK-----	98
S100A4	KR-TDEAAFOKILMSNLDNDRNEVDFOEYCVFLSCIAMMCNEFFEGFPDKQPRKK----	101
S100A2	EK-VDEEGLKKIMGNLDENSDQQVDFOEYAVFLALITVMCNDFEQGCPDR-P-----	97
S100A10	NQ-KDPLAVDKIMKDLQCRDQGVGFQSEFSLIAGLTIACNDYFVVHMKQKGKK-----	96
S100A9	KENKNEKVIEHIMEDLDTNADKQLSFEETIMLMARITWASHEKMHGEGDEGPGHHHKPGLG	110
S100A14	----	
RIK	----	
S100A13	----	
S100A4	----	
S100A2	----	
S100A10	----	
S100A9	EGTP 114	

Fig. 4 Alignment of the predicted amino acid sequences of the human S100A14 and the mouse orthologue 1110013O05RIK with the most homologous S100 family members. Homology is represented by shading of the amino acid identities. Identical amino acid residues are indicated as black boxes whereas similar amino acids are indicated as gray boxes.

3.2 Expression Profile in Tumour Cell Lines, Normal, and Neoplastic Tissues

3.2.1 *S100A14* mRNA Level in Tumour Cell Lines

To characterize *S100A14* expression in tumour cell lines from other tissues we extended the expression analysis to normal human cultured mammary epithelial cells, four immortalized epithelial cell lines, and 31 different human tumour cell lines as well as ten mouse and rat cell lines. The complete list of the examined cell lines is given in Table 2 and Table 3.

Table 2 Expression of *S100A14* mRNA in human cancer cell lines. *S100A14* transcript level was examined by Northern blot and RT-PCR analysis. The expression level was determined by semiquantitative scoring as follows: (+++) strong expression, (++) moderate expression, (+) weak expression, (RT-PCR) transcript not detectable by Northern blot but detected by RT-PCR, (–) negative expression. The tumour cell lines histopathology: SCLC, small cell lung cancer; ADC, adenocarcinoma; SCC, squamous cell carcinoma; LCLC, large cell lung cancer; Ca, carcinoma.

Cell lines	Histopathology	<i>S100A14</i>
HBE	Normal human bronchial epithelial cells	+++
SAE	Normal human small-airway epithelial cells	+++
H378	SCLC	–
H82	SCLC	–
COLO 677	SCLC	RT-PCR
H446	SCLC	–
CPC-N	SCLC	–
DMS-79	SCLC	+
H209	SCLC	RT-PCR
DMS-114	SCLC	–
H187	SCLC	RT-PCR
N417	SCLC	–
H526	SCLC metastatic	–
COLO 668	Brain metastasis of SCLC	–
SHP77	Large cell variant of SCLC	–
COLO 699	ADC	–
DV-90	ADC	+
H322	ADC	+
D51	ADC	RT-PCR
D54	ADC	RT-PCR
D117	ADC	–
H125	ADC	–
H23	ADC	–
A549	ADC	RT-PCR
H2228	ADC	RT-PCR
H2030	ADC	–
H157	SCC	–
H2170	SCC	+
H226	SCC mesothelioma	–
H596	Lung Ca	–
D40/97	Lung Ca	+
A427	Lung Ca	–
BEN	Lung Ca, lymph node metastasis	–
D97	LCLC	–
HBE-E6/E7	HBE immortalized with HPV-16	++
9442 (BET-1A)	HBE immortalized with SV40 early region	++

BEAS-2B	HBE immortalized with SV40 early region	++
YP44	HBE immortalized with SV40 early region	++
DU 145	Prostate Ca	–
PC-3	Prostate Ca	–
HMEC	Normal human mammary epithelial cells	++
HMEB	HMEC immortalized with telomerase and SV40	+
MCF-10A	Spontaneously immortalized mammary epithelial cells	++
MCF-7	Breast Ca	–
SK-BR-3	Breast Ca	–
MDA-MD-231	Breast Ca	–
Kato III	Metastasis of gastric Ca	++
HT-29	Colon Ca	+
SW-480	Colon Ca	–
HCT-116	Colon Ca	+
CaCo-2	Colon Ca	++
WiDr	Colon Ca	+
Lovo	Colon Ca	+++
CX-2	Colon Ca	+
HRT-18	Colon Ca	++
EJ	Bladder Ca	–
HeLa	Cervical Ca	–
Daudi	Burkitt's lymphoma	–
K562	Chronic myelogenous leukemia	–
HL-60	Promyelocytic leukemia	–
MOLT-4	Lymphoblastic leukemia	–
Raji	Burkitt's lymphoma	–
G361	Melanoma	–
SKOV-3	Ovarian Ca	–
OVCAR-3	Ovarian Ca	+
HT 1080	Fibrosarcoma	–
HEP-2	Head and neck Ca	–
D36-1/95	Head and neck Ca	+
D36-2/95	Head and neck Ca	+
D6/95	Head and neck Ca	+
D3/02	Head and neck Ca	–
IMR-90	Fetal lung fibroblasts	–
HAKAT	Immortalized keratinocytes	+
HEK 293	Human embryonic kidney epithelial cells	–

The *S100A14* mRNA is most abundant in cells cultured from normal human epithelial cells, but is absent from the vast majority of cancer-derived cell lines. Interestingly, most of the immortalized human cell lines also show significant

S100A14 mRNA expression. The *S100A14* mRNA level is relatively high in most of the colon tumour cell lines. We did not detect *S100a14* in any mouse or rat cell line examined using a mouse *S100a14* cDNA sequence as a hybridization probe.

Table 3 Expression of *S100A14* mRNA in other mammalian cell lines

Cell lines	Histopathology	<i>S100a14</i>
COS-7	Monkey kidney fibroblasts	–
RAW 264.7	Mouse macrophagoid immortalized cells	–
L-cells	Mouse immortalized fibroblasts	–
L-Wnt 3 cells	L-cells transfected with <i>Wnt-3A</i>	–
C57MG	Mouse mammary epithelial cells	–
ROSE 199	Rat ovarian surface epithelial cells	–
ROSE A2/1	ROSE 199 cells transfected with <i>KRas</i>	–
ROSE A2/5	ROSE 199 cells transfected with <i>KRas</i>	–
208F	Immortalized rat fibroblasts	–
FE-8	<i>HRas</i> -transformed derivative of 208F	–
IR-4	208F cells transfected with IPTG-inducible <i>Ras</i>	–

3.2.2 Expression Profile in Normal Human Tissues

We examined the expression pattern and transcript size of *S100A14* in normal human tissues by Northern blot hybridization using a cDNA probe corresponding to the complete protein coding region. The transcript of approximately 1.1 kb was expressed most abundantly in colon (Fig. 5A). Moderate levels of *S100A14* mRNA were detected in thymus, kidney, liver, small intestine, and lung. A very low expression level was detected in heart where a slightly longer transcript of approximately 1.35 kb was observed. No expression could be detected in brain, skeletal muscle, spleen, placenta, and peripheral blood leukocytes. Additionally, *S100A14* was expressed in normal breast, ovary, prostate, rectum, stomach, thyroid, and uterus as determined by hybridization to the Cancer Profiling Array (Fig. 5B).

To confirm the mRNA expression data, we analysed a panel of normal human tissues by immunohistochemistry using a polyclonal anti-S100A14 antibody raised in rabbit. The *S100A14* protein expression was predominantly associated with various epithelia as well as gland cells (Table 4). The expression

pattern was virtually consistent with the *S100A14* mRNA expression in normal human tissues. The exceptions were brain and placenta, showing a weak expression of *S100A14* protein, in contrast to the absence of the transcript in Northern blot analysis.

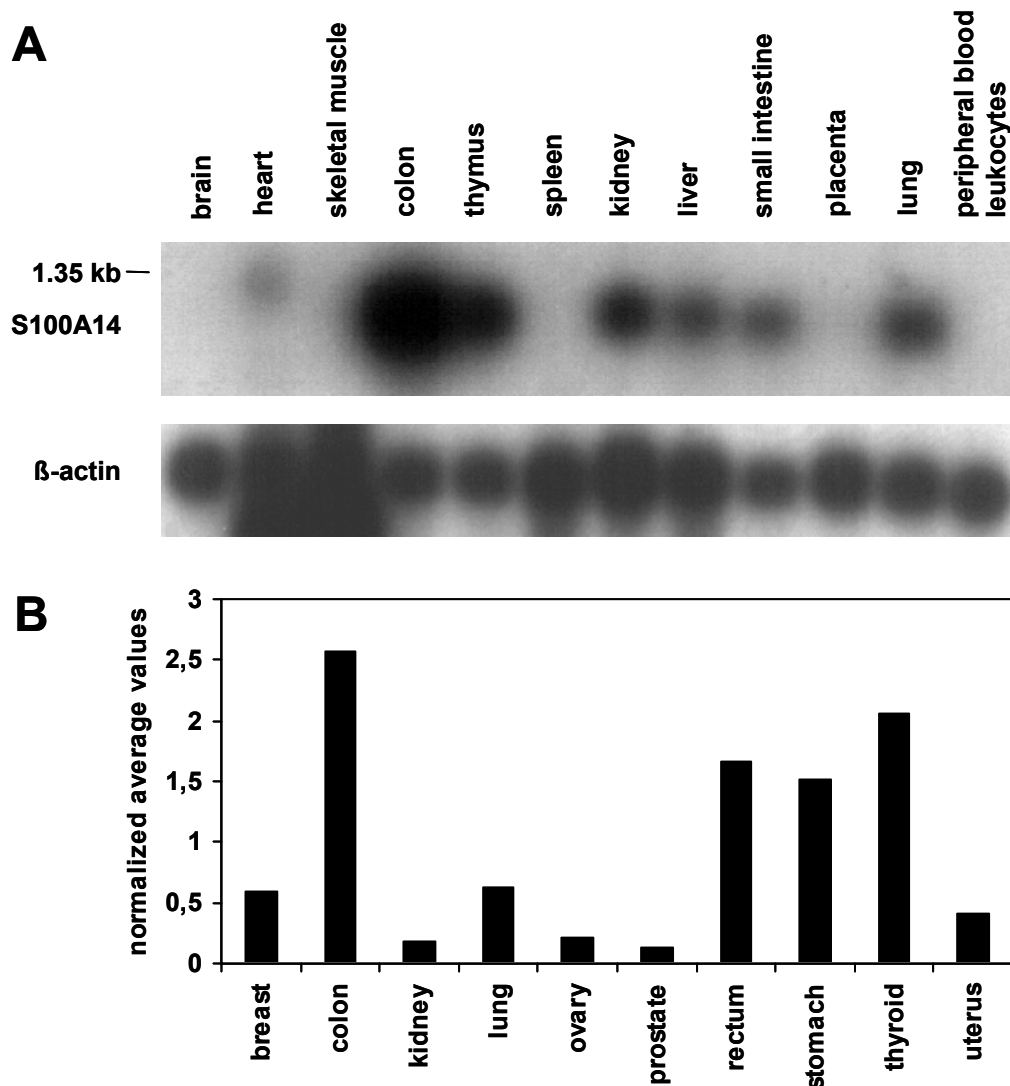


Fig. 5 Expression of the *S100A14* mRNA in normal human tissues. **A:** A human 12-lane Multiple Tissue Northern Blot (BD Biosciences) containing 2 µg poly(A)⁺ RNA in each lane was hybridized with a ³²P-labelled *S100A14* cDNA probe. β-actin was assayed as a loading control. **B:** Expression of *S100A14* mRNA in additional normal human tissues examined by hybridization to the Cancer Profiling Array (BD Biosciences).

These results suggest that there is a very low *S100A14* expression in these tissues and a not sufficient sensitivity of Northern blot to detect low abundant transcripts.

Table 4 Expression of the S100A14 protein in normal human tissues

Tissue	S100A14 Expression
Pancreas	Islet cells, endocrine pancreas
Spleen	Negative
Breast	Mammary gland cells
Smooth muscle	Muscle fibres weakly positive
Skeletal muscle	Negative
Salivary glands	Salivary gland cells, exocrine salivary glands
Gall bladder	Basal cytoplasm of goblet cells
Thyroid	Follicular epithelium
Kidney	Tubular epithelium
Tonsille	Squamous epithelium
Appendix	Epithelium
Lung	Pneumocytes
Uterus	Apical epithelium, stroma cells and smooth muscle weakly positive
Prostate	Epithelium, stroma cells and smooth muscle weakly positive
Stomach	Epithelium, gland cells weakly positive
Parathyroid gland	Epithelium
Placenta	Trophoblast cells weakly positive
Colon	Epithelium
Testis	Spermatocytes and stroma cells weakly positive
Small intestine	Epithelium
Heart	Cardiac muscle fibres weakly positive
Cervix	Suprabasal cells of squamous epithelium, basal cells weakly positive
Liver	Hepatocytes, bile duct epithelium
Brain	Ganglia cells
Skin	Squamous epithelium, hair follicles, sweat glands
Endothelium	Weakly positive

3.2.3 *S100A14 mRNA Level in Tumour Tissues*

Since *S100A14* mRNA was not expressed in most of the tumour-derived cell lines, we hypothesized that its expression might be suppressed also in primary tumour tissue. To examine its expression in primary tissue we applied a commercially available Cancer Profiling Array, which contains cDNAs from 241 tumours and corresponding normal tissues from individual patients. This analysis, however, revealed a varied expression of the gene in different tumours (Fig. 6A). Significant overexpression was detected in ovary (78.6%), breast (62%), and uterus (45.2%) tumour tissues. Also lung (38.1%), prostate (25%), and thyroid gland (16.7%) tumours showed up-regulated levels of *S100A14* transcript. In contrast, marked

underexpression was found in kidney (70%), rectum (50%), and colon (40%) tumours and to lesser extent in stomach tumours (18.5%). The expression status in cervix, small intestine and pancreas tumours could not be evaluated because of the limited number of samples available on the array. The schematic presentation of *S100A14* expression in normal and tumour tissues is shown in Fig. 6B.

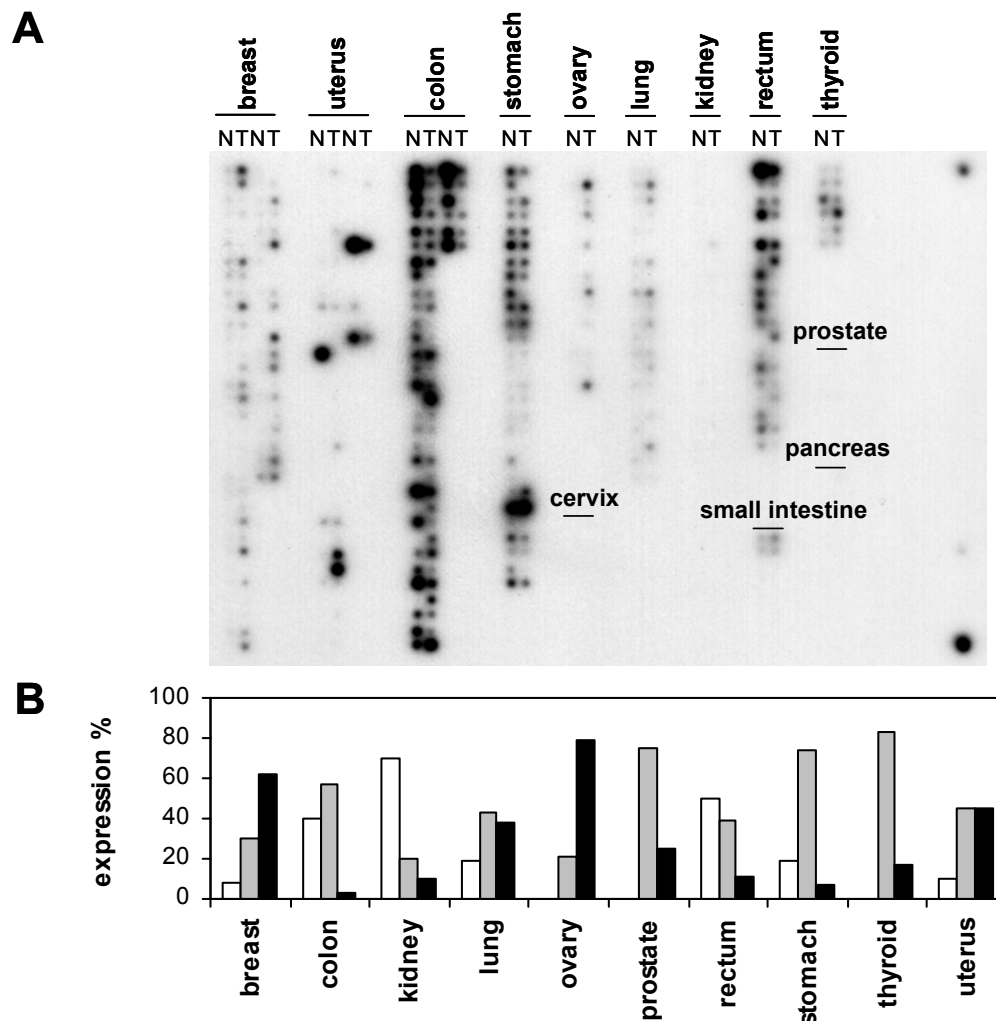


Fig. 6 Expression profile of *S100A14* in human tumours. **A:** The Cancer Profiling Array containing SMART-amplified cDNA from tumour (T) and corresponding normal (N) tissues from individual patients was hybridized with 32 P-labelled *S100A14*-specific probe. Hybridization to ubiquitin cDNA (top and bottom) and *E.coli* DNA (middle) is shown on the right side of the array. Human cancer cell lines (no detectable signal) are spotted on the right. **B:** The schematic presentation of *S100A14* expression in normal and tumour tissues determined by hybridization to the Cancer Profiling Array. Data are expressed as percentage of up-regulated, down-regulated and normal samples and normalized to all spots on the membrane to correct for RNA quantity and integrity. The grey bars represent normal expression level, the black and white bars denote up-regulated and down-regulated expression, respectively. Signal intensities were quantified after several exposure times to compensate for differences in mRNA expression between different organs.

3.2.4 S100A14 Protein Expression in Lung Tumours and Association with Clinicopathological Factors

Our transcript expression analysis in primary tumour tissues suggested that S100A14 is not a simple suppressor of tumour cell growth as might have been concluded from the cell line model system. It is possible that its altered expression is a result of, or otherwise associated with, tumour progression. To shed light on the association of S100A14 protein with malignant transformation and to verify the RNA expression data we used immunohistochemistry to investigate its expression in tumour tissues.

S100A14 protein was examined in 120 histological sections of human lung cancer and 10 specimens of normal human lung epithelium. The cohort of tumour samples included 62 cases of adenocarcinoma (51.7%) and 58 cases of squamous cell carcinoma (SCC) (48.3%). The small number of samples precluded a separate analysis of large cell lung cancer (LCLC) tumour specimens. We observed a low cytoplasmic S100A14 staining in normal lung epithelium (score 0 to 1+; Fig. 7). Therefore, we approved a scoring of 2+ and 3+ as indicative of protein overexpression for our analysis. Scores 0 or 1+ were considered as physiologically normal expression.

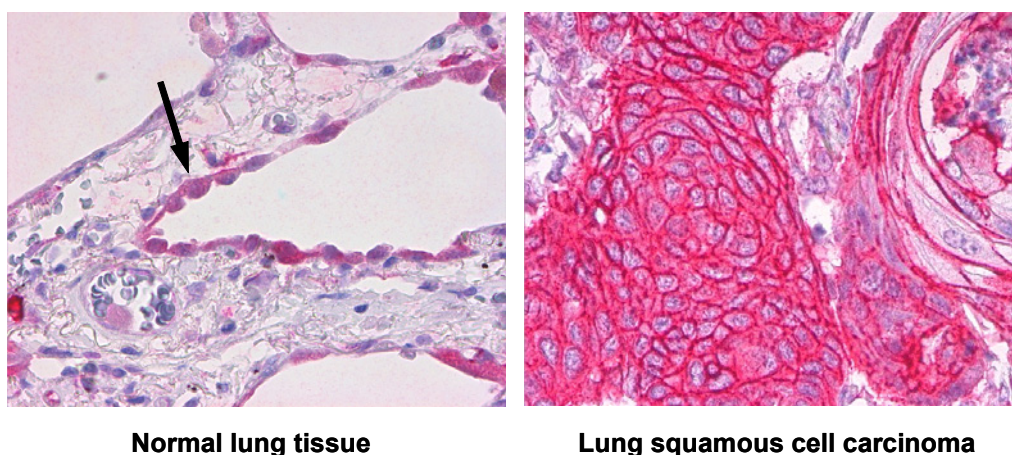


Fig. 7 S100A14 protein is overexpressed in primary lung tumour tissue in comparison to normal lung tissue. Immunohistochemical staining of S100A14 protein in tissue sections of normal lung pneumocytes (left, indicated by an arrow) and lung squamous cell carcinoma (right). Specimens were stained with an anti-S100A14 antibody. Photographs were taken with a 40x objective.

Positive staining was assessed not only as the degree of staining intensity but also as the proportion of cells with staining of both plasma membrane and cytoplasm as compared with those of cytoplasmic staining alone.

S100A14 immunoreactivity in tumour tissue scored positive in 68.3% (82/120) of cases thus validating its up-regulation in this tumour type (Fig. 7). The S100A14 staining was restricted to the cancerous epithelial cells of the tissue. Next, S100A14 expression was analysed in relation to clinicopathological criteria. No significant correlation was found between S100A14 positivity and gender, age, histological subtype, tumour size, number of positive lymph nodes, and histological grade.

We found that 57.3% (47/82) of S100A14-overexpressing lung tumours displayed cytoplasmic and membranous expression relative to exclusively cytoplasmic S100A14 staining in normal lung epithelium ($p = 0.006$; Fig. 8).

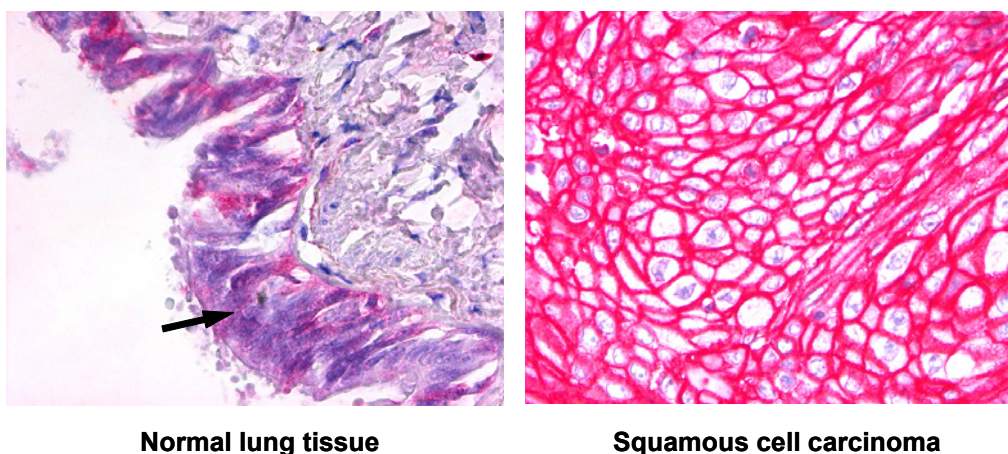


Fig. 8 S100A14 localizes to plasma membrane in lung tumour tissue. Immunohistochemical analysis of S100A14 protein in sections of normal bronchial epithelial cells (left) and lung squamous cell carcinoma (right). Panels show high power microscopy (magnification, 40x), demonstrating cytoplasmic staining of S100A14 in normal bronchial epithelial cells (left, indicated by an arrow) and distinct plasma membrane-associated staining of S100A14 in lung carcinoma cells (right).

Moreover, we observed a significant association ($p = 0.048$) between higher-grade tumours (grade 3) and S100A14 subcellular distribution. 50% (27/54) of high-grade tumours displayed S100A14 protein localized both to the cytoplasm and the plasma membrane. Another relation was found between lung tumour histology and subcellular distribution of S100A14. Cytoplasm and plasma membrane-localized S100A14 staining was associated with 61.8% (34/55) of SCC ($p = 0.02$) compared

to 38.2 % (20/58) of adenocarcinoma tumours, the latter detecting predominantly cytoplasmic S100A14 (65.5%; 38/58). S100A14-negative tumours were not included in the statistical analysis of the subcellular distribution of S100A14. These results are summarized in Table 5.

Table 5 Association of S100A14 protein expression in lung tumours with clinicopathological factors

Parameter	S100A14 positive/total	<i>p</i>	memb.+cytopl. positive/total	<i>p</i>
S100A14 overexpression	68.3% (82/120)			
Membranous+cytoplasmic	57.3% (47/82)	< 0.01		
High grade			50% (27/54)	0.048
Histological subtype				
Adenocarcinoma			38.2% (20/58)	
Squamous cell carcinoma			61.8% (34/55)	< 0.01

3.2.5 S100A14 Protein Expression in Breast Tumours and Association with Clinicopathological Factors

A significant up-regulation of *S100A14* mRNA in breast tumours prompted us to investigate this tumour type by immunohistochemistry. We examined S100A14 protein expression in 93 breast tumour samples, 14 lymph node metastases and 10 normal mammary epithelia. In our cohort of breast tumours were 77 invasive ductal carcinomas (IDC), 14 invasive lobular carcinomas (ILC) and 2 cases of mixed type (IDC+ILC).

Normal mammary epithelium stained rather weakly for S100A14 protein with cytoplasm-localized staining (score 1+; Fig. 9). Therefore we applied the same scoring as for lung tumours, *i.e.* scores 0 to 1+ were considered as normal physiological expression, whereas scores of 2+ and 3+ were assessed as positive and indicative of protein overexpression. S100A14 positivity was detected in 68.8% (64/93) of breast tumour samples and 71.4% (10/14) of lymph node metastases (Fig. 9). Clinical relevance of S100A14-overexpressing tumours was investigated only in IDC cases due to small sample number of other tumour subtypes. No significant correlation with gender, age, histological subtype, tumour size, number of positive lymph nodes or histological grade was observed.

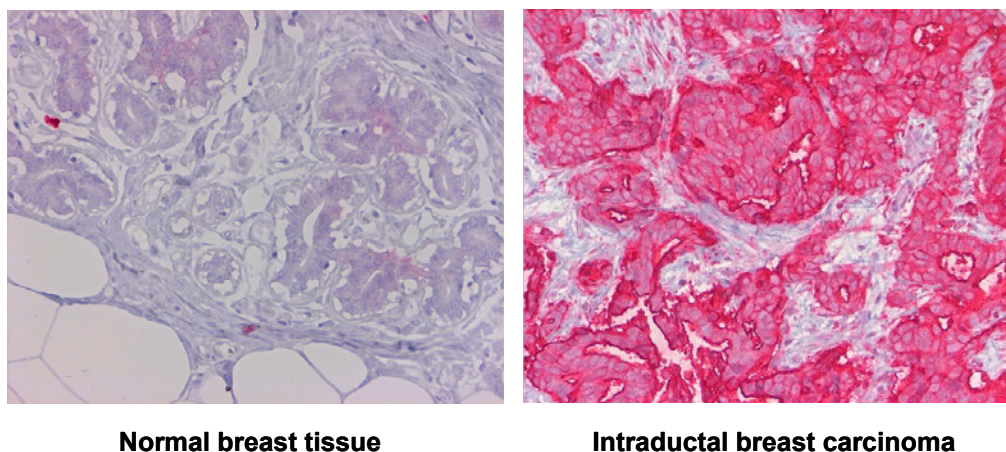


Fig. 9 S100A14 protein is up-regulated in primary breast carcinoma relative to normal breast tissue. Immunohistochemical analysis of S100A14 protein in normal breast ductal epithelial cells (left) and ductal carcinoma epithelial cells (right). Specimens were stained with an anti-S100A14 antibody. Photographs were taken with a 20x objective.

Interestingly, we found a significant correlation between a high S100A14 level and ERBB2 overexpression ($p = 0.04$). 82.9% (29/35) of ERBB2-overexpressing tumours (score 2+ and 3+) had up-regulated S100A14 expression as well (Fig. 10). To further substantiate this finding, we separately examined 31 ERBB2-overexpressing breast tumours of score 3+. We found that 90.3% (28/31) of ERBB2-positive tumours were also S100A14-positive.

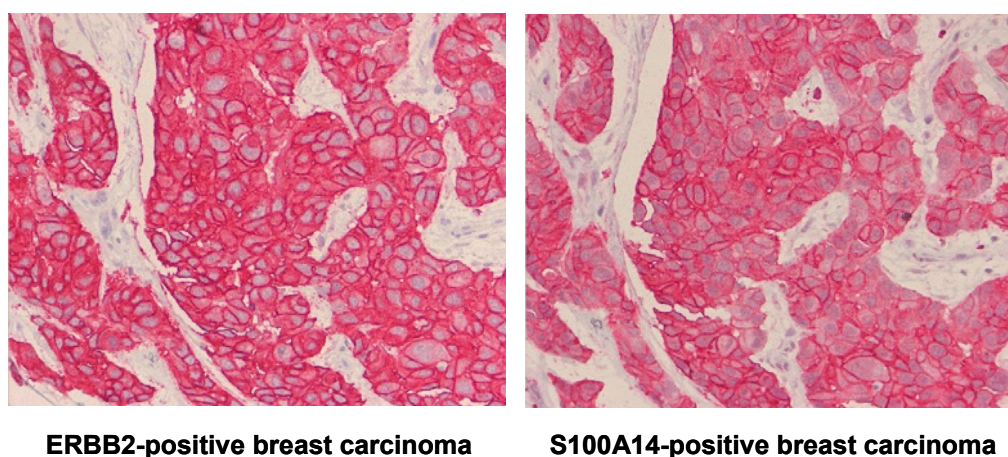


Fig. 10 S100A14 overexpression correlates with ERBB2 overexpression in primary breast tumours. Immunohistochemical analysis of a section of a breast ductal carcinoma specimen stained both with anti-ERBB2 antibody (left) and (the same section) with anti-S100A14 antibody (right). Photographs were taken with a 40x objective.

Oestrogen receptor- α (ER- α) negativity was also significantly associated with elevated levels of S100A14 ($p = 0.024$). 87.5% (21/24) of ER- α -negative tumour specimens were S100A14-positive. Moreover, a significant association to increased tumour cells proliferation index (MIB) was observed ($p = 0.033$). 100% (11/11) of tumours assessed as highly proliferating (60-100% of actively proliferating cells) stained positively for S100A14.

Also in this case the subcellular distribution of S100A14 was related to S100A14 protein abundance. 79.7% (59/74) of S100A14-overexpressing tumours displayed prominent plasma membrane and cytoplasmic localization of S100A14 ($p < 0.01$) relative to 34.8% (8/23) of low-expressing tumours showing predominantly cytoplasmic staining (65.2%; 15/23). In contrast to this tumour cell plasma membrane localization, normal human breast epithelial cells showed solely diffuse cytosolic S100A14 expression (Fig. 11). For the statistical analysis of subcellular localization of S100A14 we omitted the S100A14-negative samples. These results are summarized in Table 6.

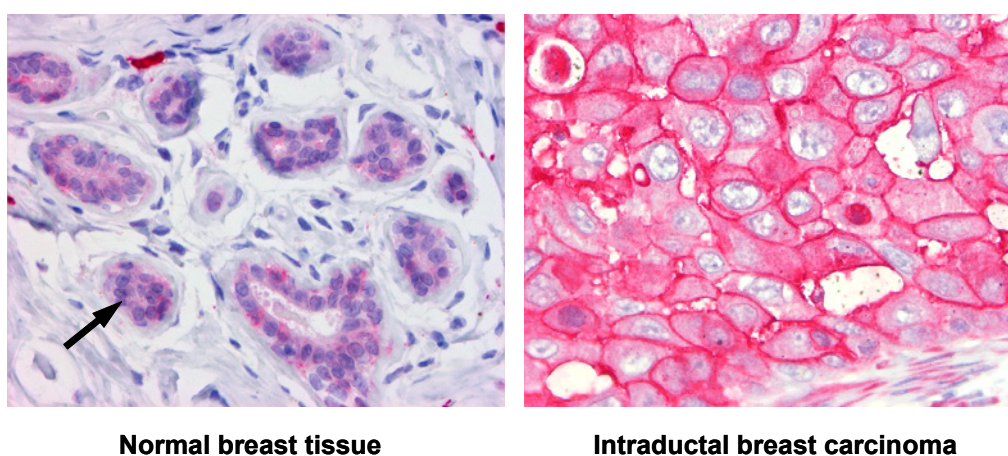


Fig. 11 S100A14 localizes to plasma membrane in breast cancer tissue. S100A14 immunostaining in sections of normal breast ductal epithelial cells (left) and breast ductal carcinoma sections (right). Panels show high power microscopy (magnification, 40x), demonstrating cytoplasmic staining of S100A14 in normal breast ductal epithelial cells (left, indicated by an arrow) and plasma membrane-associated staining of S100A14 in breast carcinoma cells (right).

Our transcriptional and protein analysis demonstrated that expression of *S100A14* in primary tumours differed from that in cell line model; the gene was significantly overexpressed in multiple lung and breast tumour samples. Nevertheless, our data also confirmed the differential expression of the gene in a wide range of primary

tumours as well as its potential clinical relevance with regard to the positive correlation with ERBB2 overexpression in breast tumours. Therefore, we decided to further characterize the gene and the molecular determinants of its regulation.

Table 6 Association of S100A14 protein expression in breast tumours with clinicopathological factors

Parameter	S100A14 positive/total	<i>p</i>
S100A14 overexpression	68.8% (64/93)	
ERBB2 overexpression	82.9% (29/35)	0.04
ER- α negativity	87.5% (21/24)	0.024
MIB	100 % (11/11)	0.033
Membranous+cytoplasmic	79.7% (59/74)	< 0.01

3.2.6 S100A14 is not Re-Expressed Following Growth of Human Cancer Cell Lines Transplanted into Mice

To determine if the absence of *S100A14* in the vast majority of cultured tumour cell lines could be due to differences between the cell model system and the primary tissue, we examined 9 mouse xenograft tumours of human cultured lung cancer cell lines. They represented the following histopathological types: SCLC (CPC-N, H526, H446, H82, H209, N417), brain metastasis of SCLC (Colo 668), adenocarcinoma (D54), and LCLC (D97). These cell lines do not express endogenous *S100A14* in Northern blot analysis.

RT-PCR analysis did not reveal re-expression of the *S100A14* transcript in the majority of the examined xenografts (Fig. 12).

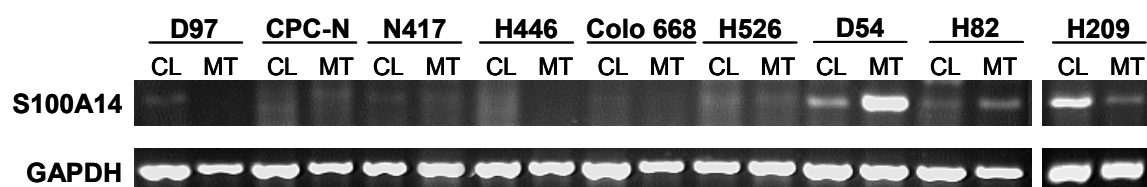


Fig. 12 S100A14 is not re-expressed in lung cancer cell line xenografts from nude mice. Nine *S100A14*-negative human lung cancer cell lines (CPC-N, H526, H446, H82, H209, N417, Colo 668, D54, and D97) were transplanted subcutaneously into immunodeficient mice. Mouse xenograft tumours (MT) and the respective lung cancer cell lines (CL) were examined by RT-PCR. GAPDH was used as a loading control.

An enhanced *S100A14* mRNA expression was clearly present only in the D54 xenograft tumour as compared with the corresponding cell line. A very weak mRNA expression was detected in the H82 cell line and the corresponding xenograft as well as in the D97 cell line. A modest mRNA expression was observed in the H209 cell line and a weak expression in the corresponding xenograft.

3.3 Subcellular Localization of the S100A14 Protein

In an attempt to achieve a better understanding of the biology of the S100A14 protein, we examined its subcellular localization by immunofluorescence. Initially, we expressed the protein as carboxyl-terminal fusion of V5-epitope, and determined expression of the fusion protein after transient transfection by confocal laser-scanning microscopy. H157, A549, and COS-7 cells were chosen for their absence of *S100A14* transcript in Northern blot analysis.

Distinct subcellular localizations were detected in all analysed cell lines. Immunoreactivity was observed in the cytoplasm with a higher expression around the nucleus in A549 and COS-7 cells (Fig. 13A, B). H157 cells displayed a pronounced immunoreactivity in the perinuclear area (Fig. 13C). Control incubation with mock-transfected cells was completely negative (Fig. 13D). Expression of the protein was also confirmed by Western blot analysis (Fig. 13E).

To confirm that the localization studies performed with epitope-tagged protein corresponded to the subcellular distribution of endogenous protein, we applied the polyclonal antibody against the endogenous S100A14 protein. Patterns of subcellular distribution and expression of S100A14 protein were examined in immortalized lung cells (9442, 2078), colon tumour (Caco-2, HCT-116, Lovo, WiDr), and lung tumour (H322) cells.

9442 and 2078 cells displayed strong plasma membrane immunoreactivity of sharp and clear pattern with the exception of cell protrusions where more diffuse staining was observed (Fig. 14A, B). Additionally, a very weak and diffuse cytoplasmic S100A14 staining was detectable. This staining pattern is consistent with our analysis of fractionated proteins in 9442 cells (see below).

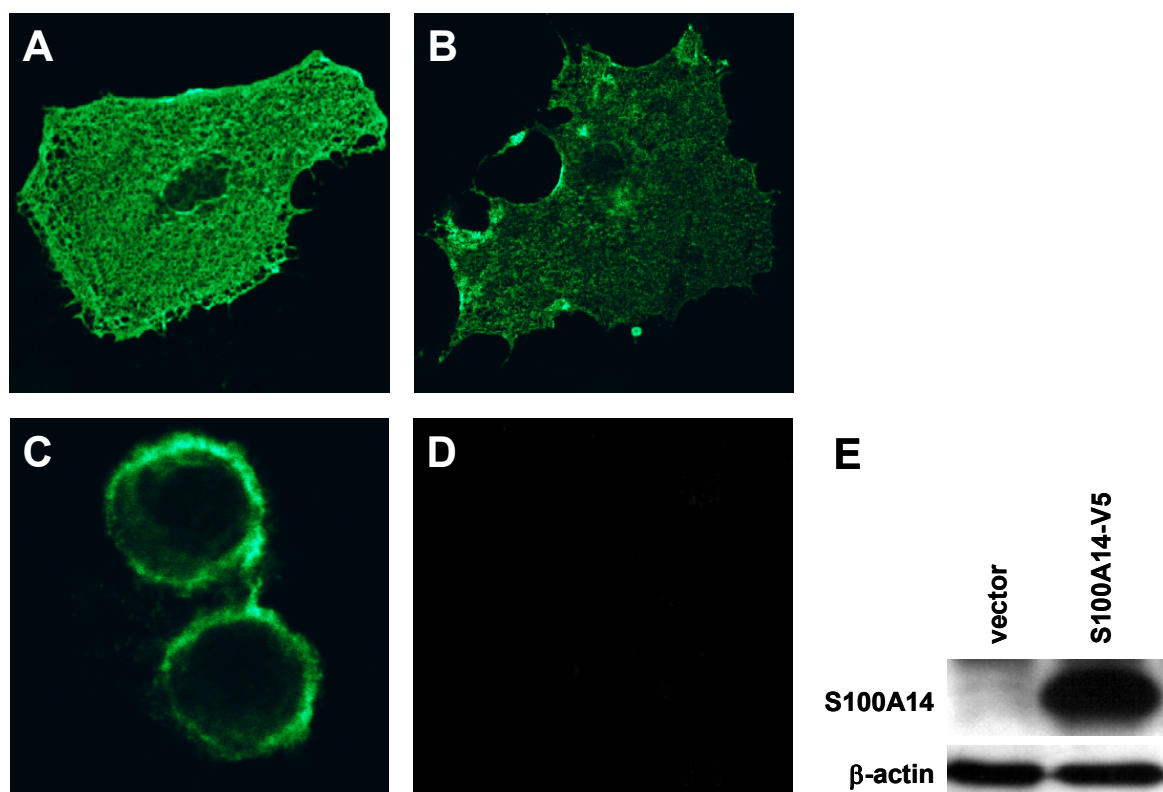


Fig. 13 Cellular localization of S100A14-V5 protein in human lung tumour and COS-7 cells. **A:** A549 (lung tumour), **B:** COS-7 (monkey kidney fibroblasts), and **C:** H157 (lung tumour) cells were transiently transfected with the S100A14-V5 expression vector. Forty-eight hours after transfection immunofluorescent analysis was performed using confocal laser scanning microscopy. Cells were examined for localization of S100A14-V5 after indirect staining with monoclonal anti-V5 primary antibody and anti-mouse FITC-conjugated secondary antibody. Magnification using 60x oil immersion objective. **D:** Control incubation with mock-transfected cells was completely negative. **E:** Expression of the protein was confirmed by immunoblotting analysis. Vector-transfected cells were used as a negative control. Equal loading was determined by immunoblotting with anti-β-actin antibody.

Moreover, strong S100A14 expression was observed in actively proliferating cells (Fig. 14C). Interestingly, staining of distinct vesicles of unknown origin was also observed in these cells (Fig. 14D). H322 and HCT-116 cells, which grow in colonies, expressed S100A14 in similar patterns (Fig. 14E, F). Immunofluorescent staining in these cells revealed distinct immunoreactivity at cell junctions with occasionally stronger plasma membrane expression relative to neighbouring cells indicating a heterogeneous expression. Weak and diffuse cytoplasmic staining was also observed. In contrast, Caco-2 cells had diffuse rather than sharp staining at cell junctions and moderately strong and homogenous cytosol immunoreactivity (Fig. 14G). Prominent membranous staining was observed in Lovo cells with focally stronger expression (Fig. 14H). Overall staining was low in WiDr cells

showing heterogenous expression at cell junctions (data not shown). Control incubation with preimmune serum was completely negative (Fig. 14I).

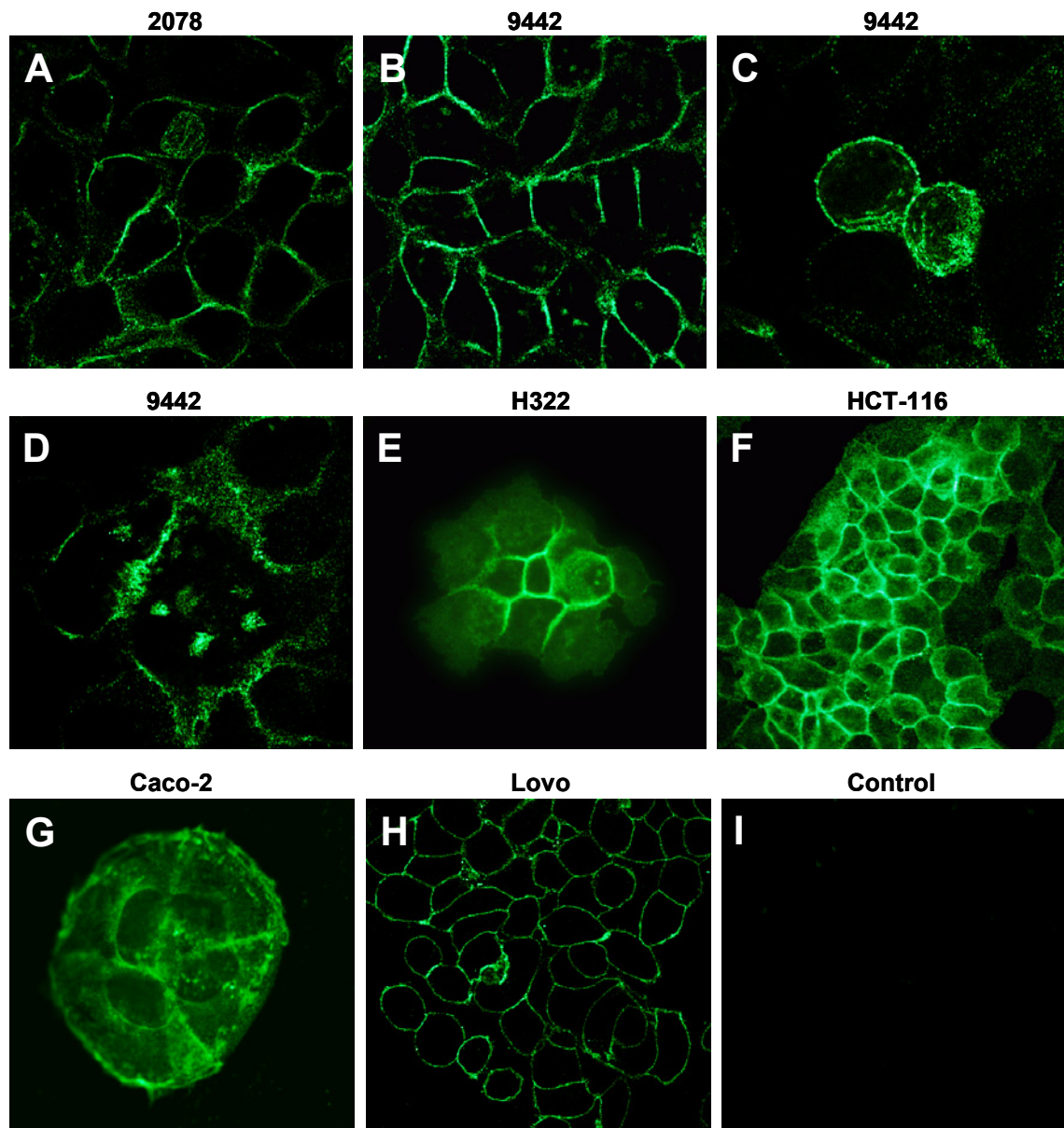


Fig. 14 Subcellular localization of the endogenous S100A14 protein in immortalized lung cells, and lung and colon tumour cells. Immunofluorescence microscopy of **A:** 2078, **B, C, D:** 9442 (immortalized lung epithelial cells), **E:** H322 (lung tumour), **F:** HCT-116, **G:** Caco-2, and **H:** Lovo. Cells were fixed and stained with the polyclonal anti-S100A14 antibody and with the secondary anti-rabbit FITC-conjugated antibody. Magnification using 60x oil immersion objective. **I:** Control incubation with preimmune serum was completely negative.

To verify the data obtained by immunofluorescence, we fractionated whole-cell extracts into membrane and soluble components. Soluble and crude membrane fractions of 9442 cells were prepared by hypotonic lysis, Dounce homogenization,

and differential centrifugation. Western blot analysis with anti-S100A14 antibody revealed that S100A14 was predominantly associated with the membrane fraction, whereas only very little S100A14 protein was detected in the soluble form (Fig. 15). These data indicate that the cells endogenously expressing S100A14 preferentially target the protein to the plasma membrane.

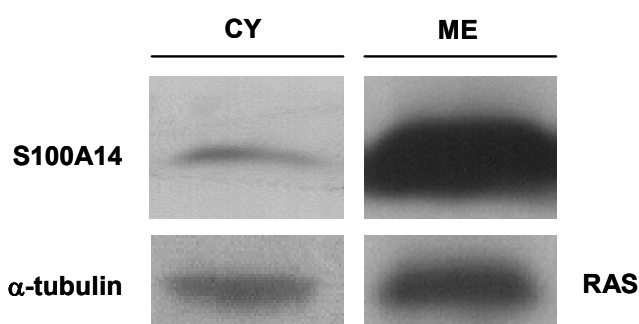


Fig. 15 The S100A14 protein is distributed through the cytoplasmic and membranous fractions of 9442 cells. Total proteins from 9442 cells were fractionated. For SDS-PAGE, 80 μ g of protein extract from each fraction was used for loading. Immunoblotting was performed with a polyclonal anti-S100A14 antibody. The specific S100A14 band was detected in the cytoplasmic (CY) and membranous fraction (ME). α -tubulin and RAS were assayed as loading controls for cytoplasmic and membranous fraction, respectively.

It was of interest to determine whether divalent cations could affect the subcellular localization of S100A14. To characterize the dependence of the subcellular distribution of S100A14 on the intracellular Ca^{2+} and Zn^{2+} levels, we treated 9442, 2078, Caco-2, WiDr, Lovo, HCT-116, and H322 cells with thapsigargin in conjunction with 1 mM CaCl_2 as well as with ZnCl_2 . Thapsigargin increases intracellular Ca^{2+} levels by blocking endoplasmic reticulum calcium pumps. We observed predominantly plasma membrane anti-S100A14 staining under all conditions tested, with no detectable alterations in distribution pattern.

3.4 Genomic Organization and Chromosomal Localization of the *S100A14* Gene

Most of the human *S100* genes are clustered on the chromosome 1q21, a region which is frequently involved in chromosomal rearrangements and deletions in human cancers. In order to identify the mechanisms of abnormal *S100A14* expression in tumours we sought to determine its genomic structure and localization.

To obtain *S100A14* genomic sequence data, human RPCI 1,3-5 PAC blood genomic libraries (RZPD) were screened with the purified insert of the full-length cDNA clone of human *S100A14* (H1043). We obtained 18 positive clones that we re-screened by PCR using several cDNA-derived primer pairs: H1043f, H1043ex1f, H1043ex2f, H1043ex3f, and H1043r.

We identified three candidate positive clones, RPCIP704 I22230Q2A, RPCIP704 A12752Q2, and RPCI P704 D11609Q2 (designated I22230, A12752, and D11609), and subjected them to a second screening by PCR to confirm their positive status. Following assembly of the genomic sequence of *S100A14* based on the Celera's human genome-unassembled fragments database (Venter et al., 2001), we designed the following PCR primers located in the flanking region of the exon/intron junctions of the relevant putative introns: H1043i1for, and H1043i1rev; H1043i2for, and H1043i2rev; H1043i3for, and H1043i3rev. The three genomic PAC clones were confirmed positive by this screening. Southern blot analysis revealed an approximately 3-kb region of overlap among the three clones that were positive for hybridization with the *S100A14* cDNA and intronic probes (Fig. 16A). The restriction enzyme-digested fragments covering that region were subcloned and sequenced to identify the genomic organization of *S100A14* (Fig. 16B).

In total, we obtained 3173 bp of continuous genomic sequence. In addition to the genomic locus of the *S100A14* gene, it included part of the putative 5' upstream promoter sequence and the 3' downstream region of the gene. It was consistent with the compiled sequence identified in Celera's human genome-unassembled fragments database using *S100A14* cDNA as a query. The sequence was submitted to GenBank under Accession No AF426828.

Comparison of the genomic and cDNA sequence revealed that the gene spanned 2165 bp. It was organized in four exons and three introns (Fig. 17). Exon 1 is untranslated, exon 2 contains the translation initiation codon and the putative N-myristoylation site, and exon 3 codes for the N-terminal EF-hand motif. The latter exon contains the C-terminal EF-hand motif and the translation termination codon followed by 630 bp of 3'-untranslated sequence. All the intron/exon boundaries confirmed to the GT-AG rule (Table 7).

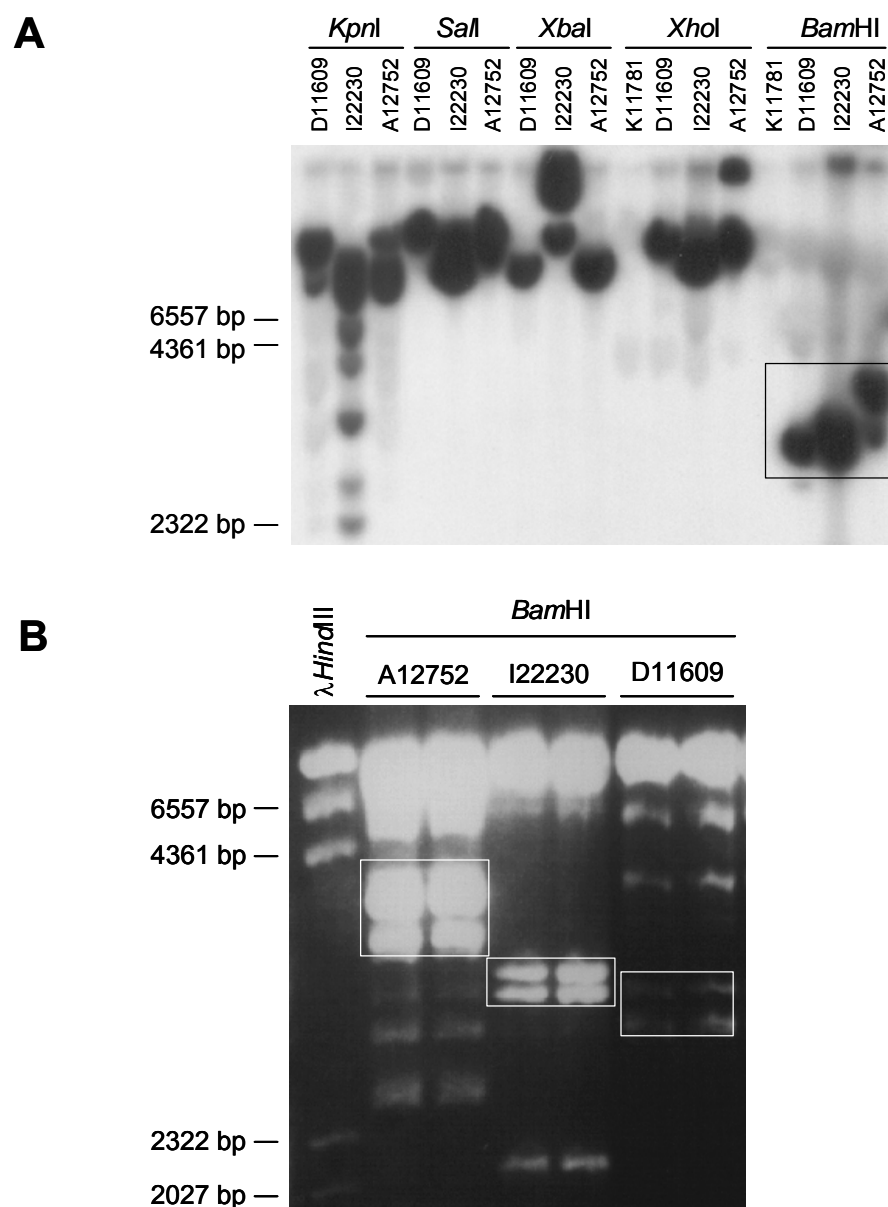


Fig. 16 Southern blot analysis of the genomic PAC clones positive for S100A14. Southern blot analysis of the candidate S100A14-positive clones, RPCIP704 I22230Q2A, RPCIP704 A12752Q2, and RPCI P704 D11609Q2. **A:** Restriction analysis with *Bam*HI, *Xba*I, *Kpn*I, *Xho*I, and *Sal*I restriction endonucleases revealed a ~3-kb region of overlap (rectangle) among the three clones that were positive for hybridization with the S100A14 cDNA and intronic probes. **B:** The *Bam*HI-digested fragments covering that region (rectangles) were subcloned and sequenced. Genomic PAC clone K11781, which was negative by PCR, was assayed as a negative control. λ *Hind*III-digested DNA was used as a molecular size marker.

We also identified a candidate TATAA box, lacking the third and fourth adenosine residues (Bucher, 1990), 26 bp upstream from the transcription initiation site determined by RACE. No other consensus promoter sequences were identified in

the entire 5' region sequenced, suggesting that the 5'-end of the cDNA sequence is in fact the major initiation site for the gene.

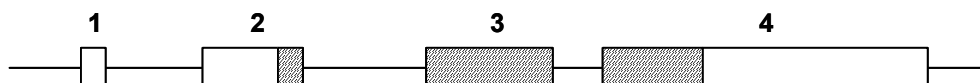


Fig. 17 Genomic structure of the human *S100A14*. Schematic representation of the exon/intron organization. Boxes represent exons, and intervening lines represent introns. The hatched region within the boxed exons denotes the coding sequence.

Sequence analysis of the entire genomic locus of *S100A14* did not reveal any CpG island. This was in accordance with our DNA hypermethylation analysis in 8 lung cancer cell lines. Treatment with 5-aza-2'-deoxycytidine (20 μ M) did not induce re-expression of the gene either.

A search for repetitive elements revealed AluY subfamily repeat of 283-bp (nt 2450-2732) located near the polyadenylation site as well as (TG)_n and (GA)_n simple repeats in the putative promoter region.

We verified the human *S100A14* genomic sequence by Southern blot hybridization to examine the possibility of deletion or gross rearrangement in the gene. The 1628-bp (*Sac*I; spanning all introns and coding exons) and 500-bp (*Eco*RI; spanning exon 3 and part of exon 4) bands were found to be informative for the verification of the assembly. Using the cDNA sequence that covers the coding region of *S100A14* as a probe for the hybridization, we observed the same restriction pattern for each enzyme in both *S100A14*-negative and *S100A14*-positive tumour cells. A single band was detected in digests of 25 tumour cell lines (Fig. 18).

Table 7 Exon/intron boundaries of the human *S100A14* gene. The exon and intron sequences are shown in upper- and lowercase letters, respectively. Splice acceptor and donor sequences are shown in boldface type.

Exon	cDNA position (bp)	Exon size (bp)	3' splice acceptor (intron/exon)	5' splice donor (exon/intron)	Intron size (bp)
1	1-30	30		GCCAACAG/ gt aaggaa	358
2	31-138	108	ctaagc ag /ATCATGAG	ACGCAGAG/ gt gggctc	447
3	139-285	147	gccctc ag /GATGCTCA	TCATGCCG/ gt atggac	212
4	286-1067	782	cccctc ag /AGCAACTG		

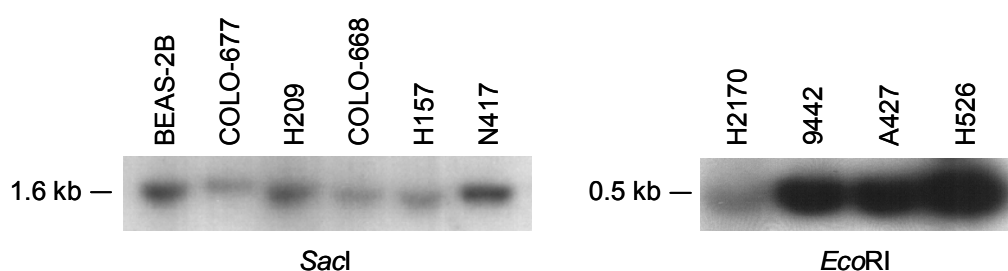


Fig. 18 Southern blot analysis of the *S100A14* gene in lung cancer cell lines. Southern blot analysis of the representative *S100A14*-positive (2078, 9442, H2170) and *S100A14*-negative (Colo 677, H209, Colo 668, H157, N417, A427, H526) cell lines. Genomic DNA (30 µg) isolated from 25 lung tumour cell lines was digested with *SacI* and *EcoRI* (300 U). The 1628-bp (*SacI*) and 500-bp (*EcoRI*) bands were detected in digests of all examined cell lines. *S100A14* cDNA sequence that covers the protein coding region was ³²P-labelled and was used as a probe for hybridization.

Next, the three PAC clones were used to determine the chromosomal localization of *S100A14* by fluorescence *in situ* hybridization (FISH) on normal human metaphase chromosomes. All clones revealed a strong signal at chromosome band 1q21 with the clone I22230 being the most specific (Fig. 19).

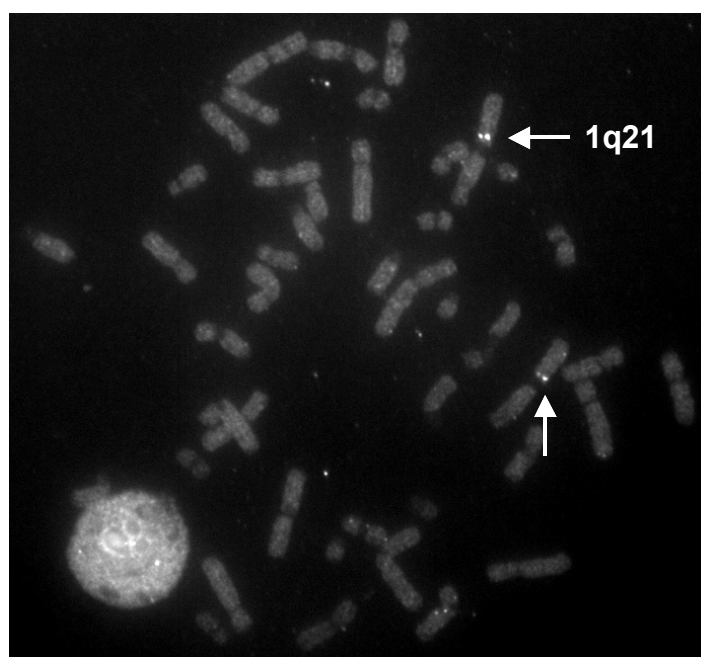


Fig. 19 Chromosomal localization of *S100A14* by FISH. The FISH analysis was performed on metaphases of normal human lymphocytes using biotin-16-dUTP-labelled genomic PAC clone I22230. White arrowheads indicate the specific signal on chromosome 1q21.

Clones A12752 and D11609 showed additional weaker signals on other different chromosomes. Due to the presence of these signals the mapping result was

confirmed and refined by hybridizing the *S100A14* cDNA to the established 6 Mb YAC contig and to the genomic restriction map of region 1q21 (Marenholz et al., 1996, 2001). The specific probe detected two of the 24 YACs of the contig, 100_f_3 and 950_e_2, which were already known to contain several other genes of the *S100* gene cluster in chromosomal region 1q21 (Schäfer et al., 1995, Marenholz et al., 1996) (Fig. 20A). *S100A14* was mapped on the same *SalI* fragment as *S100A1* and *S100A13*, the most telomeric genes of the established *S100* cluster (Fig. 20B).

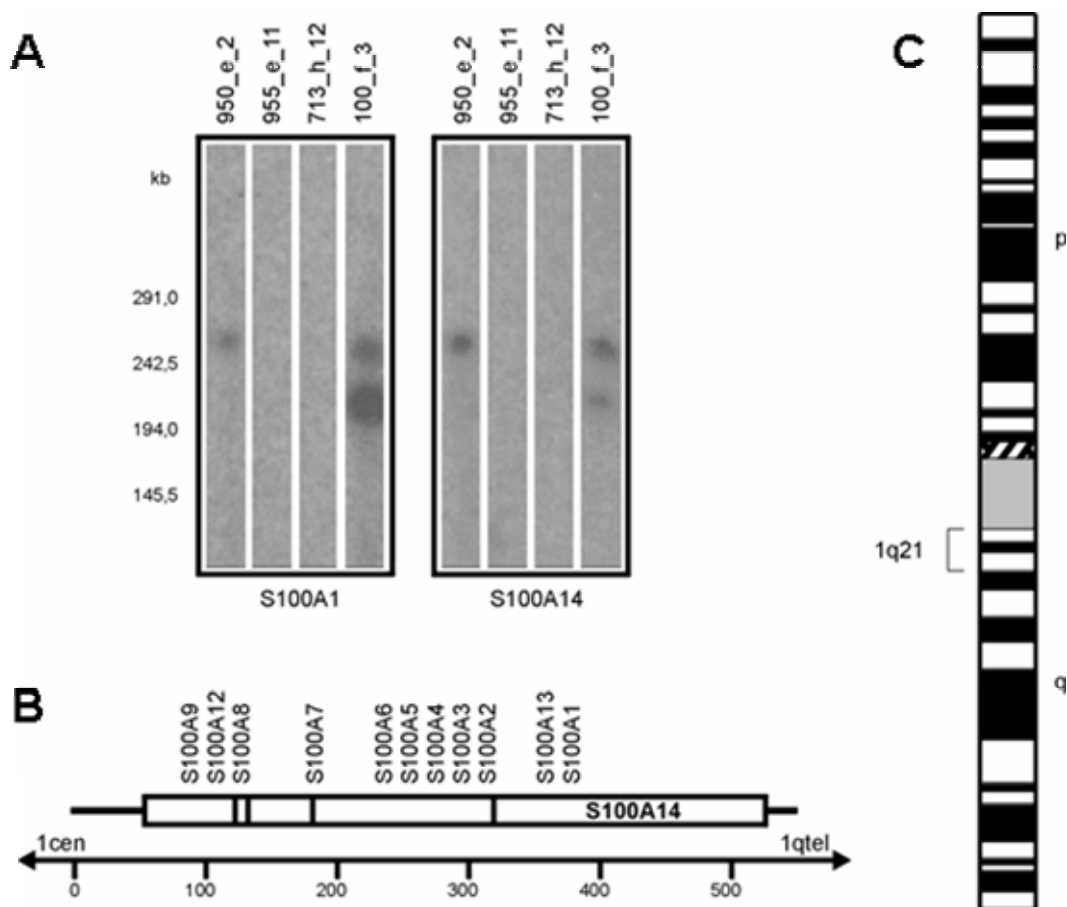


Fig. 20 *S100A14* is localized within the *S100* gene cluster on human chromosome 1q21. **A** Southern blot that contains *SalI*-digested DNA of 24 YACs covering chromosomal region 1q21 was hybridized with the ^{32}P -labelled *S100A14* cDNA. **A**: Four YACs of the contig that cover the distal *S100* genes including the adjacent regions, are shown. Two YACs were positive for the *S100A14*-specific probe (right) that detected the same restriction fragments as the *S100A1* probe (left). The second fragment identified in YAC 100_f_3 is probably due to an additional, rearranged clone in the original YAC culture. **B**: *SalI* restriction map of YAC 100_f_3. A vertical bar represents the YAC. Boxes represent *SalI* restriction fragments that were detected by the genes above. The order of genes has been resolved previously (South et al., 1999). The position of *S100A14* relative to *S100A13* and *S100A1* could not be resolved. **C**: Ideogram of human chromosome 1.

We additionally confirmed localization of the gene in the region 1q21 on the genomic restriction map of the H2LCL cell line (Marenholz et al., 1996), on which the *S100A14* probe detected the same *NotI*-, *NruI*-, *MluI*-, and *BsWI*-fragments as the adjacent *S100* genes (data not shown).

3.5 Identification and Characterization of the Promoter for the *S100A14* Gene

To further investigate the reasons for deregulated *S100A14* expression in tumours, we examined regulation of its putative promoter. As cell model system we chose HEK 293 cells, which do not express endogenous *S100A14*, and Lovo cells, which express the gene at a high level.

Isolation of *S100A14* genomic DNA provided 511 bp of the 5' upstream region of the major transcription initiation site of the gene. In order to identify potential regulatory sequences within this region, a panel of deletion mutants, covering the region of 495-bp immediately adjacent to the transcription start site, was generated and linked to a promoterless luciferase reporter gene. The presence of endogenous *SacI* and *PstI* sites was used to aid the subcloning. The p500-luc luciferase reporter driven by the longest promoter fragment showed a significant luciferase activity in extracts from HEK 293 and Lovo cells (Fig. 21A, B). Thus, we generated deletion mutants of this fragment to locate the minimal promoter region responsible for the observed activity.

The p300-luc promoter construct that covers the proximal region of the promoter (-313/-12) conferred a 4-fold activation. The other promoter fragment (p250-luc) covering the -495/-313 region showed a very low level of activity, similar to the level obtained with the control vector pGL3 Basic. This indicated that the -313/-12 region of the *S100A14* promoter is sufficient to induce a potent luciferase activity. Therefore, we investigated deletion mutants of this promoter fragment. p2A-luc and p2B-luc luciferase reporters showed activity at a level approximately equal to that of the control vector. On the contrary, transfection of a p2C-luc construct, covering the most proximal promoter fragment (-208/-12) of 196-bp, resulted in an enhanced luciferase activity that could be indicative of the presence of possible transcription factor binding sites.

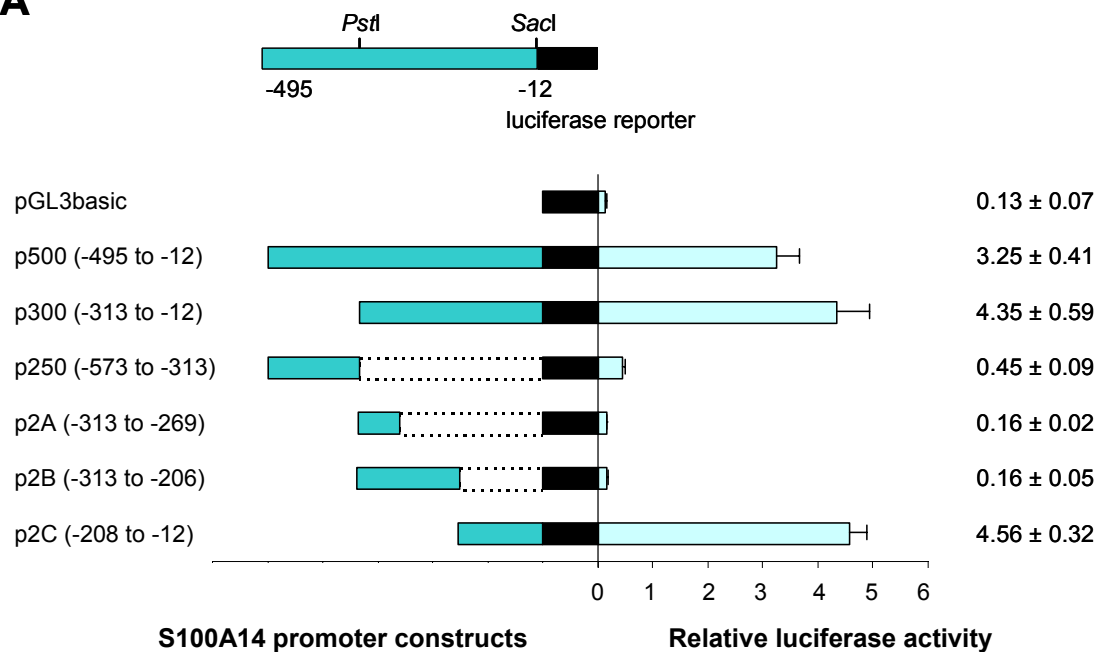
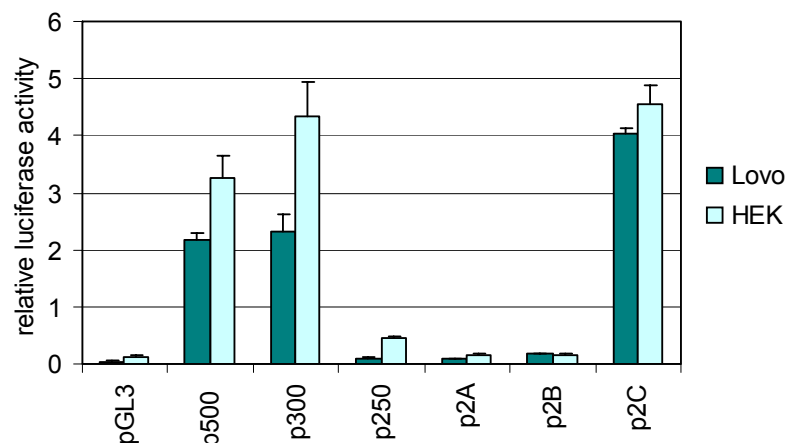
A**B**

Fig. 21 Transcription activities of *S100A14* promoter constructs. **A:** Effects of deletions of putative *cis*-acting regulatory elements on luciferase activity in HEK 293 cells. A series of 5' deletion mutants were fused with the firefly luciferase reporter gene (black box) and analysed by transient transfection. Native restriction sites used for cloning are indicated. The relative sizes of the constructs are to scale. The numbers in parentheses indicate the position of the tested promoter region within the 5' upstream region of the *S100A14* gene. Firefly luciferase activity was normalized to *Renilla* luciferase activity, which was measured to control for transfection efficiency. Means and standard deviations are indicated to the right. The data shown are representative of three experiments, each performed in triplicate. **B:** Transcription activities of the *S100A14* promoter constructs in HEK 293 and Lovo cells. Relative luciferase activity is indicated ± the standard deviation. The mean values for Lovo cells were uniformly scaled by the factor 3 to allow comparison of the two cell lines. The results represent the mean of triplicate experiments.

Computer-assisted analysis of the minimal promoter fragment revealed a TATA box, multiple potential transcription factor binding sites for Elk-1, and RFX-1, as well as single binding sites for SRF (serum response factor), AP-1, CEBP, CHOP, USF, NFκB, and N-myc.

In search for conserved elements in the human *S100A14* promoter, we retrieved 3460 bp in the sequence 5' upstream of the mouse *S100a14* gene. Comparison of the region with the 511 bp of the human *S100A14* promoter revealed presence of two fragments immediately upstream of the transcription start site that were conserved in the human gene (Fig. 22). One of the fragments (-7/-48) showed 97% identity with the human counterpart and encompassed the TATA box. The other fragment (-76/-135) showed 89% identity with the human sequence and contained a CAAT sequence. This sequence, however, lacked significance to the consensus CCAAT box in our promoter prediction analysis. Within the conserved fragment from -76 to -135 bp two possible transcription factor binding sites for CEBP and C/EBP homologous protein (CHOP), also known as growth arrest- and DNA damage-inducible gene 153 (GADD153) were detected. Both of them belong to the CCAAT/enhancer binding protein (CEBP) family of transcription factors.

Additionally, a potential NFκB consensus motif was conserved in the mouse and human DNA within the minimal promoter fragment but further upstream of the two strongly conserved promoter fragments. This putative consensus site was located in equivalent position in alignment between the two orthologous sequences. No significant homology of sequences further upstream could be detected.

To determine if the potential NFκB binding site represents a functional NFκB response element, we examined it in more detail. Therefore, it was evaluated whether the *S100A14* promoter was subjected to transactivation by wild type p65 – the DNA binding subunit of NFκB. HEK 293 cells were co-transfected with p65/Flag and the p2C-luc luciferase reporter or with empty vectors. Measurement of luciferase activity revealed a weak decrease in the p2C-luc luciferase reporter activity following transient transfection with an empty vector for p65, indicating an inhibitory effect of pcDNA3/Flag vector (data not shown). Nevertheless, no increase of activity was detected upon co-transfection of HEK 293 with p65

compared with the co-transfection with the empty vector (data not shown). Treatment with TNF- α also did not induce any significant transactivation of the promoter in any concentration tested (5-25 ng/ml) thus confirming our Northern blot results (data not shown).

```

mouse_ CCTTTCAACCTTTCATCTCTAGGCTGTCAGGACTGAGAGGCTTGACTCT-AGGTTTCAGC 59
human_ CCAGGCAGGCTTGAGTGTGTCAG---TATCCAAGCTG---GGCCTGACTGGGAGAAGTGTGC 54
      **  **  ***  *  **      *  **      ***      ***  *****  **  *  **

mouse_ AGGCCCCGAGTGATCCAAGCCAAATTAGCTCTAGTTGGAAGGGAGAGGAGAAGAGAGATGC 119
human_ GTGTGCGTGTGTGTGTGTGTGTGTGTGTGTGCACGTGA-GAGAGAGAGAGAGAGAGACAGACAG 113
      *  **  ***              *  **  *  *  *  **  *****      ***  ***

mouse_ CAAAGCACAGAGATCCATGGGCCTCGTTCAAGCTTCTCCTTCCATAAGCTTCCGTTGATC 179
human_ ACACACATGGAGGGTACAGAGGCTCCT----GCTTCTCCTTCCT--GGTCACAGAT--TC 165
      *  **  ***              *  *  ***  *      *****          *  *  *  *  **

mouse_ AGCCCTTGCTTCTCTTTTGTGCGACCCCTCTGCTCCCTGCATCATAGCTGCCTCAGGTT 239
human_ AGACCC--CCTCTCCTTCCCTGCCCCTGCAGTTCGCCAGGGCCCTTCCACTTCCTAGGGTG 223
      **  **      *  *****  *      *  **  *  *  *  **      **      **  ***  ***

mouse_ CTTACCCTCCTAGCTAAGATCCCCCTCTGCATCTCCCTAGCTTT-TCTTTTTCCTCTCCCT 298
human_ AC--CCCATGAGGTCTCGAAGTCTCTCTGTCTCCCCAGCCTTCTCGCTTCTCTTTCTCT 281
      ***      *      **      *****      *****  **  *  *  *  **  *  *  *  *

                                     NFkB Elk-1 RFX-1      SRF
mouse_ GTGACTCTGTAAGGTGATCTTGCGCCAGGGGCATCCCGTACCCAGCCCTCCACGGCTTCC 358
human_ GTGACTCTGCATGCTGATCGGAGGCCAGGGGTTTCCAGCCCCAGCCCTCTGTGGCTCCC 341
      *****  *  *  *****      *****  *****  *****  *****  **

               N-myc USF AP-1      RFX      Elk-1
mouse_ TCCTCATGATAGGGGTGGGGACTGACTCTAGAGCT-----GTAGAGGGTGGGGCTCAT 411
human_ TCCTCGTGGCAGGG-TCATGGTAGGCTCTGGAAGCTCTGGCCAGCGGAGGGTGGGGCCCAT 400
      *****  **  *****  *      *  *****  *  *  *  *  *  *  *  *  *  *

                               CEBP      CHOP
mouse_ AAAGCTGGCTCCAGCCCAGGAGGCTGCAATAGCTGGGGTGGCTGAGGGATAAGGCCCTG 471
human_ AAAGCTGGCTCATAGCCCAGGCTGCTGCAATAGCAGGGGTGGCTTAGG-----CCCA 452
      *****  *****  *****  *****  *****  *****  *****  **

mouse_ GCCCTGCCCCGTCTCCCTCCCTTCCCCCAGGTATAAGAGCAGAGCTCAGGTGAGCTGGC 531
human_ GCCC---CCTGCCTCCCTCCCTTCCCCCAGGTATAAGAGCTGAGCTCAGGTGAGCTGGC 512
      ****      **  *  *****  *****  *****  *****  *****

mouse_ TCCTCCATCCTGTCT 546
human_ TCCTCCTGTCTTGTC 527
      *****      **

```

Fig. 22 Comparison of nucleotide sequence and potential regulatory elements of the *S100A14* promoter fragment in mouse and human genomic DNAs. The consensus sequences of the potential transcription factor-binding sites are underlined or in bold. Nucleotide identities are indicated by asterisks. The predicted TATA box and CAAT sequence are represented by shading the consensus sequence. The major transcription initiation site identified in the human *S100A14* is indicated by boxes.

3.6 ERBB Ligands Induce *S100A14* Expression at the Transcriptional Level in 9442 Cells

Preliminary experiments with H322 lung tumour cells revealed that stimulation of the cells with serum induced *S100A14* transcript (Fig. 23). Furthermore, our initial analysis by immunohistochemistry of breast tumours demonstrated a significant correlation between a high *S100A14* level and ERBB2 overexpression ($p = 0.04$). This prompted us to investigate whether *S100A14* could be subjected to epidermal growth factor (EGF) regulation.

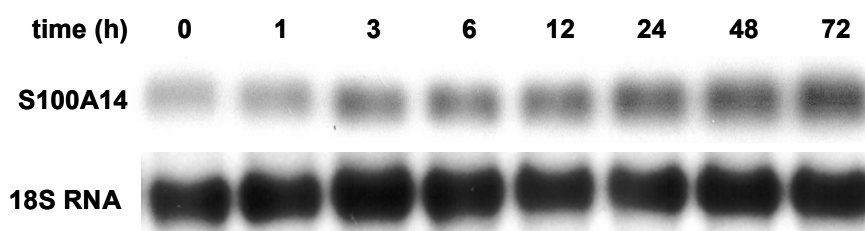


Fig. 23 Up-regulation of *S100A14* expression in H322 cells after stimulation with serum. Northern blot analysis of *S100A14* expression in H322 cells was performed after stimulation with 20% serum for the indicated times. *S100A14* cDNA sequence that covers the protein coding region was ^{32}P -labelled and used as a probe for hybridization. 18S RNA was assayed as a loading control.

Eight human cell lines were treated with recombinant human EGF and *S100A14* mRNA expression was measured by Northern blot analysis. The eight cell lines included immortalized bronchial epithelial cells (9442) and immortalized mammary epithelial cells (HMEB), which express *S100A14* as well as six *S100A14*-negative tumour cell lines: three breast (SK-BR-3, MCF-7, MDA-MB-231) and three lung (H157, DMS-114, A549) tumour cell lines. Expression of endogenous *S100A14* mRNA was remarkably induced by EGF in *S100A14*-positive 9442 and HMEB cells, but not in *S100A14*-negative tumour cell lines (Fig. 24).

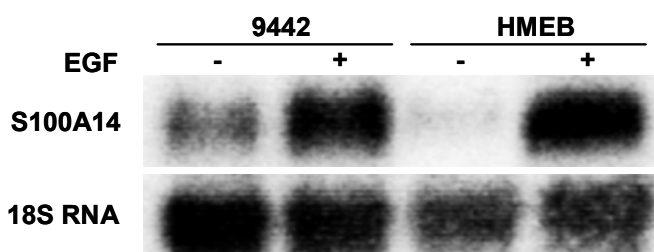


Fig. 24 Treatment of 9442 and HMEB cells with EGF leads to the induction of *S100A14*. 9442 and HMEB cells were grown for 3 days in regular culture medium and then treated for 12 hours with 50 ng/ml of EGF without medium change. 10 μg of total RNA was size-fractionated followed by Northern blot analysis. *S100A14* cDNA sequence was applied as a probe for hybridization. 18S RNA was used as a loading control.

Based on this result, we decided to further characterize regulation of the gene by EGF using 9442 cells as a cell model. The 9442 (BET-1A) cells are derived from normal human bronchial epithelial cells that were immortalized with the SV40 early region and represent non-tumorigenic cells.

First, we determined the kinetics of *S100A14* induction by EGF in 9442 cells. Following the growth factor treatment, *S100A14* levels were induced at 3 hours post-treatment and then gradually increased, reaching a maximal level at 12 hours (Fig. 25). The observed sustained response remained for up to 24 hours, with a subsequent gradual decrease to slightly above pre-stimulation level. These results clearly demonstrated an EGF-dependent induction of endogenous *S100A14* expression and indicated that *S100A14* is an EGF target gene.

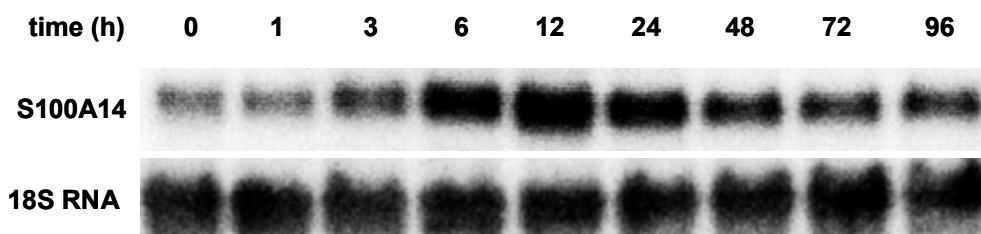


Fig. 25 *S100A14* is induced by EGF in a time-dependent manner in 9442 cells. 9442 cells were grown for 3 days in regular culture medium and then treated for the indicated times with 50 ng/ml of EGF without medium change. Northern blot analysis was performed using specific ³²P-labelled *S100A14* cDNA probe for the detection. 18S RNA was used to correct for equal loading.

Next, we examined the dose dependency of the *S100A14* mRNA induction in 9442 cells. The response appeared to be maximal at a concentration of 50 to 100 ng/ml of EGF (Fig. 26). Therefore, 50 ng/ml of EGF treatment for 12 hours was used in this study.

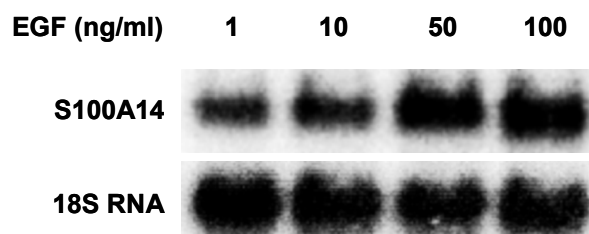


Fig. 26 Induction of *S100A14* is EGF dose-dependent. 9442 cells were grown for 3 days in regular culture medium and then treated with 1-100 ng/ml of EGF for 12 hours without medium change. *S100A14* was detected by Northern blot analysis using a specific ³²P-labelled cDNA probe. 18S RNA was used as a loading control.

Treatment of the cells with transforming growth factor- α (TGF- α), another ERBB receptor ligand, also resulted in an increase of the *S100A14* transcript level (Fig. 27). The kinetics of the TGF- α -induced response was similar for the EGF and TGF- α ligands with a delayed time course relative to the EGF-induced response. The induction was transient, starting at 6 hours post-treatment, reaching maximal levels 12 hours post-stimulation and remaining for up to 48 hours, with levels returning to basal by 72 hours.

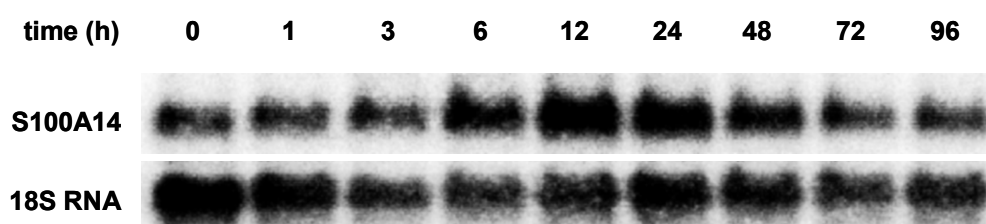


Fig. 27 TGF- α induces *S100A14* mRNA in 9442 cells. 9442 cells were grown for 3 days in regular culture medium and then treated for the indicated times with 20 ng/ml of TGF- α without medium change. 10 μ g of total RNA was size-fractionated followed by Northern blot analysis. *S100A14* cDNA sequence was 32 P-labelled and used as a probe for hybridization. 18S RNA was used as a loading control.

S100A14 was also induced in response to fresh medium or “stimulation medium” showing a maximal level at 6 hours (Fig. 28). Notably, the induction was less potent than in response to EGF.

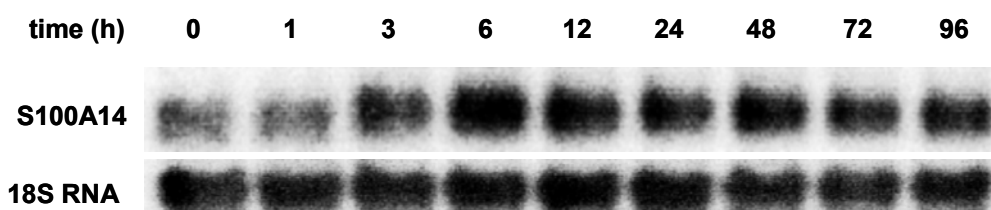


Fig. 28 Up-regulation of *S100A14* expression in 9442 cells after stimulation with fresh medium. 9442 cells were grown for 3 days in regular culture medium and then incubated for the indicated times with fresh medium. Northern blot analysis was performed using 32 P-labelled *S100A14* cDNA probe for the detection. 18S RNA was used to correct for equal loading.

It was of interest to determine whether the minimal positive promoter element, which we identified, confers EGF responsiveness to the luciferase reporter gene. Treatment of the p2C-luc-transfected HEK 293 and Lovo cells with EGF revealed no significant induction of the promoter fragment (data not shown).

The up-regulation of *S100A14* by EGF was examined at the protein level by Western blotting of the whole cell lysates. The cells were collected 24 hours after

stimulation with EGF. We did not, however, detect any substantial changes in S100A14 protein level even after increasing the EGF concentration (Fig. 29).

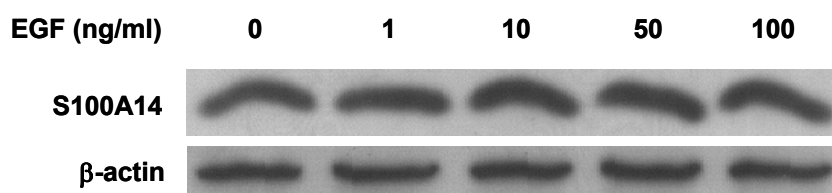


Fig. 29 S100A14 protein is not induced following treatment with EGF. 9442 cells were grown for 3 days in regular culture medium and then treated with 1-100 ng/ml of EGF for 24 hours without medium change. 10 µg of whole protein extracts were subjected to SDS-PAGE followed by Western blot analysis using anti-S100A14 antibody. β-actin was used as a loading control.

3.6.1 Effects of Signalling Pathways Inhibition on Activation of S100A14 by EGF

The major downstream signalling pathways triggered by activated ERBB receptors are ERK1/2 mitogen-activated protein kinase (MAPK), stress-activated protein kinase/c-JUN NH₂-terminal kinase (SAPK/JNK), p38 MAPK, and phosphatidylinositol 3'-kinase (PI3K) pathways. To assess which signalling pathway(s) mediated the stimulatory effect of EGF on S100A14 we applied several pharmacological agents to inhibit these pathways.

First, kinetics of the growth factor-induced response was determined for the three MAPK signalling pathways (ERK1/2, p38, JNK) and the PI3K cascade in order to establish the stimulation efficacy and the optimal treatment time. Immunoblotting with the respective antiphospho antibodies revealed that growth factor stimulation caused a significant increase in ERK1/2 activation which remained on a steady level over a period of 120 min (Fig. 30A). The p38 signalling pathway was also markedly activated reaching a maximal induction level between 5 and 30 min after treatment with levels returning to basal by 120 min (Fig. 30B). Mitogen exposure also enhanced the phosphorylation and activation of the JNK MAPK cascade in these cells with maximal response at 5 to 15 min after stimulation (Fig. 30C). Remarkably, growth factor treatment had no effect on the activation of AKT suggestive of a constitutive activation of the PI3K pathway in these cells (Fig. 30D).

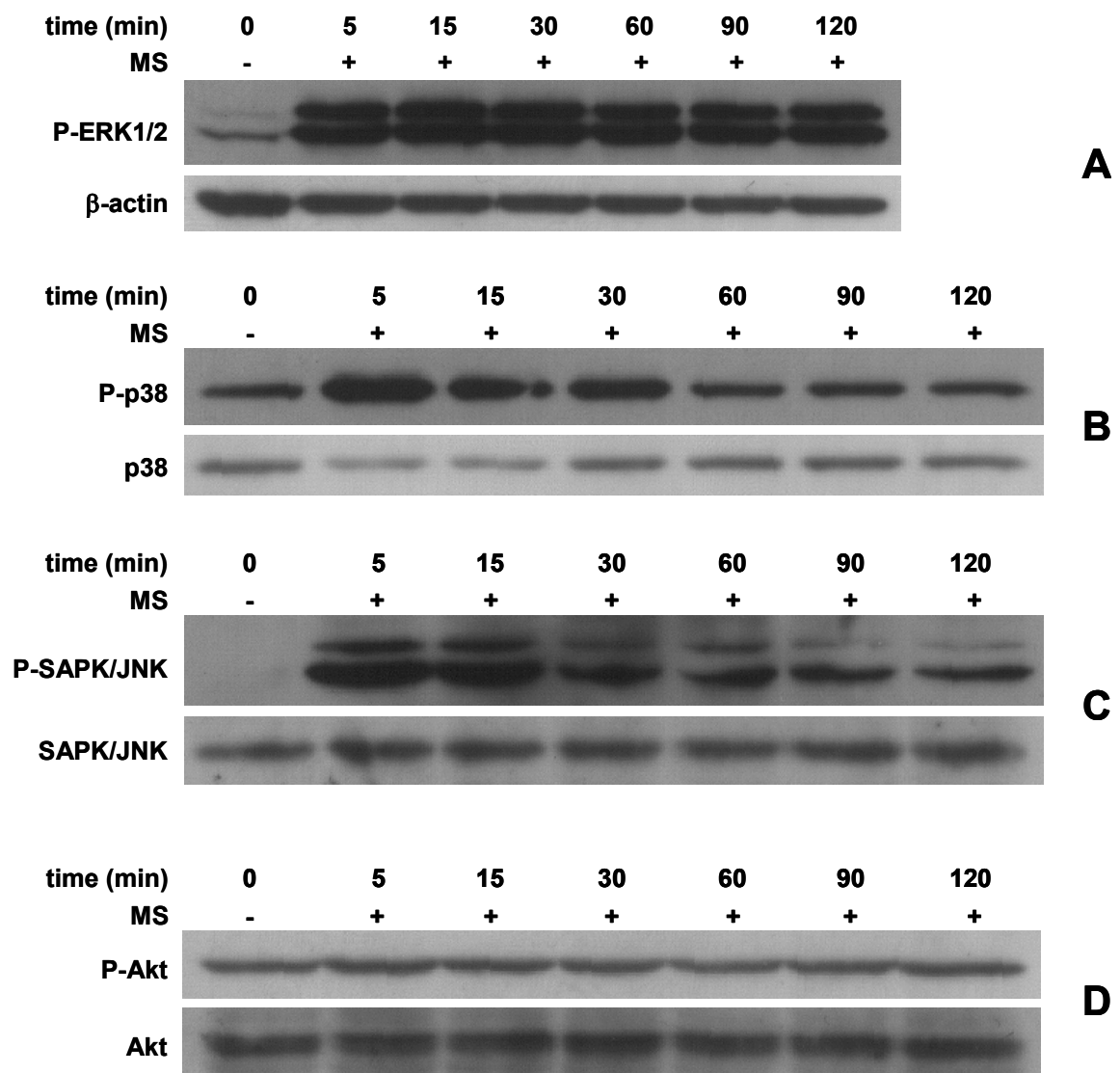


Fig. 30 Kinetics of the growth factor-induced response for the ERK1/2, p38, and JNK MAPK pathways and the PI3K cascade. 9442 cells were grown for 3 days in regular culture medium. The medium was then replaced with the medium that was supplemented with a double set of growth factors (referred to as “stimulation medium”; MS). The cells were cultured for the indicated times and harvested. 20 μ g of whole protein extracts were subjected to SDS-PAGE followed by Western blot analysis using **A**: anti-phospho ERK1/2, **B**: anti-phospho p38, **C**: anti-phospho SAPK/JNK, and **D**: anti-phospho AKT antibodies. β -actin, p38, SAPK/JNK, and AKT were used as loading controls, respectively.

Next, we examined the inhibitory efficacy of various pharmacological agents on activation of the intracellular signalling pathways triggered in response to EGF. U0126 (MEK1 and MEK2 inhibitor) markedly suppressed growth factors-induced ERK1/2 activation in 9442 cells (Fig. 31A). AG1478 (ERBB receptor tyrosine kinase inhibitor) also markedly attenuated ERK1/2 phosphorylation (Fig. 31B). The suppressive efficacy of SB203580 (p38 kinase inhibitor) on the p38 MAPK

pathway and SP600125 (JNK kinase inhibitor) on the JNK pathway was confirmed by the ability to block the activation of their downstream targets: HSP27 and c-JUN, respectively. This was determined by immunoblotting with the respective antiphospho antibodies (Fig. 31C, D). Pretreatment with LY294002 (a PI3K inhibitor) only partially inhibited the response to growth factors (Fig. 31E). Increasing concentration of the inhibitor failed to alter the inhibitory response in these cells.

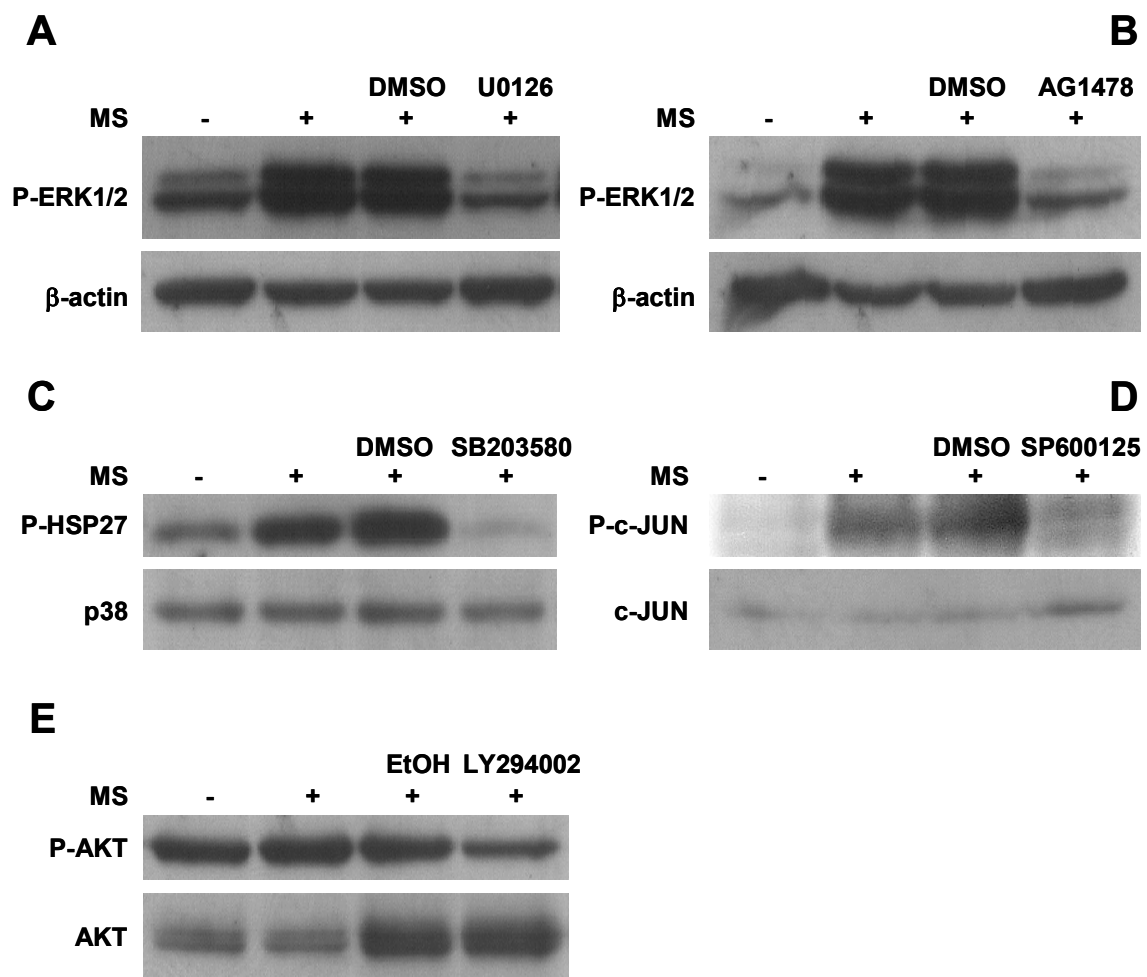


Fig. 31 The inhibitory efficacy of various pharmacological agents on activation of the ERK1/2, p38, and JNK MAPK pathways and the PI3K cascade. 9442 cells were grown in regular medium for 3 days and then preincubated for 1 hour with **A:** 20 μ M U0126, **B:** 10 μ M AG1478, **C:** 40 μ M SB203580, **D:** 40 μ M SP600125, and **E:** 40 μ M LY294002, respectively, without medium change. Next, the cells were stimulated with the medium that was supplemented with a double set of growth factors (referred as “stimulation medium”; MS) for 10 min (A), 10 min (B), 5 min (C), 5 min (D), and 10 min (E). As negative controls, cells were treated with the vehicle: DMSO (A, B, C, D) or ethanol (E). 20 μ g of whole protein extracts were subjected to SDS-PAGE followed by Western blot analysis using anti-phospho ERK1/2 (A, B), anti-phospho HSP27 (C), anti-phospho c-JUN (D), and anti-phospho AKT (E) antibodies. β -actin, p38, c-JUN, and AKT were assayed as loading controls.

To delineate the pathways involved in *S100A14* mRNA induction we treated 9442 cells with the MAPK and the PI3K pathway inhibitors prior to EGF stimulation. Treatment with LY294002 does not abrogate growth factor-dependent induction of *S100A14* mRNA (Fig. 32A). Its expression was also unaffected by SB203580 and SP600125 inhibitors. In contrast with this result, U0126 completely abrogated EGF-induced *S100A14* mRNA expression at the time of optimal gene induction (after 12 hours) and this treatment reduced mRNA levels to those seen in unstimulated cells (Fig. 32B). To examine whether the intact tyrosine kinase activity of the EGF receptor was necessary for the EGF-induced *S100A14* expression, cells were preincubated with AG1478. AG1478 completely prevented EGF-induced *S100A14* up-regulation (Fig. 32B). None of the concentrations of the inhibitors that were used in this study caused cell detachment or cell death.

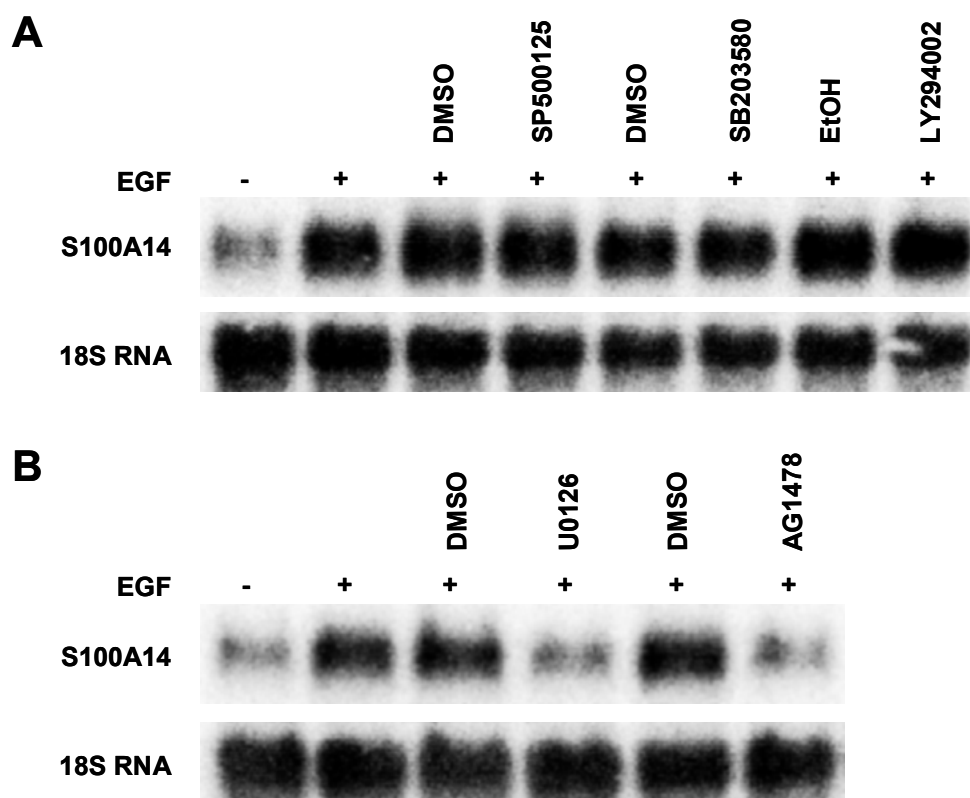


Fig. 32 ERK1/2 MAPK signalling pathway determines *S100A14* induction following stimulation with EGF. 9442 cells were grown in regular medium for 3 days and then preincubated for 1 hour with **A**: 40 μ M SP600125, 40 μ M SB203580, 40 μ M LY294002, **B**: 20 μ M U0126, and 10 μ M AG1478, respectively, without medium change. As negative controls, cells were treated with the vehicle: DMSO or ethanol. Next, the cells were stimulated with 50 ng/ml of EGF for 12 hours and harvested. 10 μ g of total RNA was size-fractionated followed by Northern blot analysis using 32 P-labelled *S100A14* cDNA probe for the detection. 18S RNA was used to correct for equal loading.

These results demonstrated that ERK1/2 MAPK signalling plays a prominent role in regulation of *S100A14* transcript in response to growth factors.

No inhibition of S100A14 protein was detected following treatment with the U0126 and AG1478 inhibitors (data not shown). Experiments included both whole cell lysates as well as subcellular fractionated lysates (membrane and soluble fraction). Similarly, no shift in the S100A14 subcellular localization was observed and S100A14 remained compartmentalized to crude membrane and soluble fractions upon induction by EGF, as determined by Western blotting with anti-S100A14 antibody (data not shown).

3.6.2 EGF-Induced *S100A14* Gene Expression is Dependent on *de novo* Protein Synthesis

To further investigate the mechanisms of EGF-mediated *S100A14* transcriptional activation, we employed cycloheximide (CHX) – an inhibitor of protein synthesis. Pretreatment of cells with CHX led to a partial reduction in the EGF-induced *S100A14* mRNA levels in a dose-dependent manner (Fig. 33). Based on this result, we concluded that the induction of *S100A14* following EGF treatment requires a new protein synthesis. Therefore, *S100A14* is likely to be an indirect transcriptional target of EGF signalling and it is conceivable that the synthesis of other protein(s) is involved in its transcriptional activation.

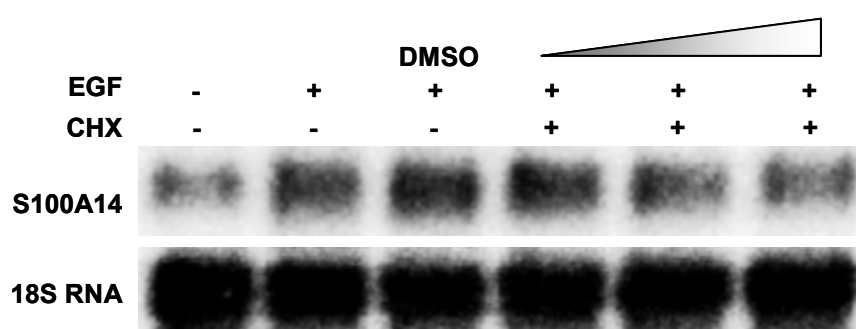


Fig. 33 EGF-induced *S100A14* expression is dependent on *de novo* protein synthesis. 9442 cells were grown in regular medium for 3 days and then preincubated for 1 hour with 2, 5, and 10 µg/ml of cycloheximide (CHX), respectively, without medium change. As negative controls, cells were treated with the vehicle DMSO. Next, the cells were stimulated with 50 ng/ml EGF for 12 hours and harvested. 10 µg of total RNA was size-fractionated followed by Northern blot analysis using ³²P-labelled *S100A14* cDNA probe for the detection. 18S RNA was used as a loading control.

3.7 Transcriptional Induction by Protein Kinase C

Screening for transcriptional modulators of *S100A14* revealed phorbol ester 12-myristate 13-acetate (PMA) as a potential activator of the gene. PMA acts as a specific agonist of both conventional and novel protein kinase C (PKC) isoenzymes activation. The phospholipase C γ – PKC pathway is well known to be coupled to activation of ERBB receptors and PKC has often been implicated as a mediator of ERBB receptor transactivation. The involvement of PKC was therefore investigated to determine whether PKC could mediate *S100A14* mRNA induction.

PMA induced *S100A14* mRNA in 9442 cells reaching a maximal level by 12 hours and returning to a level slightly above basal by 24 hours (Fig. 34A). The kinetics of this response paralleled the time course of the EGF effect, although PMA was less potent than EGF in inducing *S100A14*.

To confirm that *S100A14* induction in response to PMA was PKC-dependent, we tested the ability of the PKC inhibitor bisindolylmaleimide I to block PMA-stimulated *S100A14* induction. As demonstrated in Fig. 34B, bisindolylmaleimide I (5 μ M) did not abrogate *S100A14* induction in response to PMA.

The ability of PMA to cause the phosphorylation and activation of ERK1/2 MAP kinases is well established and has been shown to depend upon PKC-mediated activation of upstream elements of the ERK1/2 MAPK pathway, including RAS and RAF-1. We therefore addressed the question whether PMA had the capacity to activate the ERK1/2 MAPK pathway in 9442 cells. PMA induced a rapid increase in the amount of phospho-ERK1/2 in 9442 cells and this activation continued for at least 60 min (Fig. 34C). To determine whether the PMA-induced increase in *S100A14* mRNA also depends upon the activation of ERK1/2, we stimulated 9442 cells with PMA and tested by Northern blot analysis the ability of U0126 to inhibit *S100A14* mRNA. In the presence of U0126, the *S100A14* mRNA level decreased to slightly above pre-stimulation level (Fig. 34B).

The ability of both EGF and PMA to stimulate ERK1/2 activity in 9442 cells could suggest that the capacity of EGF to stimulate *S100A14* might be PKC-dependent. We therefore tested the effect of the PKC inhibitor on *S100A14* induction in response to EGF. Pretreatment of cells with bisindolylmaleimide I did not significantly influence *S100A14* up-regulation in response to EGF suggesting that the induction is not mediated by PKC (Fig. 34D).

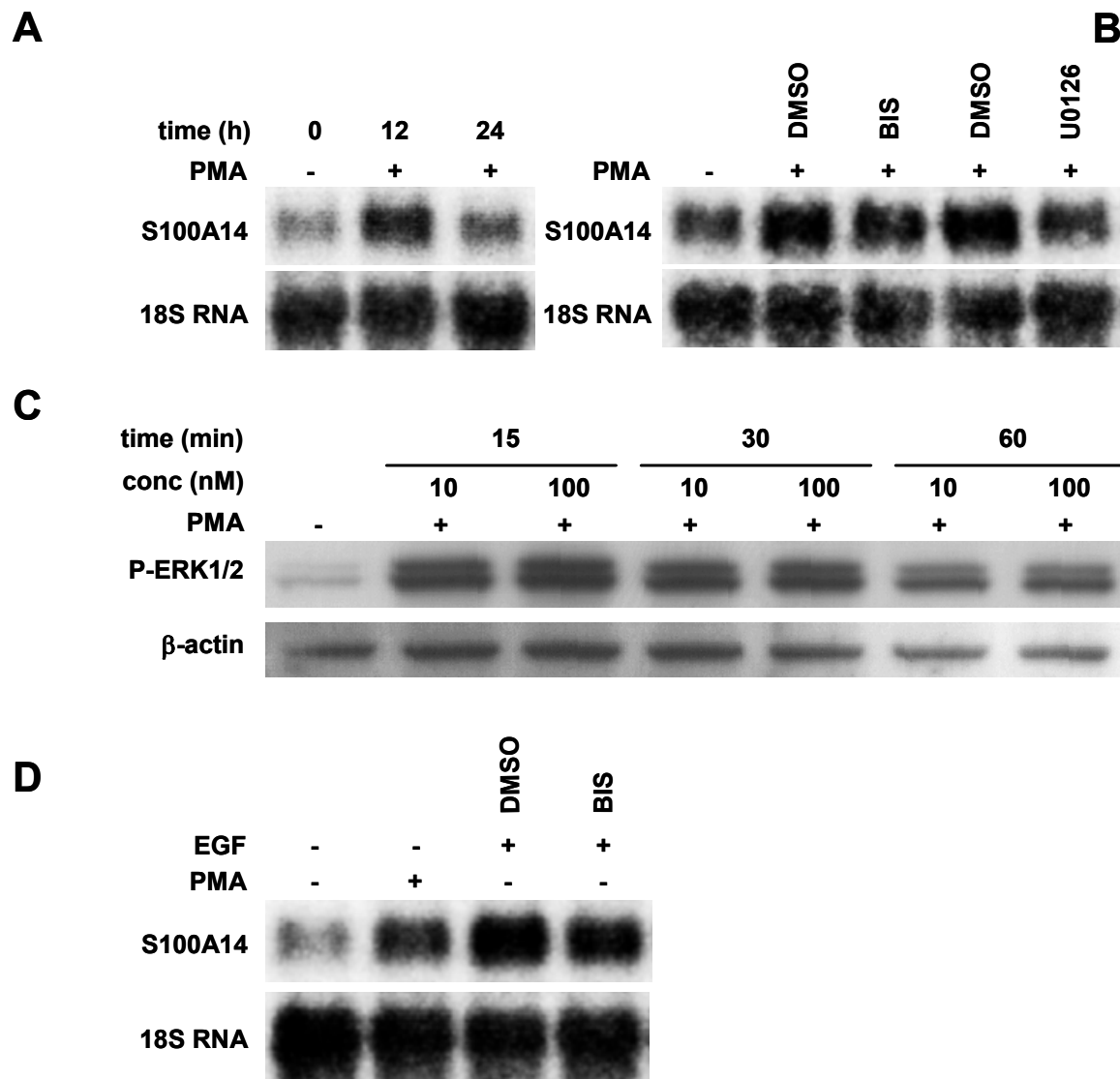


Fig. 34 PMA exerts stimulation of *S100A14* via PKC activation. 9442 cells were grown for 3 days in regular culture medium. **A:** The cells were then treated without medium change with 100 nM of PMA for the indicated times and harvested for Northern blot analysis. **B:** The cells were preincubated for 1 hour with 5 μ M of bisindolylmaleimide I (BIS) or 20 μ M of U0126, respectively, without medium change. As negative controls, cells were treated with the vehicle DMSO. Next, the cells were stimulated with 100 nM of PMA for 12 hours and harvested. 10 μ g of total RNA was size-fractionated followed by Northern blot analysis using 32 P-labelled *S100A14* cDNA probe for the detection. 18S RNA was used as a loading control. **C:** The cells were stimulated without medium change with 10 and 100 nM of PMA for the indicated times and harvested. 20 μ g of whole protein extracts were subjected to SDS-PAGE followed by Western blot analysis using anti-phospho ERK1/2 antibody. β -actin was used as a loading control. **D:** The cells were preincubated for 1 hour with 5 μ M of bisindolylmaleimide I (BIS) without medium change. Next, the cells were stimulated with 100 nM of PMA or 50 ng/ml of EGF, respectively, for 12 hours and harvested. As negative controls, cells were treated with the vehicle DMSO. Northern blot analysis was performed using 32 P-labelled *S100A14* cDNA probe for the detection. 18S RNA was used as a loading control.

4 Discussion

4.1 Identification of the *S100A14* cDNA

This study was undertaken in order to identify tumour-associated genes with potential application in the detection or treatment of the disease. For this purpose, suppression subtractive hybridization (SSH) was performed using cDNA synthesized from normal human bronchial epithelial cells and cells derived from a metastatic small cell lung carcinoma (Difilippantonio et al., 2003).

SSH was developed by Diatchenko and colleagues (Diatchenko et al., 1996) providing a powerful approach for identification of genes differentially expressed in one cell population compared to another. The technique has been successfully used in many experimental settings and two important applications are differential gene expression in multiple tumour systems and identification of tumorigenesis relevant genes. Although cDNA microarrays are increasingly used for the global analysis of gene expression, SSH is still widely applied. It not only permits identification of tumour-associated genes with known function but also unbiased isolation of novel sequences that are not yet available on microchips. Moreover, it enables the recovery of abundant as well as low-copy-number mRNA transcripts.

Using this approach, we recovered a set of genes differentially expressed in lung tumour cells compared to normal lung cells. These genes then provided the groundwork for identifying unknown transcripts with diagnostic and prognostic value for cancer. In this set of cDNAs, it was then confirmed that one of the under-represented transcripts, with no homology to any known gene, was differentially expressed in a panel of lung tumour cell lines. Hence, we decided to analyse this transcript more extensively.

The isolated full-length cDNA is 1067 bp in length and encodes a putative protein of 104 amino acids. The predicted protein contains the S100-specific EF-hand calcium-binding domain and shares the highest sequence homology with S100A13. We therefore assigned this unknown transcript as a novel member of the *S100* gene family and designated it *S100A14* (Pietas et al., 2002).

The S100 protein family forms a growing subfamily of proteins related by Ca^{2+} -binding motifs to the EF-hand Ca^{2+} -binding protein superfamily. The

members of this family are involved in Ca^{2+} -, Zn^{2+} -, and Cu^{2+} -dependent regulation of many cellular processes, including tumour development and acquisition of metastatic phenotype (Donato, 2001; Heizmann et al., 2002). The homology to the protein family known to be associated with tumorigenesis prompted us to investigate the involvement of *S100A14* in tumour biology.

Further analysis of the cDNA sequence revealed that the S100-specific N-terminal EF-hand of *S100A14* consists of 13 amino acids. This is in contrast with the 14 amino acid loop characteristic for the S100 family. However, it should still be a functional calcium-binding domain since the critical Glu45 is present (Kawasaki et al., 1998). The carboxyl terminal canonical EF-hand, also referred to as the high affinity calcium-binding site, seems to be mutated as only 2 out of 6 conserved amino acid residues are present. The presence of the N-myristoylation site at the N-terminus of *S100A14* poses the possibility of an interaction with a membrane receptor or with the lipid bilayer itself. In contrast to other S100 protein family members the deduced protein contains an extended hydrophilic loop at the N-terminus spanning at least 17 amino acids. The calculated molecular weight and isoelectric point for the *S100A14* protein are in accordance with characteristic features of the S100 family as small acidic proteins. Also the structural organization of the protein based on hydropathy plots is similar to other members of the family.

4.2 *S100A14* is Differentially Expressed in Human Tumours

Expression of *S100A14* was found in epithelial cells of a variety of tissues including colon, thymus, kidney, liver, small intestine, lung, breast, cervix, ovary, uterus, pancreas, prostate, rectum, stomach and thyroid gland, most of them having mainly an epithelial-parenchymal phenotype. In contrast, most mesenchymal-stromal tissues like skeletal muscle, white blood cells and spleen are negative (Fig. 5). This is largely consistent with our database searches indicating many *S100A14*-related ESTs present in libraries of normal as well as tumour tissue such as squamous cell carcinoma of the skin, colon, stomach and pancreas adenocarcinoma as well as uterus and lung cancers. Normal tissues were additionally represented by head and neck as well as placenta. In contrast, we did not observe detectable mRNA expression in placenta even after prolonged

exposure indicating that the expression level of the protein must be very low (data not shown). We found mouse *S100a14* transcript mainly in libraries of embryonal origin.

We were primarily interested in identifying transcripts differentially expressed in a wide range of tumours. Differential expression of *S100A14* was therefore confirmed by Northern blot analysis of various immortalized and tumour cell lines from different tissues. *S100A14* was abundantly expressed in cells cultured from normal human epithelial cells, moderately expressed in immortalized epithelial cells, and absent from most of the examined tumour cell lines. The relatively high *S100A14* expression in most of the colon tumour cell lines could be due to its high basal expression level in normal colon tissue. These results indicate that altered *S100A14* expression occurs in most of the human tumour cell lines. Therefore, we hypothesized that its expression might be also suppressed in primary tumour tissue.

Using the BD Biosciences array with 241-matched tumour/normal cDNA samples from individual patients we determined the expression status of *S100A14* in 10 different human tumour types. The gene is preferentially overexpressed in ovary, breast, and uterus tumours, and mainly underexpressed in kidney, rectum, and colon tumours. Most notably, increased rather than decreased expression of *S100A14* has been found in lung tumours. The reason for this discrepancy is unclear, although it may be due to differences between the cell model system and the primary tissue. This highlights the need to supplement cell culture-derived transcript abundance data with transcriptional or immunohistochemical analysis of primary material. Thus, using immunohistochemistry, we sought to determine *S100A14* protein expression in lung tumour specimens. Additionally, we examined breast tumour samples since this tumour type showed significant *S100A14* overexpression in our transcriptional analysis.

Whilst normal lung and breast epithelial cells express *S100A14* at a low level, we observed strong tumour cell-localized cytoplasmic and membranous *S100A14* protein expression in over 60% of the analysed tumour samples. Thus, our analysis on the expression of *S100A14* in primary tumours differs from the cell culture data by demonstrating a consistent and strong overexpression of this gene in multiple lung and breast tumour samples. We therefore speculated that the

expression of the gene might be modulated by extrinsic factors or by the microenvironment in which the cancer cells reside.

The influence of cell culture conditions on gene expression patterns of cultured cell lines is a longstanding concern. Cells grown in culture have unlimited access to nutrients under conditions most favourable for growth and proliferation and only little exposure to extrinsic factors that modulate growth and differentiation, e.g. cytokines. In contrast, cells in a tumour growing in a host tissue environment face conditions with more limited nutrients and oxygen and are subjected to or benefit from a wide variety of host factors. Recently, global gene expression profiling of tumour cells grown *in vitro* versus the same cells transplanted into an *in vivo* environment (nude mice) have been performed (Creighton et al., 2003). This revealed specific up-regulation of one set of genes related to cell growth and proliferation when in culture and a different set of genes related to cell adhesion, extracellular matrix, growth substances, and neovascularization when developing as an *in vivo* tumour.

Our expression analysis of nine *S100A14*-negative lung tumour cell lines transplanted into immunodeficient mice as well as spheroides of 2 ovary tumour cell lines did not reveal a general re-expression of the gene (Fig. 12). Thus, our results cannot imply an essential physiological role of the tumour environment for *S100A14* expression. The interpretation of this finding remains to be elucidated.

Our expression analysis also suggests that up-regulation of *S100A14* is not a universal feature of epithelial cell tumours. A potential mechanism for the apparently contradictory role of *S100A14* in renal, colon and rectum cancer could be context-dependent. Since most genes act within networks, differences in *S100A14* expression pattern may arise from differences in the expression profile of its interacting proteins as well as differential availability of signalling pathways involved in its regulation in various cell types. A growing number of genes regulated by the relative contributions of specific signalling pathways in a particular cell type have been revealed in the recent years as exemplified by *S100A2* and maspin. *S100A2* was found to be frequently down-regulated early in lung cancer development (Feng et al., 2001). Supporting these data, a number of expression studies implicated this gene as a breast tumour suppressor gene (Liu et al., 2000; Wicki et al., 1997). However, contrary to the proposed role of *S100A2* as a tumour

suppressor protein, it was found to be overexpressed in gastric and ovarian tumours (El-Rifai et al., 2002; Hough et al., 2001).

Maspin (SERPIN B5) was also found to be down-regulated in breast and prostate cancer and was suggested to be a suppressor of metastasis (Seftor et al., 1998). Paradoxically, it was reported that the gene was strongly expressed relative to normal tissue in pancreatic tumours (Maas et al., 2001) and lung tumours (Heighway et al., 2002). The seemingly contradictory results of *S100A14*, *S100A2* and maspin suggest that these and other genes perhaps not only behave differently in particular tumours, but also that they may play different roles in various tissue types and perhaps even within distinct components of a tissue.

Significant up-regulation of *S100A14* in lung and breast tumours directed our attention towards its clinical significance in these tumours. Most interestingly, we found that *S100A14* overexpression was significantly associated with ERBB2 overexpression in breast tumours.

The ERBB family of receptor tyrosine kinases (RTKs) couples binding of extracellular growth factor ligands to intracellular signalling pathways regulating diverse biologic responses, including proliferation, differentiation, cell motility, and survival (reviewed in Prenzel et al., 2001; Olayioye et al., 2000; Marmor et al., 2004). It consists of four receptors: ERBB1 (also called epidermal growth factor receptor – EGFR or HER1), ERBB2 (HER2/neu), ERBB3 (HER3), and ERBB4 (HER4). All the family members have in common an extracellular ligand-binding domain, a single membrane-spanning region and a cytoplasmic tyrosine kinase domain. A family of ERBB ligands, the EGF-related peptide growth factors, have been characterized, including epidermal growth factor (EGF), transforming growth factor- α (TGF- α), amphiregulin, heparin-binding EGF-like growth factor, betacellulin, epiregulin, and neuroregulins (NRG-1,-2,-3,-4). The binding affinity of the EGF-like ligands to various ERBB receptors differs as is their potency to induce signalling. No direct ligand for ERBB2 has yet been discovered. However, increasing evidence suggests that the primary function of ERBB2 is as a co-receptor. In fact, ERBB2 is the preferred heterodimerization partner for all other ERBB family members and plays a role in the potentiation of ERBB receptor signalling.

The ERBB RTKs have a broad expression pattern on epithelial, mesenchymal, and neuronal cells. Signalling through these receptors plays a critical developmental role in inductive cell fate determination in many organ systems. This is exemplified by the perinatal (ERBB1) or early embryonic lethality (ERBB2, -3, and -4) of knock-out mice as a result of insufficient heart and nervous system development (Burden and Yarden, 1997). Furthermore, ERBB RTKs are involved in mammary gland development during puberty and pregnancy.

Ligand binding drives receptor dimerization leading to the formation of both homo- and heterodimers. Dimerization consequently stimulates the intrinsic tyrosine kinase activity of the receptors and triggers autophosphorylation of specific tyrosine residues within the cytoplasmic domain. Each ERBB receptor displays a distinct pattern of C-terminal autophosphorylation sites. These phosphorylated residues serve as docking sites for signalling effector molecules containing Src homology 2 (SH2) or phosphotyrosine binding (PTB) domains. Examination of the binding preferences of different effector proteins revealed a great deal of overlap in the signalling pathways activated by the four ERBB receptors. All ERBB family members apparently utilize the mitogen-activated protein (MAP) kinase pathways as the major signalling routes.

A wealth of clinical data demonstrates the importance of ERBB receptors, in particular ERBB1 and ERBB2, in multiple human cancers, including lung, colon, breast, prostate, brain, head and neck, thyroid, ovarian, bladder, gliomas, and renal carcinoma (Yarden and Slivkowski, 2001). Several phenomena are responsible for hyperactivation of ERBB receptors in tumours, including overexpression, amplification, and constitutive activation of mutant receptors or autocrine growth factor loops. Most notably, ERBB2 is overexpressed in 20-30% of breast and ovarian tumours and its overexpression correlates with tumour chemoresistance and poor patient prognosis, yielding a median survival of 3 years, compared with 6-7 years when unassociated with ERBB2 (Miles et al., 1999; Witton et al., 2003).

Due to their frequent overexpression in various cancers and their high signalling capacity ERBB receptors are promising targets for therapeutic intervention in human cancers. Monoclonal antibodies raised against several epitopes of the ERBB1 and ERBB2, as well as EGF and TGF- α blocking

antibodies, have been validated in the clinic as an ERBB-directed therapeutic approach. Herceptin, a monoclonal antibody that targets the extracellular domain of ERBB2, was the first target-selective drug raised against an oncogenic cell surface receptor and therefore represents the first example of a new era of anti-cancer therapy. This antibody is now applied in the treatment of metastatic breast cancer patients.

The immunohistochemical detection of ERBB2 in our study (29.3%) is in keeping with the reported frequency of the protein overexpression in breast cancer. In contrast to a number of previous reports, however, ERBB2 expression was not related to oestrogen receptor negativity in our study.

Immunohistochemical analysis of primary lung and breast tumours revealed a significant association between the subcellular distribution of S100A14 and the protein abundance. The majority of S100A14-overexpressing tumours displayed both plasma membrane and cytoplasmic localization of S100A14 relative to low-expressing tumours showing predominantly cytoplasmic staining. Also, there was a significant correlation between higher-grade (grade 3) lung tumours and S100A14 cytoplasmic and plasma membrane localization. Moreover, subcellular distribution of S100A14 was related to lung tumour histology. Both cytoplasmic and plasma membrane-localized staining were associated with squamous cell carcinomas compared to adenocarcinomas detecting cytoplasmic-only S100A14.

In contrast to this tumour cell plasma membrane localization, normal human breast and lung epithelial cells showed exclusively diffuse cytosolic S100A14 expression (Fig. 8 and Fig. 11). These data suggest that translocation of S100A14 to the plasma membrane could be unique to cancer cells over normal lung and breast epithelial cells and could represent the disease-associated state.

Many S100 proteins translocate to different cellular compartments in response to elevated intracellular Ca^{2+} and Zn^{2+} level and this process was shown to be cell type specific (Hsieh et al., 2004). Exposure of several different cell lines to elevated Ca^{2+} and Zn^{2+} level did not affect the subcellular localization of S100A14 in our study, suggesting that fluctuations of divalent cations do not regulate S100A14 protein distribution. The prevalence and the clinical relevance of the plasma membrane relative to cytoplasmic S100A14 distribution remains to be established in other tumour types. It is conceivable that the subset of lung and

breast cancers that show both plasma membrane and cytoplasmic localization define a molecularly different mechanism of regulation on the protein.

Analysis of cultured cells demonstrated predominantly plasma membrane-localized endogenous S100A14 (Fig. 14). Most notably, prominent staining at cell junctions was detected in several tumour cell lines suggesting a potential role in establishing cell-cell contacts. Cellular fractionation of 9442 cells and testing the different fractions with anti-S100A14 antibody confirmed the immunofluorescence data. S100A14 can be detected in both membrane-bound and soluble forms, although the soluble protein is present only in very small amounts (Fig. 15). Analysis of cells transiently transfected with epitope-tagged protein showed predominantly cytoplasmic and perinuclear localization of the S100A14 protein (Fig. 13). This result, however, requires further confirmation by cellular fractionation. A challenge of future investigations will be to address whether the sites of action of S100A14 are in the cytosol or in membranes.

4.3 Identification and Characterization of the Genomic Locus of *S100A14*

Numerous studies have described frequent alterations of the chromosomal region 1q21 in tumours where the human *S100* gene cluster is located. In order to elucidate the rationale for the differential *S100A14* expression in tumours, we defined its chromosomal localization as well as the nature of its genomic locus in size, structure, and sequence of its introns and exons. Furthermore, we analysed its immediately upstream regulatory region to get some insights into the regulation of the gene.

The human *S100* gene family encodes a set of structurally related proteins sharing a common genomic organization of three exons and two introns, with the first exon being short and untranslated and the second and third exons containing the coding sequence (Fig. 35). Exceptions are *S100A5* consisting of four exons with exon three and four being the coding ones, *S100A4* containing an additional alternatively spliced untranslated exon, *S100A11* with the coding sequence beginning already in the first exon, and *S100A16*, which is composed of four exons and three introns with coding sequence in the third and fourth exon and the first and second exon being alternatively transcribed.

Unlike other *S100* genes, *S100A14* contains an additional intron that interrupts the sequence encoding the N-terminal part of the protein. Lack of nucleotide sequence homology to any of the *S100* family members and lack of strong conservation of the genomic structure may indicate that *S100A14* is less closely related to other members of the *S100* family.

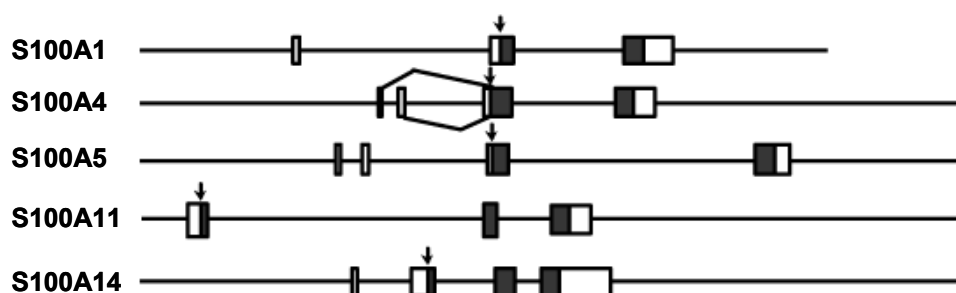


Fig. 35 Generic *S100* gene structure. A typical *S100* gene, e.g. *S100A1* is composed of three exons (boxes) with exon 1 being not translated (open boxes) and exons two and three containing the coding region (black boxes). Exceptions to this general rule are depicted below with straight lines in *S100A4* indicating alternative splicing and arrows indicating the translational start.

An Alu element belonging to the “young” Alu subfamily (AluY) was identified in the direct proximity of the polyadenylation signal in the 3’ UTR reaching beyond the genomic locus of *S100A14*. This family of repetitive DNA has been implicated in the stimulation of homologous and non-homologous recombination and triggering chromosomal rearrangements (Deininger and Batzer, 1999). The frequent involvement of the highly conserved 26-bp core sequence of Alu elements in gene rearrangements suggested that this sequence might represent a recombinational hotspot (Rüdiger et al., 1995). The Alu element present in the genomic locus of *S100A14* contains the 26-bp core sequence and therefore might contribute specifically to gene rearrangements.

We mapped *S100A14* to the chromosome band 1q21 where 16 other *S100* genes are tightly clustered (Heizmann et al., 2002). This region is known to be involved in structural and numerical aberrations in various human tumours (Weternan et al., 1996; Gendler et al., 1990). Our Southern blot analysis of *S100A14*-negative as well as *S100A14*-positive lung cancer cell lines, however, so far indicates that the *S100A14* gene itself is not affected by rearrangements. *S100A14* was present in all tumour cell lines examined and showed no detectable

deletions or gross rearrangements (Fig. 18). Thus, it seems likely that the differential expression observed in tumour cell lines is not driven by dramatic gene deletions or gross rearrangements. This, however, does not completely rule out a possible correlation of *S100A14* expression with the frequently observed chromosome 1q21 rearrangements in solid tumours.

It has been previously shown that the chromosome region 1q21-q22 contains extended regions of high CpG island density (Wright et al., 2001). Consistent with this observation are reports of site-specific methylation associated with transcriptional repression in the promoter region of *S100A2* in tumorigenic cells (Wicki et al., 1997; Lee et al., 1992). Examination of the 5' upstream region as well as introns of *S100A14* did not reveal any CpG island. Similarly, we did not observe re-expression of the gene in eight lung cancer cell lines on treatment with 5-aza-2'-deoxycytidine as determined by Northern blot and RT-PCR analysis (data not shown).

In the course of our studies on the genomic organization of *S100A14*, we identified the *S100A14* promoter fragment, located within 511 bp upstream of the transcription initiation site, and containing constitutive promoter elements (TATA box) that might support basal transcription at this promoter.

The primary aim of our promoter analysis was to determine whether the aberrant regulation of *S100A14* at the promoter level might be responsible for its altered expression in tumours. Therefore, we chose for the transient expression analysis HEK 293 cells, which are well established in promoter assays but do not express endogenous *S100A14*, and Lovo cells, which have a high level of *S100A14* mRNA. Another reason for selecting these cell lines was the high transfection efficiency with standard procedures. Using a luciferase reporter system, a panel of deletion mutants covering the entire putative promoter fragment was constructed in the promoterless pGL3 Basic vector.

Transient luciferase expression experiments indicated the presence of a core promoter located within 196 bp immediately upstream of the major transcription initiation site (Fig. 21). The 4.5-fold activation of the promoter fragment in HEK 293 and Lovo cells compared with the control vector-transfected cells is in accord with many previously published promoter analyses supporting the significance of our data (Perrais et al., 2002; Nichols et al., 2003; Diaz-Guerra et al., 1997; Bordonaro

et al., 2002). Besides a TATA box and an incomplete CCAAT box, consensus motifs for transcription factors located within the promoter region included Elk-1, RFX-1, SRF, AP-1, CEBP, CHOP, USF, NF κ B, and N-myc, many of which are associated with proliferative response.

Site conservation is a good indicator of its functional importance and comparative genome sequence analysis (phylogenetic footprinting) can eliminate up to 90% of false binding-site predictions (Wasserman and Sandelin, 2004). Therefore, we compared the region immediately upstream of the mouse orthologue with the 511-bp fragment of the human *S100A14* promoter. The analysis revealed the presence of two fragments immediately upstream from the transcription start site that were conserved in the mouse and the human gene (Fig. 22). They encompassed the TATA box and the CAAT sequence. Additionally, a potential NF κ B consensus motif was conserved in the mouse and the human DNA within the minimal promoter fragment but further upstream of the two highly conserved promoter fragments. No other sequences matching the further upstream consensus transcription factor binding sites related to mitogenic response could be detected.

Thus, the strong conservation between the mouse and the human *S100A14* promoter fragment concerns only constitutive promoter elements that probably contribute to the basal activity of the promoter. It is therefore conceivable that the respective homologous promoter fragment is present further upstream in the mouse promoter or that the regulation of the mouse *S100a14* is different from the regulation of the human counterpart.

A potential NF κ B transcription factor binding site was conserved in the mouse and the human promoter fragment. NF κ B has been reported to be involved in TNF- α -induced expression of other *S100* genes (Joo et al., 2003). Therefore, we have analysed the potential role of NF κ B in the regulation of the *S100A14* transcription. We found that NF κ B could not transactivate *S100A14* by co-transfection experiments with the NF κ B subunit p65 and the *S100A14* luciferase reporter. Similarly, treatment of cells with TNF- α , which induces degradation of I κ B and translocation of NF κ B to the nucleus, did not enhance the *S100A14* promoter-driven reporter gene transcription. Moreover, TNF- α did not induce *S100A14*

expression at the mRNA level in Northern blot analysis. Thus, we found no evidence that NF κ B transactivates the *S100A14* promoter fragment.

Taken together, our analysis of two cell lines although differing in *S100A14* expression yielded the same activation pattern of the analysed promoter fragment. This means that the transcription regulatory region that we identified is most probably not the critical determinant of *S100A14* expression in tumours. Based on these findings, we suggest that a further distal promoter or enhancer confers induction to *S100A14* and possibly influences its expression in tumours.

4.4 Oncogenic Signalling Pathways Mediate *S100A14* Transcriptional Induction

S100A14 is differentially expressed in many human tumours and its expression is enhanced in lung and breast tumours (Pietas et al., 2002). No data pertinent to the molecular mechanisms responsible for the regulation of the *S100A14* gene are available.

Based on our initial finding that serum stimulation enhanced *S100A14* expression in H322 cells, we reasoned that this effect could be mediated by growth factors. In this context, the additional finding of positive correlation with ERBB2 overexpression in breast tumours raised the possibility that epidermal growth factor (EGF) might function as a positive regulator of the gene. To elucidate mechanisms whereby *S100A14* expression is enhanced in lung tumours, we studied the effects of EGF on *S100A14* expression in 9442 human immortalized bronchial epithelial cells as well as the signal transduction pathways that trigger its expression.

EGF induced a significant increase in *S100A14* mRNA expression in a time- and dose-dependent manner in 9442 cells but not in *S100A14*-negative cell lines (Fig. 25 and Fig. 26). This result implies that a low EGF concentration in culture media cannot account for the absence of *S100A14* transcript in the examined negative cell lines. The EGF effects on *S100A14* expression were also detected in another cell line examined in this study – HMEB, indicating similar transcriptional regulation in immortalized breast epithelial cells (Fig. 24).

Moreover, treatment of 9442 cells with transforming growth factor- α (TGF- α), a member of the EGF ligand family that binds to and activates the ERBB receptor,

also enhanced *S100A14* transcript with similar kinetics to EGF, thus confirming the involvement of ERBB receptor signalling in growth factor-induced *S100A14* expression (Fig. 27).

TGF- α is an essential mediator of oncogenesis and malignant progression. Its overexpression in transgenic mice leads to hyperplasia as well as malignancy in pancreas and breast tissues (Sandgren et al., 1990). TGF- α also acts as a strong collaborator in promoting carcinogenesis by other oncogenes (Sandgren et al., 1993) and chemical carcinogens (Takagi et al., 1993). Among the ERBB family members, TGF- α binds only to the ERBB1 receptor and is best known as an autocrine stimulatory growth factor (Riese et al., 1996). Strong expression of TGF- α has been found in 67% of pulmonary adenocarcinomas (Tateishi et al., 1991) pointing to an important role in non-small cell lung cancer (Rusch et al., 1997; Fontanini et al., 1998).

S100A14 was also induced in response to fresh medium or “stimulation medium” showing, however, an earlier and less potent maximal response relative to the response induced by EGF (Fig. 28). The less potent response in comparison to that induced by stimulation with EGF could be due to the lower EGF concentration present in the medium than the concentration applied in our EGF-stimulation experiments (50 ng/ml). In addition, other unknown growth factors could contribute to this more rapid stimulation.

Regulatory promoter regions responsive to EGF or PMA could not be identified in this study, neither in the 511-bp fragment nor in the minimal *S100A14* upstream regulatory fragment. This suggests the existence of other cooperative elements present at more distant site or in the intervening sequences of the *S100A14* gene.

The analysis of *S100A14* expression at the protein level did not reveal any induction following EGF treatment (Fig. 29). Moreover, treatment with U0126 and AG1478 inhibitors also had no impact on the *S100A14* protein level as determined by Western blotting of whole cell- and fractionated cell-extracts. These findings raise the possibility of an additional post-transcriptional regulation of the gene.

Regulatory elements modulating mRNA half-life are often found within 3' untranslated regions (3' UTR) (Chen et al., 1995; Hollams, 2002). They include AU-rich elements (AREs) that are associated with stabilization-destabilization of

the mRNA or hairpin (stem-loop) structure. Binding of a *trans*-acting factor to these elements influences the turnover of the mRNA or its translational efficiency (Baker et al., 2000; Ranganathan et al., 2000). AREs are found in the 3' UTR of many mRNAs that code for proto-oncogenes, nuclear transcription factors, and cytokines e.g. COX-2, p21^{Waf1}, TNF- α , interferon- β , GM-CSF, c-myc, and c-fos (Dixon et al., 2000; Giles et al., 2003; Wang et al., 1997; Kruys et al., 1989; Han et al., 1990; Levine et al., 1993). The 644-bp 3' UTR of *S100A14* accounts for over 60% of the transcript length suggesting that it might be a target of post-transcriptional regulation.

Although, long tracts of the highly conserved AREs could not be found in the 3' UTR of *S100A14*, we cannot exclude that the few poorly conserved AREs found in the 3' UTR of *S100A14* confer post-transcriptional control to its mRNA. Moreover, it is possible that sequestration of some factors involved in translation that are present in limiting amounts may be responsible for the observed inhibition of translation of the *S100A14* mRNA.

The development of efficient and selective inhibitors against protein kinases involved in signalling has made significant progress. These inhibitors provide a suitable alternative to transfection experiments using dominant-negative mutants of protein kinases, in particular for cells which cannot be transfected efficiently in culture with standard procedures. In the present study, we used several inhibitors to characterize the signalling events involved in EGF-induced expression of *S100A14* (Fig. 36).

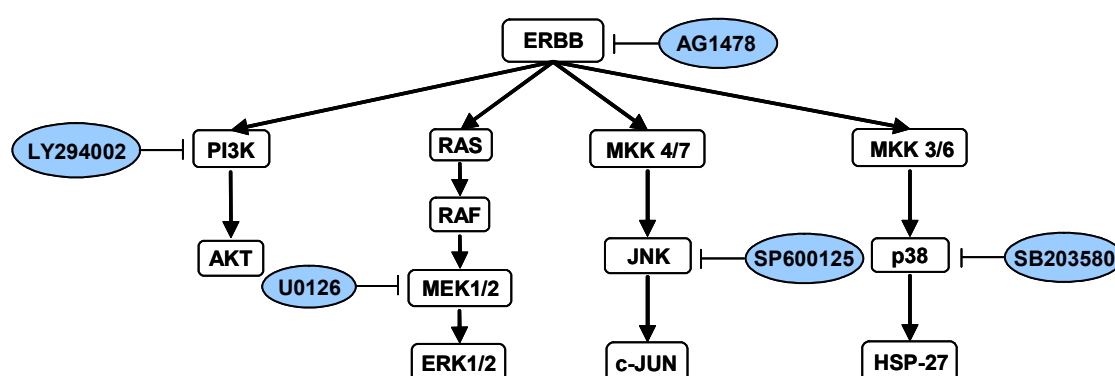


Fig. 36 Pharmacological modulation of the ERBB-induced signalling pathways

In order to determine the effects of the inhibitors on the signalling cascades we first carried out an analysis of the kinetics of the mitogen-induced response for the three MAPK signalling pathways (ERK1/2, p38, JNK) and the PI3K cascade in 9442 cells.

Growth factor stimulation caused a significant increase in phosphorylation and activation of ERK1/2, p38, and JNK kinases but had no effect on the activation of AKT, suggestive of a constitutive activation of the PI3K pathway in these cells (Fig. 30). The EGF-induced *S100A14* expression was inhibited by mitogen-activated protein (MAP) kinase kinase (MEK) inhibitor U0126 but not by p38, JNK, and PI3K pathway inhibitors (Fig. 32). Inhibition of ERBB receptor tyrosine kinase activity by AG1478 inhibitor also resulted in a reduction of *S100A14* mRNA levels to those seen in unstimulated cells, thus confirming the results obtained with the MEK1/2 inhibitor. Taken together, these inhibitor studies demonstrate that the activation of ERBB tyrosine kinase by its ligands EGF and TGF- α , leads to the synthesis of *S100A14* mRNA via the activation of the RAS-RAF-MEK-ERK signalling pathway.

The importance of constitutively activated mitogenic signalling pathways in oncogenesis is well established. Binding of extracellular growth factor ligands couples the ERBB family of receptor tyrosine kinases to intracellular signalling pathways regulating diverse biologic responses including proliferation, differentiation, cell motility, and survival, all of them implicated in tumorigenesis. The RAS-RAF-MEK-ERK pathway is at the heart of signalling networks that govern these processes. It may be noted that about 30% of human tumours carry *RAS* gene mutations that may prolong the activation of mitogenic signalling pathways (Khosravi-Far and Der, 1994). Of the three genes in this family (composed of *KRAS*, *NRAS*, and *HRAS*), *KRAS* is the most frequently mutated member in human tumours, including adenocarcinoma of the pancreas (~70-90% incidence), colon (~50%), and lung (~25-50%) (Pellegata et al., 1994; Bos et al., 1987; Mills et al., 1995).

Thus, multiple components of mitogenic signal transduction pathways are either overexpressed (ERBB receptor family and ligands, and cyclin D1) or mutated (*KRAS*) in cancer, leading to excessive activation of these important growth-modulating cascades. We therefore suggest that the involvement of ERBB

receptor signalling and the RAS-RAF-MEK-ERK pathway in *S100A14* transcript regulation links the gene to oncogenic signalling pathways in cancer. Identification of target genes of ERBB signalling such as *S100A14* may, therefore, prove important for a clearer understanding of the output of the ERBB module and consequently contribute to future ERBB-directed approaches that are more beneficial for cancer treatment.

S100 family members have been specifically related to the ERBB status in breast tumorigenesis including *S100A4* and *S100P* (Perou et al., 2000; Rudland et al., 2000; Sorlie et al., 2001; Mackay et al., 2003). *S100A4* is a direct target of ERBB2 signalling in medulloblastoma cells and levels of ERBB2 and *S100A4* are tightly correlated in samples of primary medulloblastoma (Hernan et al., 2003). The induction involves phosphatidylinositol 3-kinase, AKT and ERK1/2 kinase.

In this context, it should be noted that signalling by ERBB receptors is accompanied in many cell types by a transient increase in the cytosolic concentration of Ca^{2+} . This process is mediated by phospholipase C-protein kinase C (PLC γ -PKC) pathway (Marmor et al., 2004). PLC γ phosphorylation by ERBB1 and ERBB2 results in its activation. PLC γ hydrolyzes phosphatidylinositol 4,5-bisphosphate to generate the second messengers diacylglycerol and inositol triphosphate. Binding of inositol triphosphate to receptors on the endoplasmic reticulum results in Ca^{2+} release, which lead to the activation of calcium/calmodulin-dependent protein kinases and phosphatases, including Pyk2 and calcineurin. Furthermore, Ca^{2+} and diacylglycerol activate protein kinase C (PKC), resulting in the phosphorylation of a large variety of substrates. PKC also mediates a feedback attenuation of the signalling by ERBB receptors due to its capacity to phosphorylate ERBBs and to inhibit the receptor's tyrosine kinase activity (Welsh et al., 1991).

ERBB receptors also play an important role in the regulation of cell motility and cytoskeletal reorganization mainly by the recruitment of Ca^{2+} and phosphatidylinositol 4,5-bisphosphate (Feldner and Brandt, 2002). Many experimental data support the notion that PLC γ is the most important molecule in the ERBB2-mediated migratory/invasive ability of certain tumour cells (Brandt et al., 1999). Interestingly, ERBB1 homodimers and ERBB1:ERBB2 heterodimers differentially modulate the time course of PLC γ activation thereby generating

different patterns of oscillations in Ca^{2+} level (Dittmar et al., 2002). EGF-induced breast tumour cell migration was attributed to a transient, rather than sustained, activation of PLC γ due to ERBB2 signalling.

There are multiple ways how EGF signalling could have an effect on the expression level of S100A14: 1) direct transcriptional regulation, 2) influence on the mRNA stability or 3) indirectly through other transcription factors/signalling pathways. We wished to determine which of these mechanisms is responsible for EGF-mediated S100A14 transcriptional activation. Although the effect of EGF on the stability of S100A14 mRNA was not examined in this study, cycloheximide – an inhibitor of protein synthesis – partially blocked S100A14 induction by EGF, indicating requirement for *de novo* protein synthesis (Fig. 33). Therefore, we suggest that S100A14 is an indirect transcriptional target of EGF signalling.

Treatment with the phorbol ester PMA enhanced S100A14 expression in 9442 cells (Fig. 34A). PMA is a potent tumour promoter as well as a growth regulator of many different cell types (Hunter and Karin, 1992). It activates protein kinase C (PKC), a ubiquitous family of serine/threonine kinases. These kinases play key regulatory roles in a multitude of cellular processes, including proliferation, apoptosis, differentiation, cell migration, and adhesion (Mellor and Parker, 1998; Lafon et al., 2000; Zhao et al., 2000). The PKC family consists of at least 11 isoforms. Specific isoforms are activated, depending on isoform, by Ca^{2+} , phospholipids or diacylglycerol generated by phospholipase C γ (PLC γ) or phospholipase D (PLD) from phosphatidylinositol 4,5-bisphosphate.

We used bisindolylmaleimide I which acts as a competitive inhibitor for the ATP-binding site of PKC to inhibit PKC in 9442 cells. Bisindolylmaleimide I shows high selectivity for PKC- α , - β_1 , - β_2 , - γ , - δ , and - ϵ isozymes with a ranked order of potency $\alpha > \beta_1 > \epsilon > \delta$ (Martiny-Baron et al., 1993). Pretreatment with the inhibitor did not significantly affect PMA-induced S100A14 expression in 9442 cells (Fig. 34B). The reason for this is unclear considering that the concentration of the inhibitor we applied was shown by others to block completely the activity of PKCs in bronchial epithelial cells (Reibman et al., 2000; Graness et al., 2002). Furthermore, the range of phorbol ester-sensitive isoforms of PKC (PKC- α , - β_1 , - β_2 , - γ , - δ , - ϵ , - η , - θ) virtually matches that of isoforms inhibited by bisindolylmaleimide I. Nevertheless,

we cannot exclude that the PKC isotypes that are not inhibited or only weakly inhibited by the inhibitor are responsible for *S100A14* induction.

We next examined whether EGF-induced stimulation of *S100A14* was mediated by PKC. Preincubation of cells with bisindolylmaleimide I does not prevent the EGF-induced stimulation of *S100A14* indicating that this induction is not mediated by PKC, in agreement with the finding that EGF activates the ERK1/2 cascade in a PKC-independent manner, via the RAS-dependent pathway (Boulikas, 1995), see Fig. 34D.

Previous studies have demonstrated that acute treatment with phorbol esters leads to a rapid activation of ERK MAPK in most cell types (Rossomando et al., 1989). Since PKC is the major target for these tumour promoters, it has been implicated in the activation of the ERK MAPK pathway and the consequent triggering of cellular responses such as differentiation and proliferation (Mischak et al., 1993; Murray et al., 1993). Accordingly, it has been demonstrated that members of all three groups of PKC isoforms (conventional, novel, and atypical) are able to activate upstream elements of the ERK MAPK pathway, including RAS and RAF-1, and the mechanism of activation shows some isotype specificity (Schönwasser et al., 1998; Marais et al., 1998).

We found that PMA indeed induces activation of the ERK1/2 signalling pathway in 9442 cells (Fig. 34C). Moreover, MEK1/2 inhibitor – U0126 inhibited PMA-induced *S100A14* expression indicating that the ERK1/2 MAPK pathway is the signalling pathway that targets *S100A14* expression in response to PMA (Fig. 34B).

Protein kinase C overexpression is associated with increased tumorigenicity and metastatic potential in several experimental models, and its activity is increased in tumours of breast and lung as compared with their normal counterparts (Blobe et al., 1994; O'Brian et al., 1989; Clegg et al., 1999). The essential role of PKC in processes relevant to neoplastic transformation and tumour invasion renders it a potentially suitable target for anticancer therapy (Basu, 1993). PKC- α , an important tumour-promoting factor is currently being studied as a target in treating patients with cancer.

In summary, our results demonstrate that PMA exerts stimulation of *S100A14* via PKC activation in 9442 cells. We also show that the PMA-induced *S100A14*

expression in 9442 cells requires activation of the ERK1/2 MAPK pathway. Overexpression of PKC in lung and breast tumours could therefore contribute to the enhanced expression of *S100A14* in these tumours. Our data also indicate that both PKC- and ERBB-dependent signalling converge on the ERK1/2 cascade to regulate the expression of *S100A14* and are probably necessary for its full activity (Fig. 37).

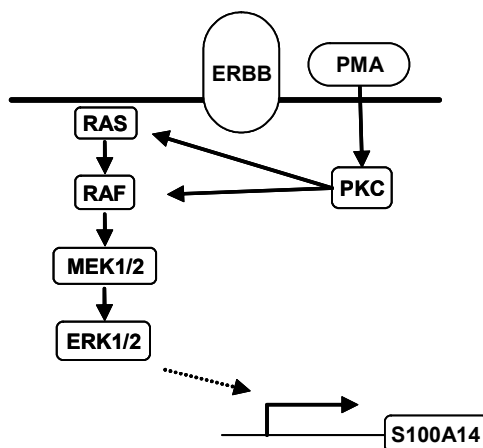


Fig. 37 Schematic representation of the signalling pathways leading to *S100A14* up-regulation in response to EGF and PMA in 9442 cells

A recent study of the protein arylation targets in human bronchial epithelial cells dosed with 1,4-benzoquinone (BQ) and 1,4-naphthoquinone (NQ), common tobacco smoke and environmental pollutants, revealed that the *S100A14* protein was one of the major cellular targets (Lamé et al., 2003).

Many quinonoid compounds are reactive electrophiles capable of causing cellular injury by two mechanisms: 1) direct disruption of the function of critical proteins or regulatory pathways, or 2) secondary activation of the immune system by the modified protein. For quinonoid compounds, a third mechanism might be considered where the adducted protein acts as a platform for quinone redox cycling producing reactive oxygen species that in turn damage the protein and its surrounding environment, including oxidative DNA damage. The toxicity of arylating quinones can be magnified by the redox cycling properties of quinone metabolites, e.g. glutathione (GSH) conjugates.

Specifically, Lamé and his colleagues, found that *S100A14* protein formed substantial amounts of adducts with BQ and NQ, as well as with GSH-BQ on two cysteine containing peptides (residues 1-5 and 68-78), providing evidence for a

cycle of oxidation of the resulting BQ-GSH conjugate metabolite followed by attachment to the protein. Formation of such protein adducts is expected to increase the residence time of redox cycling substances and therefore induce single and double strand breaks in DNA.

The finding of the modification of S100A14 protein by quinones is the first report, to our knowledge, implicating one of the putative functions of this protein. Future research aimed at identifying target proteins of S100A14 needs to be done to determine further functions of this novel gene and elucidate its role in neoplastic transformation.

In summary, by analysing a human lung tumour cell line subtraction cDNA library, we have identified and characterized a novel member of the human *S100* gene family that we designated *S100A14*. It encodes an mRNA that is ubiquitously expressed in normal human tissues of epithelial origin. We demonstrated that *S100A14* transcript is down-regulated in many immortalized and tumour cell lines from different tissues. In contrast, studies on human primary tumours, including lung and breast, revealed predominantly up-regulation of the gene at the mRNA and protein level.

We mapped the *S100A14* gene to a region of chromosomal instability on human chromosome 1q21 and subsequently resolved the gene structure of *S100A14* in human by demonstrating its organization of four exons and three introns spanning a total of 2165 bp of genomic sequence. By analysing the 5' upstream proximal region of the *S100A14* gene, we identified and characterized the minimal promoter fragment of the gene.

Studies on regulation of *S100A14* in 9442 immortalized bronchial epithelial cells identified it as a growth factor-inducible gene that is induced by epidermal growth factor (EGF) and transforming growth factor- α (TGF- α). EGF-mediated transcriptional induction of *S100A14* depends on extracellular signal-regulated kinase (ERK1/2) signalling and requires *de novo* protein synthesis. In support of these findings, we demonstrated co-existence of ERBB2 overexpression and S100A14 protein accumulation in primary breast tumours.

Further studies identified phorbol ester 12-myristate 13-acetate (PMA) as an activator of *S100A14* in 9442 cells suggesting regulation by protein kinase C (PKC). The PMA-induced *S100A14* expression is mediated by activation of the ERK1/2 signalling cascade indicating that both PKC- and ERBB-dependent signalling converge on the ERK1/2 cascade to regulate the expression of *S100A14*. Considering the frequent incidence of aberrant activation of the ERK1/2 and PKC signalling pathways in tumours as well as their oncogenic potential we suggest that it is the impaired regulation of these signalling cascades that couples *S100A14* to malignant transformation.

The challenge of future investigations will be to define the binding partners of *S100A14* to determine the function of this novel gene in cancer, and to further elucidate the functional importance of ERBB- and PKC-dependent signalling for the *S100A14* gene regulation.

5 References

- Ambartsumian N.S., Grigorian M.S., Larsen I.F., Karlstrom O., Sidenius N., Rygaard J., Georgiev G., Lukanidin E. Metastasis of mammary carcinomas in GRS/A hybrid mice transgenic for the mts1 gene. *Oncogene*. 1996. 13, 1621-1630
- Arai K., Teratani T., Nozawa R., Yamada T. Immunohistochemical investigation of S100A9 expression in pulmonary adenocarcinomas: S100A9 expression is associated with tumour differentiation. *Oncol Rep*. 2001. 8, 591-596
- Arumugam T., Simeone D.M., Schmidt A.M., Logsdon C.D. S100P stimulates cell proliferation and survival via receptor for activated glycation end products (RAGE). *J Biol Chem*. 2004. 7, 5059-5065
- Averboukh L., Liang P., Kantoff P.W., Pardee A.B. Regulation of S100P expression by androgen. *Prostate*. 1996. 29, 350-355
- Baker D.M., Wang S.L., Bell D.J., Drevon C.A., and Davis R.A. One or more labile proteins regulate the stability of chimeric mRNAs containing the 3'-untranslated region of cholesterol-7 α -hydroxylase mRNA. *J Biol Chem*. 2000. 275, 19985-19991
- Beer D.G., Kardia S.L., Huang C.C., Giordano T.J., Levin A.M., Misek D.E., Chen G., Gharib T.G., Thomas D.G., Lizyness M.L., Kuick R., Hayasaka S., Taylor J.M., Iannettoni M.D., Orringer M.B., Hanash S. Gene-expression profiles predict survival of patients with lung adenocarcinoma. *Nat Med*. 2002. 8, 816-824
- Bernards R., Weinberg R.A. A progression puzzle. *Nature*. 2002. 418, 823
- Berridge M.J., Lipp P., Bootman M.D. The versatility and universality of calcium signalling. *Nat Rev Mol Cell Biol*. 2000. 1, 11-21
- Bertram J., Palfner K., Hiddemann W., Kneba M. Elevated expression of S100P, CAPL and MAGE 3 in doxorubicin-resistant cell lines: comparison of mRNA differential display reverse transcription-polymerase chain reaction and

- subtractive suppressive hybridization for the analysis of differential gene expression. *Anticancer Drugs*. 1998. 9, 311-317
- Blobe G.C., Obeid L.M., Hannun Y.A. Regulation of protein kinase C and role in cancer biology. *Cancer Met Rev*. 1994. 13, 411-431
- Bordonaro M., Lazarova D.L., Augenlicht L.H., Sartorelli A.C. Cell type- and promoter-dependent modulation of the Wnt signaling pathway by sodium butyrate. *Int J Cancer*. 2002. 97, 42-51
- Bos J.L., Fearon E.R., Hamilton S.R., Verlaan-de Vries M., van Boom J.H., van der Eb A.J., Vogelstein B. Prevalence of ras gene mutations in human colorectal cancers. *Nature*. 1987. 327, 293-297
- Boulikas T. The phosphorylation connection to cancer. *Int J Oncol*. 1995. 6, 271-279
- Böttiger B.W., Möbes S., Glätzer R., Bauer H., Gries A., Bärtsch P., Motsch J., Martin E. Astroglial protein S100 is an early and sensitive marker of hypoxic brain damage and outcome after cardiac arrest in humans. *Circulation*. 2001. 103, 2694-2698
- Brandt B.H., Roetger A., Dittmar T., Nikolai G., Merschjann A., Nofer J.R., Dehmer-Moller G., Junker R., Assmann G., Zaenker K.S. erbB-2/EGF-R as dominant heterodimerization partners determine the motogenic phenotype in human breast cancer cells. *FASEB J*. 1999. 13, 1939-1949
- Bucher P. Weight matrix descriptions of four eukaryotic RNA polymerase II promotor elements derived from 502 unrelated promotor sequences. *J Mol Biol*. 1990. 212, 563-578
- Burden S., Yarden Y. Neuregulins and their receptors: A versatile signalling module in organogenesis and oncogenesis. *Neuron*. 1997. 18, 847-855
- Camby I., Nagy N., Lopes M.B., Schäfer B.W., Muraige C.A., Ruchoux M.M., Murmann P., Pochet R., Heizmann C.W., Brothi J., Salmon I., Kiss R., Decaestecker Ch. Supratentorial pilocytic astrocytomas, astrocytomas, anaplastic astrocytomas and glioblastomas are characterized by a differential expression of S100 proteins. *Brain Pathol*. 1999. 9, 1-19

- Camby I., LeFranc F., Titeca G., Neuci S., Fastrez M., Dedecken L., Schäfer B.W., Brotchi J., Heizmann C.W., Pochet R., Salmon I., Kiss R., Decaestecker Ch. Differential expression of S100 calcium-binding proteins characterizes distinct clinical entities in both WHO grade II and III astrocytic tumors. *Neuropathol Applied Neurobiol.* 2000. 26, 76-90
- Carmeliet P., Jain R.K. Angiogenesis in cancer and other diseases. *Nature.* 2000. 407, 249-257
- Chang C., Werb Z. The many faces of metalloproteases: cell growth, invasion, angiogenesis and metastasis. *Trends Cell Biol.* 2001. 11, S37-S43
- Chen C.Y., Shyu A.B. AU-rich elements: characterization and importance in mRNA degradation. *Trends Biochem Sci.* 1995. 20, 465-470
- Clegg R.A., Gordge P.C., Miller W.R. Expression of enzymes of covalent protein modification during regulated and dysregulated proliferation of mammary epithelial cells: PKA, PKC and NMT. *Advan Enzyme Regul.* 1999. 39, 175-203
- Coussens L.M., Raymond W.W., Bergers G., Laig-Webster M., Behrendtsen O., Werb Z., Cughey G.H., Hanahan D. Inflammatory mast cells up-regulate angiogenesis during squamous epithelial carcinogenesis. *Genes Dev.* 1999. 13, 1382-1397
- Coussens L.M., Tinkle C.L., Hanahan D., Werb Z. MMP-9 supplied by bone marrow-derived cells contributes to skin carcinogenesis. *Cell.* 2000. 103, 481-490
- Creighton C., Kuick R., Misek D.E., Rickman D.S., Brichory F.M., Rouillard J.-M., Omenn G.S., Hanash S. Profiling of pathway-specific changes in gene expression following growth of human cancer cell lines transplanted into mice. *Genome Biology.* 2003. 4, R46
- Davey G.E., Murmann P., Heizmann C.W. Intracellular Ca^{2+} and Zn^{2+} levels regulate the alternative cell density-dependent secretion of S100B in human glioblastoma cells. *J Biol Chem.* 2001. 276, 30819-30826

- Davies M.P., Rudland P.S., Robertson L., Parry E.W., Jolicoeur P., Barraclough R. Expression of the calcium-binding protein S100A4 (p9Ka) in MMTV-neu transgenic mice induces metastasis of mammary tumours. *Oncogene*. 1996. 13, 1631-1637
- Deininger P.L., Batzer M.A. Alu repeats and human disease. *Mol Genet Metabol*. 1999. 67, 183-193
- Diatchenko L., Lau Y.F., Campbell A.P., Chenchik A., Moqadam F., Huang B., Lukyanov S., Lukyanov K., Gurskaya N., Sverdlov E.D., Siebert P.D. Suppression subtractive hybridization: a method for generating differentially regulated or tissue-specific cDNA probes and libraries. *Proc Natl Acad Sci USA*. 1996. 93, 6025-6030
- Diaz-Guerra M.J.M., Velasco M., Martin-Sanz P., Bosca L. Nuclear factor κ B is required for the transcriptional control of type II NO synthase in regenerating liver. *Biochem J*. 1997. 326, 791-797
- Difilippantonio S., Chen Y., Pietas A., Schlüns K., Pacyna-Gengelbach M., Deutschmann N., Padilla-Nash H.M., Ried T., Petersen I. Gene expression profiles in human non-small and small-cell lung cancer. *Eur J Cancer*. 2003. 39, 1936-1947
- Dittmar T., Husemann A., Schewe Y., Nofer J.-R., Niggemann B., Zänker K.S., Brandt B.H. Induction of cancer cell migration by epidermal growth factor is initiated by specific phosphorylation of tyrosine 1248 of c-erbB-2 receptor via EGFR. *FASEB J*. 2002. 16, 1823-1825
- Dixon D.A., Caplan C.D., McIntyre T.M., Zimmerman G.A., Prescott S.M. Post-transcriptional control of cyclooxygenase-2 gene expression. *J Biol Chem*. 2000. 16, 11750-11757
- Donato R. S100: a multigenic family of calcium-modulated proteins of the EF-hand type with intracellular and extracellular functional roles. *J. Biochem. Cell Biol*. 2001. 33, 637-668

- Du X.-J., Cole T.J., Tennis N., Gao X.-M., Köntgen F., Kemp B.E., Heierhorst J. Impaired cardiac contractility response to hemodynamic stress in S100A1-deficient mice. *Mol Cell Biol.* 2002. 22, 2821-2829
- El-Rifai W., Moskaluk C.A., Abdrabbo M.K., Harper J., Yoshida C., Frierson H.F. Jr., Powell S.M. Gastric cancers overexpress S100A calcium-binding proteins. *Cancer Res.* 2002. 62, 6823-6826
- Emberley E.D., Niu Y., Njue C., Kliever E.V., Murphy L.C., Watson P.H. Psoriasin (S100A7) expression is associated with poor outcome in estrogen receptor-negative invasive breast cancer. *Clin Cancer Res.* 2003. 9, 2627-2631
- Feldner J.C., Brandt B.H. Cancer cell motility – on the road from c-erbB-2 receptor steered signalling to actin reorganization. *Exp Cell Res.* 2002. 272, 93-108
- Feng G., Xu X., Youssef E.M., Lotan R. Diminished expression of S100A2, a putative tumor suppressor, at early stage of human lung carcinogenesis. *Cancer Res.* 2001. 61, 7999-8004
- Fontanini G., De Laurentiis M., Vignati S., Chine S., Lucchi M., Silvestri V., Mussi A., De Placido S., Tortora G., Bianco A.R., Gullick W., Angeletti C.A., Bevilacqua G., Ciardiello F. Evaluation of epidermal growth factor-related growth factors and receptors and of neoangiogenesis in completely resected stage I-III non-small cell lung cancer: amphiregulin and microvessel count are independent prognostic indicators of survival. *Clin Cancer Res.* 1998. 4, 241-249
- Gebhardt C., Breitenbach U., Tuckermann J.P., Dittrich B.T., Richter K., Angel P. Calgranulins S100A8 and S100A9 are negatively regulated by glucocorticoids in a c-Fos-dependent manner and overexpressed throughout skin carcinogenesis. *Oncogene.* 2002. 21, 4266-4276
- Gendler S.J., Cohen E.P., Craston A., Duhig T., Johnstone G., Barnes D. The locus of the polymorphic epithelial mucin (PEM) tumor antigen on chromosome 1q21 shows a high frequency of alteration in primary human breast tumors. *Int J Cancer.* 1990. 45, 431-435

- Gerlai R., Roder J. Abnormal exploratory behaviour in transgenic mice carrying multiple copies of the human gene for S100 beta. *J Psychiatry & Neurosci.* 1995. 20, 105-112
- Giles K.M., Daly J.M., Beveridge D.J., Thomson A.M., Voon D.C., Furneaux H.M., Jazayeri J.A., Leedman P.J. The 3'-untranslated region of p21^{WAF1} mRNA is a composite *cis*-acting sequence bound by RNA-binding proteins from breast cancer cells, including HuR and poly(C)-binding protein. *J Biol Chem.* 2003. 5, 2937-2946
- Godsen J.R. Molecular Analysis of Chromosome Aberrations. *Methods in Molecular Biology.* 29. Humana Press Inc. Totowa, NJ. 1994
- Graness A., Chwieralski C.E., Reinhold D., Thim L., Hoffmann W. Protein kinase C and ERK activation are required for TFF-peptide stimulated bronchial epithelial cell migration and tumor necrosis factor- α -induced interleukin-6 (IL-6) and IL-8 secretion. *J Biol Chem.* 2002. 277, 18440-18446
- Guerreiro Da Silva I.D., Hu Y.F., Russo I.H., Ao I.H., Salicioni X., Yang A.M., Russo J. S100P calcium-binding protein overexpression is associated with immortalization of human breast epithelial cells in vitro and early stages of breast cancer development in vivo. *Int J Oncol.* 2000. 16, 231-240
- Han J., Brown T., Beutler B. Endotoxin-responsive sequences control cachectin/tumor necrosis factor biosynthesis at the translational level. *J Exp Med.* 1990. 171, 465-475
- Hanahan D., Weinberg R.A. The hallmarks of cancer. *Cell.* 2000. 100, 57-70
- Hancq S., Salmon I., Brotchi J., De Witte O., Gabius H.J., Heizmann C.W., Kiss R., Decaestecker C. S100A5: a marker of recurrence in WHO grade I meningiomas. *Neuropathol Appl Neurobiol.* 2004. 30, 178-187
- Heighway J., Knapp T., Boyce L., Brennand S., Field J.K., Betticher D.C., Ratschiller D., Gugger M., Donovan M., Lasek A., Rickert P. Expression profiling of primary non-small cell lung cancer for target identification. *Oncogene.* 2002. 21, 7749-7763

- Heizmann C.W., Fritz G., Schäfer B.W. S100 proteins: structure, functions and pathology. *Frontiers Biosci.* 2002. 7, 1356-1368
- Hernan R., Fasheh R., Calabrese Ch., Frank A.J., Maclean K.H., Allard D., Barraclough R., Gilbertson R.J. ERBB2 up-regulates *S100A4* and several other prometastatic genes in medulloblastoma. *Cancer Res.* 2003. 63, 140-148
- Hofmann M., Drury S., Caifeng F., Qu W., Lu Y., Avila C., Kambhan N., Slattery T., McClary J., Nagashima M., Morser J., Stern D., Schmidt A.-M. RAGE mediates a novel proinflammatory axis: the cell surface receptor for S100/calgranulin polypeptides. *Cell.* 1999. 97, 889-901
- Hollams E.H., Giles K.M., Thomson A.M., Leedman P.J. mRNA stability and the control of gene expression: implications for human disease. *Neurochem Res.* 2002. 27, 957-980
- Hough C.D., Cho K.R., Zonderman A.B., Schwartz D.R., Morin P.J. Coordinately up-regulated genes in ovarian cancer. *Cancer Res.* 2001. 61, 3869-3876
- Hoyaux D., Alao J., Fuchs J., Kiss R., Keller B., Heizmann C.W., Pochet R., Frermann D. S100A6, a calcium- and zinc-binding protein, is overexpressed in SOD1 mutant mice, a model for amyotrophic lateral sclerosis. *Biochim Biophys Acta.* 2000. 1498, 264-272
- Hsieh H.-L., Schäfer B.W., Cox J.A., Heizmann C.W. S100A13 and S100A6 exhibit distinct translocation pathways in endothelial cells. *J Cell Sci.* 2002. 115, 3149-3158
- Hsieh H.-L., Schäfer B.W., Weigle B., Heizmann C.W. S100 protein translocation in response to extracellular S100 is mediated by receptor for advanced glycation endproducts in human endothelial cells. *Bioch Bioph Res Com.* 2004. 316, 949-959
- Hunter T., Karin M. The regulation of transcription by phosphorylation. *Cell.* 1992. 70, 375-87
- Huttunen H.J., Kuja-Panulat J., Sorci G., Agneletti A.L., Donato R., Rauvala H. Coregulation of neurite outgrowth and cell survival by amphotericin and S100

- proteins through receptor for advanced glycation end products (RAGE) activation. *J Biol Chem.* 2000. 275, 40096-40105
- Joo J.H., Kim J.W., Lee Y., Yoon S.Y., Kim J.H., Paik S.-G., Choe I.S. Involvement of NF κ B in the regulation of S100A6 gene expression in human hepatoblastoma cell line HepG2. *Biochem Biophys Res Commun.* 2003. 307, 274-280
- Kawasaki H., Nakayama S., Kretsinger R.H. Classification and evolution of EF-hand proteins. *BioMetals.* 1998. 11, 277-295
- Khosravi-Far R., Der C.J. The Ras signal transduction pathway. *Cancer Met Rev.* 1994. 13, 67-89
- Kiewitz R., Acklin C., Minder E., Huber P.R., Schäfer B.W., Heizmann C.W. S100A1, a new marker for acute myocardial ischemia. *Biochem Biophys Res Commun.* 2000. 274, 865-871
- Kinzler K.W., Vogelstein B. Lessons from hereditary colorectal cancer. *Cell.* 1996. 87, 159-170
- Kozak M. Interpreting cDNA sequences: some insights from studies on translation. *Mamm. Genome.* 1996. 7(8), 563-574
- Krähn G., Kaskel P., Sander S., Pereira J., Waizenhöfer Y., Wortmann S., Leiter U., Peter R.U. S100 β is a more reliable tumor marker in peripheral blood for patients with newly occurred melanoma metastases compared with MIA, albumin and lactate-dehydrogenase. *Anticancer Res.* 2001. 21, 1311-1316
- Kriajevska M., Fischer-Larsen M., Moertz E., Vorm O., Tulchinsky E., Grigorian M., Ambartsumian N., Lukanidin E. Liprin β 1, a member of the family of LAR transmembrane tyrosine phosphatase-interacting proteins, is a new target for the metastasis-associated protein S100A4 (Mts1). *J Biol Chem.* 2002. 277, 5229-5235
- Kruys V., Marinx O., Shaw G., Deschamps J., Huez G. Translational blockade imposed by cytokine-derived UA-rich sequences. *Science.* 1989. 245, 852-855

- Lafon C., Mazars P., Guerrin M., Barboule N., Charcosset J.Y., Valette A. Early gene responses associated with transforming growth factor-beta 1 growth inhibition and autoinduction in MCF-7 breast adenocarcinoma cells. *Bioch Biophys Acta*. 1995. 1266, 288-295
- Lauriola L., Michetti F., Maggiano N., Galli J., Cadoni G., Schäfer B.W., Heizmann C.W., Ranelletti F.O. Prognostic significance of the Ca^{2+} binding protein S100A2 in laryngeal squamous-cell carcinoma. *Int J Cancer*. 2000. 89, 345-349
- Lee S.W., Tomasetto C., Swisshelm K., Keyomarsi K., Sager R. Down-regulation of a member of the S100 gene family in mammary carcinoma cells and re-expression by azadeoxycytidine treatment. *Proc Natl Acad Sci USA*. 1992. 89, 2504-2508
- Levine T.D., Gao F., King P.H., Andrews L.G., Keene J.D. Hel-N1: an autoimmune RNA-binding protein with specificity for 3' uridylate-rich untranslated regions of growth factor mRNAs. *Mol Cell Biol*. 1993. 13, 3494-3504
- Liu D., Rudland P.S., Sibson D.R., Platt-Higgins A., Barraclough R. Expression of calcium-binding protein S100A2 in breast lesions. *Br J Cancer*. 2000. 83, 1473-1479
- Logsdon C.D., Simeone D.M., Binkley C., Arumugam T., Greenson J.K., Giordano T.J., Misek D.E., Hanash S. Molecular profiling of pancreatic adenocarcinoma and chronic pancreatitis identifies multiple genes differentially regulated in pancreatic cancer. *Cancer Res*. 2003. 63, 2649-2657
- Maass N., Hojo T., Ueding M., Luttges J., Kloppel G., Jonat W., Nagasaki K. Expression of the tumor suppressor gene Maspin in human pancreatic cancers. *Clin. Cancer Res*. 2001. 7, 812-817
- Mackay A., Jones Ch., Dexter T., Silva R.L.A., Bulmer K., Jones A., Simpson P., Harris R.A., Parmjit S.J., Neville A.M., Reis L.F.L., Lakhani S.R., O'Hare M.J. cDNA microarray analysis of genes associated with *ERBB2* (HER2/neu)

- overexpression in human mammary luminal epithelial cells. *Oncogene*. 2003. 22, 2680-2688
- Mandinova A., Soldi R., Graziani I., Bagala C., Bellum S., Landriscina M., Tarantini F., Prudovsky I., Maciag T. S100A13 mediates the copper-dependent stress-induced release of IL-1 α from both human U937 and murine NIH 3T3 cells. *J Cell Sci*. 2003. 116, 2687-2696
- Marais R., Light Y., Mason C., Paterson H., Olson M.F., Marshall C.J. Requirement of Ras-GTP-Raf complexes for activation of Raf-1 by protein kinase C. *Science*. 1998. 280, 109-112
- Marenholz I., Volz A., Ziegler A., Davies A., Ragoussis I., Korge B.P., Mischke D. Genetic analysis of the epidermal differentiation complex (EDC) on human chromosome 1q21: chromosomal orientation, new markers, and a 6-Mb YAC contig. *Genomics*. 1996. 37, 295-302
- Marenholz I., Zirra M., Fischer D.F., Backendorf C., Ziegler A., Mischke D. Identification of human epidermal differentiation complex (EDC)-encoded genes by subtractive hybridization of entire YACs to a gridded keratinocyte cDNA library. *Genome Res*. 2001. 11, 341-355
- Marenholz I., Heizmann C.W. S100A16, a ubiquitously expressed EF-hand protein which is up-regulated in tumors. *Biochem Biophys Res Commun*. 2004. 313, 237-244
- Marmor M.D., Kochupurakkal B.S., Yarden Y. Signal transduction and oncogenesis by ERBB/HER receptors. *Int J Rad Oncol Biol Phys*. 2004. 58, 903-913
- Martiny-Baron G., Kazanietz M.G., Mischak H., Blumberg P.M., Kochs G., Hug H., Marme D., Schachtele C. Selective inhibition of protein kinase C isozymes by the indolocarbazole Go 6976. *J Biol Chem*. 1993. 268, 9194-9197
- Mellor H., Parker P.J. The extended protein kinase C superfamily. *Biochem J*. 1998. 332, 281-292
- Miles D.W., Harris W.H., Gillett C.E., Smith P., Barnes D.M. Effect of c-erbB(2) and estrogen receptor status on survival of women with primary breast

- cancer treated with adjuvant cyclophosphamide/methotrexate/fluorouracil. *Int. J. Cancer*. 1999. 84, 354-359
- Mills N.E., Fishman C.L., Rom W.N., Dubin N., Jacobson D.R. Increased prevalence of K-ras oncogene mutations in lung adenocarcinoma. *Cancer Res*. 1995. 55, 1444-1447
- Millward T.A., Heizmann C.W., Schafer B.W., Hemmings B.A. Calcium regulation of Ndr protein kinase mediated by S100 calcium-binding proteins. *EMBO J*. 1998. 17, 5913-5922
- Mischak H., Pierce J.H., Goodnight J., Kazanietz M.G., Blumberg P.M., Mushinski J.F. Phorbol ester-induced myeloid differentiation is mediated by protein kinase C- α and - δ . *J Biol Chem*. 1993. 268, 20110-20115
- Murray N.R., Baumgardner G.P., Burns D.J., Fields A.P. Protein kinase C isotypes in human erythroleukemia (K562) cell proliferation and differentiation. Evidence that beta II protein kinase C is required for proliferation. *J Biol Chem*. 1993. 268, 15847-15853
- Nichols A.F., Toshiki I., Zolezzi F., Hutsell S., Linn S. Basal transcriptional regulation of human damage-specific DNA-binding protein genes DDB1 and DDB2 by Sp1, E2F, N-myc and NF1 elements. *Nucleic Acids Res*. 2003. 31, 562-569
- Ninomiya I., Ohta T., Fushida S., Endo Y., Hashimoto T., Yagi M., Fujimura T., Nishi-mura G., Tani T., Shimizu K., Yonemura Y., Heizmann C.W., Schäfer B.W., Sasaki T., Miwa K. Increased expression of S100A4 and its prognostic significance in esophageal squamous cell carcinoma. *Int J Cancer*. 2001. 18, 715-720
- Nishikawa T., Lee I.S., Shiraishi N., Ishikawa T., Ohta Y., Nishikimi M. Identification of S100b protein as copper-binding protein and its suppression of copper-induced cell damage. *J Biol Chem*. 1997. 272, 23037-23041
- Nowell P.C. The clonal evolution of tumor cell populations. *Science*. 1976. 194, 23-28

- O'Brian C.A., Vogel V.G., Singletary S.E., Ward N.E. Elevated protein kinase C expression in human breast tumor biopsies relative to normal breast tissue. *Cancer Res.* 1989. 49, 3215-3217
- Olayioye M.A., Neve R.M., Lane H.A., Hynes N.E. The ERBB signalling network: receptor heterodimerization in development and cancer. *EMBO J.* 2000. 19, 3159-3167
- Olumi A.F., Grossfeld G.D., Hayward S.W., Carroll P.R., Tlsty T.D., Cunha G.R. Carcinoma-associated fibroblasts direct tumor progression of initiated human prostatic epithelium. *Cancer Res.* 1999. 59, 5002-5011
- Ostergaard M., Wolf H., Orntoft T.F., Celis J.E. Psoriasin (S100A7): a putative urinary marker for the follow-up of patients with bladder squamous cell carcinomas. *Electrophoresis.* 1999. 20, 349-354
- Passey R.J., Williams E., Lichanska A.M., Wells C., Hu S., Geczy C.L., Little M.H., Hume D.A. A null mutation in the inflammation-associated S100 protein S100A8 causes early resorption of the mouse embryo. *J Immunol.* 1999. 163, 2209-2216
- Pellegata N.S., Sessa F., Renault B., Bonato M., Leone B.E., Solcia E., Ranzani G.N. K-ras and p53 gene mutations in pancreatic cancer: ductal and nonductal tumors progress through different genetic lesions. *Cancer Res.* 1994. 54, 1556-1560
- Perou C.M., Sorlie T., Eisen M.B., van de Rijn M., Jeffrey S.S., Rees C.A., Pollack J.R., Ross D.T., Johnsen H., Akslen L.A., Fluge O., Pergamenschikov A., Williams C., Zhu S.X., Lonning P.E., Borresen-Dale A.L., Brown P.O., Botstein D. Molecular portraits of human breast tumours. *Nature.* 2000. 406, 747-752
- Perrais M., Pigny P., Copin M.-Ch., Aubert J.-P., Van Seuning I. Induction of MUC2 and MUC5AC mucins by factors of the epidermal growth factor (EGF) family is mediated by EGF receptor/Ras/Raf/extracellular signal-regulated kinase cascade and Sp1. *J Biol Chem.* 2002. 277, 32258-32267

- Pietas A., Schluns K., Marenholz I., Schafer B.W., Heizmann C.W., Petersen I. Molecular cloning and characterization of the human S100A14 gene encoding a novel member of the S100 family. *Genomics*. 2002. 79, 513-522
- Platt-Higgins A.M., Renshaw Ch.A., West Ch. R., Winstanley J.H.R., De Silva Rudland S., Barraclough R., Rudland Ph.S. Comparison of the metastasis-inducing protein S100A4 (p9Ka) with other prognostic markers in human breast cancer. *Int J Cancer*. 2000. 89, 198-208
- Prenzel N., Fischer O.M., Streit S., Hart S., Ullrich A. The epidermal growth factor receptor family as a central element for cellular signal transduction and diversification. *Endocrine Cancer*. 2001. 8, 11-31
- Ranganathan G., Li C., Kern P.A. The translational regulation of lipoprotein lipase in diabetic rats involves the 3'-untranslated region of the lipoprotein lipase mRNA. *J Biol Chem*. 2000. 275, 40986-40991
- Reibman J., Talbot A.T., Hsu Y., Ou G., Jover J., Nilsen D., Pillinger M.H. Regulation of expression of granulocyte-macrophage colony-stimulating factor in human bronchial epithelial cells: roles of protein kinase C and mitogen-activated protein kinases. *J Immun*. 2000. 165, 1618-1625
- Riese D.J., Kim E.D., Elenius K., Buckley S., Klagbrun M., Plowman G.D., Stern D.F. The epidermal growth factor receptor couples transforming growth factor- α , heparin-binding epidermal growth factor-like factor, and amphiregulin to Neu, ERBB-3, and ERBB-4. *J Biol Chem*. 1996. 271, 20047-20052
- Renan M.J. How many mutations are required for tumorigenesis? Implications from human cancer data. *Mol. Carcinogenesis*. 1993. 7, 139-146
- Rossomando A.J., Payne D.M., Weber M.J., Sturgill T.W. Evidence that pp42, a major tyrosine kinase target protein, is a mitogen-activated serine/threonine protein kinase. *Proc Natl Acad Sci USA*. 1989. 86, 6940-6943
- Rudland P.S., Platt-Higgins A., Renshaw C., West C.R., Winstanley J.H., Robertson L., Barraclough R. Prognostic significance of the metastasis-

- inducing protein S100A4 (p9Ka) in human breast cancer. *Cancer Res.* 2000. 60, 1596-1603
- Rüdiger N.S., Gregersen N., Kielland-Brandt M. C. One short well conserved region of *Alu*-sequences is involved in human gene rearrangements and has homology with prokaryotic *chi*. *Nucleic Acids Res.* 1995. 23, 256-260
- Rusch V., Klimstra D., Venkatraman E., Pisters P.W., Langenfeld J., Dmitrovsky E. Overexpression of the epidermal growth factor receptor and its ligand transforming growth factor alpha is frequent in resectable non-small cell lung cancer but does not predict tumor progression. *Clin Cancer Res.* 1997. 3, 515-522
- Salomon D.S., Brandt R., Ciardiello F., Normanno N. Epidermal growth factor-related peptides and their receptors in human malignancies. *Crit Rev Oncol Hematol.* 1995. 19, 183-232
- Sandgren E.P., Luetkeke N.C., Palmiter R.D., Brinster R.L., Lee D.C. Overexpression of TGF- α in transgenic mice: induction of epithelial hyperplasia, pancreatic metaplasia, and carcinoma of the breast. *Cell.* 1990. 61, 1121-1135
- Sandgren E.P., Luetkeke N.C., Qiu T.H., Palmiter R.D., Brinster R.L., Lee D.C. Transforming growth factor α dramatically enhances oncogene-induced carcinogenesis in transgenic mouse pancreas and liver. *Mol Cell Biol.* 1993. 13, 320-330
- Sakaguchi M., Miyazaki M., Inoue Y., Tsuji T., Kouchi H., Tanaka T., Yamada H., Namba M. Relationship between contact inhibition and intranuclear S100C of normal human fibroblasts. *J Cell Biol.* 2000. 149, 1193-1206
- Sakaguchi M., Miyazaki M., Takaishi M., Sakaguchi Y., Makino E., Kataoka N., Yamada H., Namba M., Huh N. S100C/A11 is a key mediator of Ca^{2+} -induced growth inhibition of human epidermal keratinocytes. *J Cell Biol.* 2003. 163, 825-835
- Schaffner W., Weissmann C. A rapid, sensitive, and specific method for the determination of protein in dilute solution. *Anal Biochem.* 1973. 56, 502-514

- Schäfer B.W., Wicki R., Engelkamp D., Mattei M.G., Heizmann C.W. Isolation of a YAC clone covering a cluster of nine S100 genes on human chromosome 1q21: rationale for a new nomenclature of the S100 calcium-binding protein family. *Genomics*. 1995. 25, 638-643
- Schäfer B.W., Fritschy J.-M., Murmann P., Troxler H., Durussel I., Heizmann C.W., Cox J.A. Brain S100A5 is a novel calcium-, zinc-, and copper ion-binding protein of the EF-hand superfamily. *J Biol Chem*. 2000. 275, 30623-30630
- Schmidt A.M., Yan S.D., Yan S.F., Stern D.M. The biology of the receptor for advanced glycation end products and its ligands. *Biochim Biophys Acta*. 2000. 1498, 99-111
- Schönwasser D.C., Marais R.M., Marshall C.J., Parker P.J. Activation of the mitogen-activated protein kinase/extracellular signal-regulated kinase pathway by conventional, novel, and atypical protein kinase C isotypes. *Mol Cell Biol*. 1998. 18, 790-798
- Seftor R.E., Seftor E.A., Sheng S., Pemberton P.A., Sager R., Hendrix M.J. Maspin suppresses the invasive phenotype of human breast carcinoma. *Cancer Res*. 1998. 58, 5681-5685
- Sorlie T., Perou C.M., Tibshirani R., Aas T., Geisler S., Johnsen H., Hastie T., Eisen M.B., van de Rijn M., Jeffrey S.S., Thorsen T., Quist H., Matese J.C., Brown P.O., Botstein D., Lonning P., Borresen-Dale A.L. Gene expression patterns of breast carcinomas distinguish tumor subclasses with clinical implications. *Proc Natl. Acad Sci USA*. 2001. 98, 10869-10874
- South A.P., Cabral A., Ives J.H., James C.H., Mirza G., Marenholz I., Mischke D., Backendorf C., Ragoussis J., Nizetic D. Human epidermal differentiation complex in a single 2.5 Mbp long continuum of overlapping DNA cloned in bacteria integrating physical and transcript maps. *J Invest Dermatol*. 1999. 112, 910-918
- Stulik J., Osterreicher J., Koupilova K., Knizek K., Macela A., Bures J., Jandik P., Langr F., Dedic K., Jungblut P.R. The analysis of S100A8 and S100A9 expression in matched sets of macroscopically normal colon mucosa and

- colorectal carcinoma: the S100A9 and S100A8 positive cells underlie and invade tumour mass. *Electrophoresis*. 1999. 20, 1047-1054
- Takagi H., Sharp R., Takayama H., Anver M.R., Ward J.M., Merlino G. Collaboration between growth factors and diverse chemical carcinogens in hepatocarcinogenesis of transforming growth factor α transgenic mice. *Cancer Res*. 1993. 53, 4329-4336
- Teratani T., Watanabe T., Kuwahara F., Kumagai H., Kobayashi S., Aoki U., Ishikawa A., Arai K., Nozawa R. Induced transcriptional expression of calcium-binding protein S100A1 and S100A10 genes in human renal cell carcinoma. *Cancer Lett*. 2002. 175, 71-77
- Venter J.C., et al. The sequence of the human genome. *Science*. 2001. 291, 1304-1351
- Wang E., Ma W.-J., Aghajanian C., Spriggs D. R. Posttranscriptional regulation of protein expression in human epithelial carcinoma cells by adenine-uridine-rich elements in the 3'-untranslated region of tumor necrosis factor- α messenger RNA. *Cancer Res*. 1997. 57, 5426-5433
- Wasserman W.W., Sandelin A. Applied bioinformatics for the identification of regulatory elements. *Nat Rev Genet*. 2004. 5, 276-287
- Welsh J.B., Gill G.N., Rosenfeld M.G., Wells A. A negative feedback loop attenuates EGF-induced morphological changes. *J Cell Biol*. 1991. 114, 533-543
- Weternan M.A.J., Wilbrink M., Dijkhuizen T., van den Berg E., van Kessel A.G. Fine mapping of the 1q21 breakpoint of the papillary renal cell carcinoma-associated (X;1) translocation. *Hum Genet*. 1996. 98, 16-21
- Wicki R., Franz C., Scholl F.A., Heizmann C.W., Schäfer B.W. Repression of the candidate tumor suppressor gene S100A2 in breast cancer is mediated by site-specific hypermethylation. *Cell Calcium*. 1997. 22, 243-254
- Witton C.J., Reeves J.R., Going J.J., Cooke T.G., Bartlett J.M.S. Expression of the HER1-4 family of receptor tyrosine kinases in breast cancer. *J Pathol*. 2003. 200, 290-297

- Wright F.A., Lemon W.J., Zhao W.D., Sears R., Zhuo D., Wang J.P., Yang H.Y., Baer T., Stredney D., Spitzner J., Stutz A., Krahe R., Yuan B. A draft annotation and overview of the human genome. *Genome Biol.* 2001. 2(7), 0025.1-0025.18
- Xiong Z., O'Hanlon D., Becker L.E., Roder J., MacDonalds J.F., Marks A. Enhanced calcium transients in glial cells in neonatal cerebellar cultures derived from S100B null mice. *Exp Cell Res.* 2000. 257, 281-289
- Yarden Y., Sliwkowski M.X. Untangling the ERBB signalling network. *Nature Rev.* 2001. 2, 127-137
- Yonemura Y., Endou Y., Kimura K., Fushida S., Bandou E., Taniguchi K., Kinoshita K., Ninomiya I., Sugiyama K., Heizmann C.W., Schäfer B.W., Sasaki T. Inverse expression of S100A4 and E-cadherin is associated with metastatic potential in gastric cancer. *Clin Cancer Res.* 2000. 6, 4234-4242
- Zhang L., Fogg D.K., Waisman D.M. RNA interference-mediated silencing of the *S100A10* gene attenuates plasmin generation and invasiveness of Colo 222 colorectal cancer cells. *J Biol Chem.* 2004. 279, 2053-2062
- Zhao Y., Neltner B.S., Davis H.W. Role of MARCS in regulating endothelial cell proliferation. *Am J Physiol.* 2000. 279, C1611-C1620
- Zhi H., Zhang J., Hu G., Lu J., Wang X., Zhou C., Wu M., Liu Z. The deregulation of arachidonic acid metabolism-related genes in human esophageal squamous cell carcinoma. *Int J Cancer.* 2003. 106, 327-333

Danksagung

Meinem Betreuer Herrn Prof. Dr. Iver Petersen, dem Leiter der Arbeitsgruppe Tumorgenetik am Institut für Pathologie der Charité, möchte ich für die Projektleitung, seine fachliche Unterstützung und den großen Freiraum bei der Bearbeitung des Themas danken.

Prof. Dr. Harald Saumweber möchte ich für die fachlichen Diskussionen, seine stimulierenden Hinweise und insbesondere seine Bereitschaft danken, mich beim Promotionsverfahren am Fachbereich Biologie der Humboldt Universität Berlin zu betreuen.

Frau Priv. Doz. Dr. Christine Sers danke ich herzlich für ihre wertvollen Anregungen, ihre Diskussionsbereitschaft und ihre freundliche Unterstützung während der gesamten Zeit meiner Doktorarbeit.

Mein besonderer Dank gilt Herrn Prof. Dr. Reinhold Schäfer für seine wertvolle Hilfestellung, seinen vielseitigen fachlichen Rat und insbesondere die Bereitschaft, mir die Teilnahme an den wissenschaftlichen Kolloquien seiner Arbeitsgruppe zu ermöglichen.

Herrn Dr. Karsten Jürchott danke ich für seine konstruktiven Hinweise, die wesentlicher Anstoß in einer wichtigen Etappe der Arbeit waren, für die stete Diskussionsbereitschaft und besonders für die intensive Durchsicht des Manuskripts.

Unserem Institutsdirektor Prof. Dr. Manfred Dietel danke ich für die angenehme Arbeitsatmosphäre und die Bereitstellung der technischen und materiellen Infrastruktur am Institut für Pathologie.

Nicht zuletzt gilt mein großer Dank Herrn Dr. Karsten Schlüns, der mich durch seine wissenschaftliche, aber auch persönliche Unterstützung durch alle Höhen und Tiefen dieser Arbeit begleitet hat.

Frau Nicole Deutschmann möchte ich für ihre Mithilfe in der Zellkultur, Anfertigung der Gewebe-Arrays und für das Heraussuchen unzähliger Paraffinblöcke danken.

Nicht versäumen will ich, mich bei dem MTA-Team der Abteilung Immunhistochemische Diagnostik für die hochwertigen immunhistochemischen Färbungen zu bedanken.

Den gesamten Arbeitsgruppen Schäfer und Sers danke ich herzlich für unschätzbare Hilfen in vielen molekularbiologischen Methoden.

Nicht unerwähnt möchte ich jene lassen, die mir unermüdlich und immer freundlich in den Laboren des Instituts für Pathologie tatkräftige Hilfen waren, sowie alle, die mir zur praktischen Umsetzung und Fertigstellung der Arbeit verhalfen. Ihnen allen gilt mein herzlicher Dank.

Curriculum Vitae

14.4.1975	Born in Lublin, Poland
1982-1990	Szkola podstawowa im. Tadeusza Kosciuszki (primary school), Poland
1990-1994	Jan Zamoyski Liceum (high school), Poland
May 1994	School-leaving Exams
1994-1999	Study of Biotechnology at the Maria Curie-Sklodowska University, Lublin, Poland
Sept 1997 - Feb 1998	Work at the Telomere Biology Laboratory, Institute of Pathology, University Hospital Charité, Berlin, Germany
June 1999	Master Thesis "Analysis of telomerase activity in human testicular germ cell tumours" at Maria Curie Memorial Cancer Centre and Institute of Oncology, Warsaw, Poland
Sept 1999 - Dec 1999	Visiting Scholar, Institute of Immunology and Virology, Würzburg, Germany
Jan 2000	Begin of PhD thesis
Since Jan 2000	Research Assistant, Tumour Genetics Group (Prof. Dr. Iver Petersen), Institute of Pathology, University Hospital Charité, Berlin, Germany

.....
 Berlin, den 28. Juni 2004

Agnieszka Pietas

Publications

Nowak R., Sikora K., Pietas A., Skoneczna I., Chrapusta S.J. Germ cell-like telomeric length homeostasis in nonseminomatous testicular germ cell tumors. *Oncogene*. 2000. 19 (35), 4075-4078

Pietas A., Schluns K., Marenholz I., Schafer B.W., Heizmann C.W., Petersen I. Molecular cloning and characterization of the human S100A14 gene encoding a novel member of the S100 family. *Genomics*. 2002. 79 (4), 513-522

Chen Y., Petersen S., Pacyna-Gengelbach M., Pietas A., Petersen I. Identification of a novel homeobox-containing gene, LAGY, which is downregulated in lung cancer. *Oncology*. 2003. 64 (4), 450-458

Chen Y., Knosel T., Kristiansen G., Pietas A., Garber M.E., Matsushashi S., Ozaki I., Petersen I. Loss of PDCD4 expression in human lung cancer correlates with tumour progression and prognosis. *J Pathol*. 2003. 200 (5), 640-646

Difilippantonio S., Chen Y., Pietas A., Schluns K., Pacyna-Gengelbach M., Deutschmann N., Padilla-Nash H.M., Ried T., Petersen I. Gene expression profiles in human non-small and small-cell lung cancers. *Eur J Cancer*. 2003. 39 (13), 1936-1947

Oral Presentations and Posters

Pietas A., Schluns K., Petersen I. Molecular cloning and characterization of the human S100A14 gene encoding a novel member of the S100 family. 85th Annual Meeting of the German Society of Pathology, Vienna, Austria, April 2002 (oral presentation)

Pietas A., Schluns K., Marenholz I., Schafer B.W., Heizmann C.W., Petersen I. Molecular cloning and characterization of the human S100A14 gene encoding a novel member of the S100 family. European Conference on Calcium Signaling in Normal and Transformed Cells, Brussels, Belgium, June 2002 (poster)

Pietas A., Schluns K., Petersen I. Epidermal growth factor induces S100A14 in human lung and mammary tumour cells via the mitogen-activated protein kinase pathway. 87th Annual Meeting of the German Society of Pathology, Rostock, Germany, June 2004 (poster)

Pietas A., Schluns K., Petersen I. Epidermal growth factor induces S100A14 in human lung and breast tumour cells via the extracellular signal-regulated kinase cascade. European Conference on Calcium Signaling in Normal and Transformed Cells, Cambridge, England, July 2004 (accepted poster)

.....
Berlin, den 28. Juni 2004

Agnieszka Pietas

Eidesstattliche Erklärung

Hiermit erkläre ich, dass ich die vorliegende Dissertation selbstständig verfasst und keine anderen als die angegebenen Quellen und Hilfsmittel verwendet habe.

.....

Berlin, den 28. Juni 2004

Agnieszka Pietas